CMC

CONSTRUCTION MATERIALS CONSULTANTS, INC.

Laboratory Investigation of Anchoring Grout And Concrete Composite Cores From Balcony Slabs Of A Condominium

Anchoring Grout & Concrete Composite Cores From Balconies of Bee Street Lofts

Core 1 From Floor 7 Zone 1 | Core 2 From Floor 5 Zone 7 | Core 3 From Floor 4 Zone 3

Building Façade and Waterproofing Repairs
Bee Street Lofts
150 Bee Street Condominiums
Charleston, South Carolina

July 9, 2020
CMC 0620132

Table Of Contents

EXECUTIVE SUMMARY

Cracking observed in the concrete balconies of a condominium complex located in Charleston, South Carolina has prompted the present detailed laboratory investigation of three cores collected from three different floors of the complex. Cracks are preferentially located around anchoring grout pockets poured for handrails. The grout pockets are 4 in. deep in 8 in. thick balcony and showed relatively sound, crack-free conditions, whereas the concrete adjacent to grouts showed cracking. Both the grout and the concrete component in each core were examined by: (a) detailed petrographic examinations according to the procedures of ASTM C 856 for evaluation of their compositions, conditions, and evidence of any potentially deleterious chemical and/or physical reactions; (b) X-ray diffraction to determine the presence of any potentially deleterious constituents in the grout and/or concrete, which might have been responsible for cracking; and (c) X-ray fluorescence spectroscopy to determine the bulk chemical compositions, particularly the sulfate contents of grout and concrete components since sulfate plays a major role in deterioration of many anchoring grouts in a moist outdoor environment. No information about the composition or specification of grout, or any prior laboratory tests of grout are available at the time of this investigation for assessment of its potential for expansions at the hardened state in the presence of moisture during service.

The grout component in all three cores are compositionally similar, and indicative of use of the same grout mix at all three core locations from three different floors. The grout sand is lightly crushed natural siliceous sand made using major amounts of quartz and subordinate amounts of quartzite, which are nominal 0.5 mm or less in size, clear, subrounded to angular, dense, hard, well-graded, well-distributed, equidimensional to elongated, unaltered, uncoated, and uncracked. There is no evidence of alkali-aggregate reaction of sand particles, which are present in sound conditions during their service.

Paste in the grout component in all three cores are very dense and hard, indicative of a low water-cementitious materials ratio mix. Most distressed grouts typically show soft, porous, dusty paste, which is not the case in these grout samples where paste shows no evidence of leaching or softening during service. Portland cement was used as the major cementitious component in the grout. There is no evidence of fly ash, or slag addition as supplementary cementitious materials. However, there are evidence of addition of some other proprietary pozzolanic and/or cementitious materials as minor components besides Portland cement, which were observed during optical microscopical examinations of paste. Such evidence include some spherical fly ash-like empty particles that have vesicular glassy margins but are not as ubiquitous as would have been if a fly ash component was intentionally added. There are also indications of possible addition of silica fume or microsilica as evidenced from some brown clusters of ultrafine particles in the paste. A polymer component may also have been added as polymers commonly impart a densified paste microstructure as seen in the paste in present grouts. In summary, the densified paste microstructure showed more than that usually obtained from hydration of Portland cement alone. Densification of paste indicates use of a combination of low-water-cementitious materials ratio, high cementitious materials content, and, water-reducer type mix, which did not leave enough capillary pores in the paste to be readily detected by optical microscopy.

Grout samples in all three cores are excessively air-entrained having air contents estimated to be 18 to 20 percent by volume. Such high air entrainment has reduced the overall compressive strengths of grouts at the expense of added freeze-thaw durability during service. The observed cracks in the field are judged not due to freezing-related distress on the grout *per se*.

Bulk sulfate contents in the grout range from 4 to 5 percent, which is normal for a shrinkage-compensating anchoring grout where high sulfate contributes to an early expansion of the grout needed for shrinkage-compensation and anchorage. Sulfate contents, however, are not too high (e.g., >15 percent) as found in many gypsum-based anchoring grouts, where a lot of unused ‘excess’ sulfate stays after initial hydration reactions at the plastic state and those unreacted sulfates cause potential sulfate-aluminate reactions in the hardened state, which introduce late expansion at the hardened state and cracking in grout. The present grout is Portland cement-based, not gypsum-based, which is confirmed by bulk sulfate content of the grout, which also removes the possibility of having an excess sulfate in the grout to cause late-stage expansion and cracking.

XRD studies of grout showed quartz as the dominant mineral from silica sand and minor portlandite and calcite from paste. None of the grout samples showed any potentially deleterious components or reactions to introduce cracking or affect the performance beyond what is anticipated for the chemistry and mineralogy of the grout. Ettringite detected in the XRD patterns of all three grouts is normal anticipated hydration product of this grout and not indicative of a deleterious product.

Similar to grouts, the concrete components in all three cores are found to be compositionally similar, and indicative of use of the same concrete mix at all three core locations from three different floors. Coarse aggregates are compositionally similar crushed granite in all three cores having nominal maximum sizes of 1 inch (25 mm). Particles are dense, hard, light to dark gray, brown, angular, equidimensional to elongated, unaltered, uncracked, and uncoated. Coarse aggregate particles are well-graded and well-distributed. There is no evidence of any potentially deleterious alkali-aggregate reaction of crushed granite particles found in the cores. Coarse aggregate particles have been sound during their service and did not contribute to the observed cracking of balconies.

Fine aggregates are compositionally similar crushed silica sand having nominal maximum sizes of $^{3}/_{8}$ in. (9.5 mm) and contain major amounts of quartz, and subordinate amounts of quartzite, feldspar, granite, and sandstone particles. Particles are

variably colored, angular, dense, hard, equidimensional to elongated, unaltered, uncoated, and uncracked. Fine aggregate particles are well-graded and well-distributed. There is no evidence of alkali-aggregate reaction of fine aggregates found in the cores. Fine aggregate particles have been sound during their service in concrete and did not contribute to the cracking of balconies.

Pastes are moderately dense, medium gray, uniform in color throughout the depth of concrete. Freshly fractured surfaces have subvitreous lusters and subconchoidal textures. Residual and relict Portland cement particles are present and estimated to constitute 8 to 10 percent of the paste volumes. Besides Portland cement, no other pozzolanic or cementitious materials are found. Hydration of Portland cement is normal in the interior bodies. The textural and compositional features of the pastes are indicative of Portland cement contents estimated to be 6 to $6^{1}/_{2}$ bags per cubic yard, and, water-cement ratios (*w/c*) estimated to be 0.40 to 0.45 in the interior bodies of concrete. Carbonation is 3 to 4 mm from exposed surface of balcony. Aggregate-paste bonds are tight. There is no evidence of any chemical deterioration of paste found in the concretes to introduce the cracks. Neither the grout nor the concrete showed any deleterious reactions in the respective pastes.

Unlike grout, which is excessively air-entrained having at least 18 to 20 percent air, however, the concrete is at the other extreme, i.e., non-air-entrained, having less than 1 to 2 percent air at the most. Air occurs as a few near-spherical and irregularly-shaped voids that are characteristic of entrapped air in concrete. There is no evidence of intentional addition of an air-entraining agent found in the concrete. Due to the non-air-entrained nature of the concrete, some of the observed cracks if not all could have been introduced from cyclic freezing and thawing of a non-air-entrained concrete at critically saturated conditions, especially in areas along the interfaces to grout pockets due to inherently higher absorptive nature of the grout from its excessive air entrainment than the less absorptive non-air-entrained concrete.

Sulfate contents in the concrete ranges from 0.4 to 0.6 percent, which is consistent with addition of approximately 15 percent by mass of Portland cement in the concrete having about 3 percent sulfate in Portland cement, which are the normal cement content and sulfate content in cement, respectively, for the concrete found in the present three cores. In other words, sulfate contents of concrete do not show any evidence of external introduction of sulfate from the adjacent grout or from any other source besides the Portland cement as the main contributor of sulfate in concrete. There is, therefore, no evidence of cracking in the concrete from external sulfate attack or introduction of sulfate from the grout.

XRD studies showed quartz and feldspar (microcline, orthoclase, and albite) as the dominant minerals from crushed granite coarse aggregate particles and minor portlandite, calcite, and occasional secondary ettringite from paste where secondary ettringite found in the XRD are innocuous, and similar to the ones found in optical microscopy lining the walls of air voids that are indicative of the presence of moisture during service.

In summary, laboratory examinations of anchoring grouts and adjacent concrete in three cores collected from three different balcony floors of the condominium complex showed no deleterious reactions within the grout or in concrete *per se* to introduce the observed cracking concentrated mostly in the concrete around grout pockets. The grout in all three cores is compositionally similar dense, excessively air-entrained (18 to 20% air), silica sand and Portland cement-based, having 4 to 6 percent bulk sulfate (as SO_3), having a very dense low *w/cm* paste microstructure, and present in sound condition with no evidence of leaching, softening, carbonation, cracking, or any moisture-related alteration or distress of grout during service that are common in many other anchoring grouts showing expansion and cracking. Field photos of grout pockets showed no expansion or bulging, cracking, or softening of grout *per se*, except some visible cracks mostly confined to the concrete around the grout pockets. The high cementitious materials factor in the grout can introduce some shrinkage-related microcracks during drying. In fact, a few shallow-depth vertical surface microcracks found in the grout components in cores are judged to have formed from unaccommodated drying shrinkage which is not unusual for loss of some mix water during drying. Adequate curing of grout could delay formation of such surface microcracks but not necessarily prevent it from occurring at the hardened state after the curing period is over.

The concrete in three cores are compositionally similar and present in sound condition. However, the non-air-entrained nature of concrete can introduce some of the visible cracks in the field from cyclic freezing and thawing of concrete at critically saturated conditions. Excessive air in the grout pockets can absorb moisture and create a local moisture mass within the concrete to saturate the concrete during freezing and hence introduce cracking from freezing of concrete mostly at grout-concrete interfaces at saturated condition. The grout itself, however, should not crack by freezing due to its abundant entrained voids, which would accommodate all freezing-related expansions.

In summary, cracking of concrete around grout in the field photos are mostly formed due to one or a combination of the following factors: (a) continued expansion of grout after semi-plastic state to exert stresses to the neighboring concrete mass, which, however, seems unlikely due to reasonable 4 to 6 percent bulk sulfate content of grout to not leave any excess sulfate for continued sulfate-aluminate reactions at the semi-plastic or hardened states, and very dense and sound paste microstructure with no evidence of leaching softening or any moisture-induced alteration of paste during service; (b) restrain from expansion of grout at the plastic and semi-plastic state from concrete and metal plate installed above the grout; (c) freezing of non-air-entrained concrete at critically saturated conditions at the grout-concrete interface; and (d) some other factors not possible to evaluate from the present study. The present study found no deleterious reactions within the grout or concrete for cracking.

INTRODUCTION

Reported herein are the results of detailed laboratory studies of three composite cores consisting of anchoring grouts and associated concrete into which the grout was poured for anchorage of handrails. The cores were collected from balconies of a condominium constructed circa 2005.

BACKGROUND INFORMATION

Three cores were retrieved from balconies of a condominium constructed circa 2005, which recently removed the handrail to complete repairs to the condominium's façade. The intent was to reinstall the handrail using the existing anchors after the façade repairs were completed. Once the handrail was removed cracking and distress was observed in the concrete under the handrail anchor plates. Upon closer inspection, it was noted that two 4″x4″x4″ grout pockets existed under the handrail post anchor plates. It is believed that the handrail post were initially going to be embedded into pockets at the perimeter of the balconies. This anchoring method was abandoned, and the pockets were filled with grout. The handrail posts at the face of the balcony are double post and the handrail post at the building is a single post. The grout pockets follow the same layout as the handrail.

The grout pockets along the face of the balcony are double pockets and a single grout pocket is located at the building. The grout pockets are approximately 3.5 to 4.5 in. deep. The balcony is approximately 8 in. deep. There are horizontal cracks occurring at the face of the balcony that appear to align with the approximate depths of the grout pockets also. The thickness of the concrete between the double grout pockets ranges from 1-$^{1}/_{4}$" to $^{1}/_{2}$" thickness. The grout was reportedly placed during the original construction of the handrails and have not been altered or repaired. No information was available regarding the type of grout or of the concrete mix design.

FIELD PHOTOGRAPHS

Field photographs in Figures 1 through 3 show cracking around the perimeter of the grout pockets, which extends to edges and face of the slab.

Core samples provided for this study were reportedly collected from the corner of the slab. Not only the corners of the slab but the in-line handrail post at the face of the slab are distressed as well. The corners of the slab were selected to avoid taking samples in proximity to the post-tensioned anchors located on the face of the slab. Of the three cores provided, Core 1 was from Floor 7, Zone 1, Core 2 was from Floor 5, Zone 7, and Core 3 was from Floor 4, Zone 3.

PURPOSES OF PRESENT INVESTIGATION

Based on the background information, the purposes of the present investigation are to determine:

a. Compositions, qualities, and overall conditions of the composite grout and concrete cores received;
b. Chemical, mineralogical, and microstructural features of grouts and concretes to investigate any potential for expansions or shrinkage due to any chemical or physical deteriorations to introduce the observed cracking around the perimeters of grout pockets that have extended into the adjacent concrete; and,
c. Based on detailed laboratory investigation, investigation of all possible reasons to explain the observed and reported distress of grout and associated concrete.

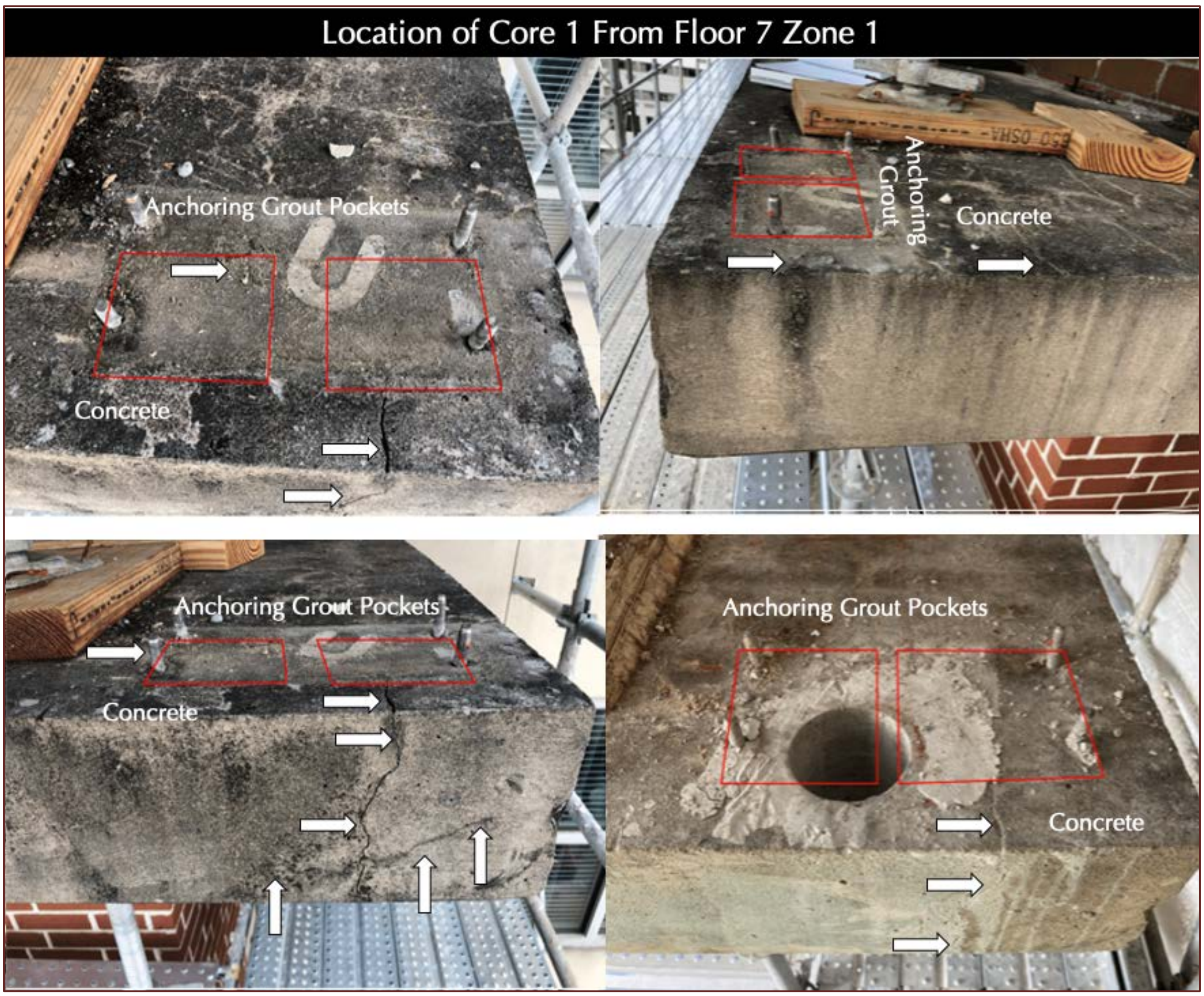

Figure 1: Field photographs showing cracking around the perimeter of the grout pocket indicated by arrows, which extend to the edges and face of the slab, and the location of Core 1 from Floor 7, Zone 1.

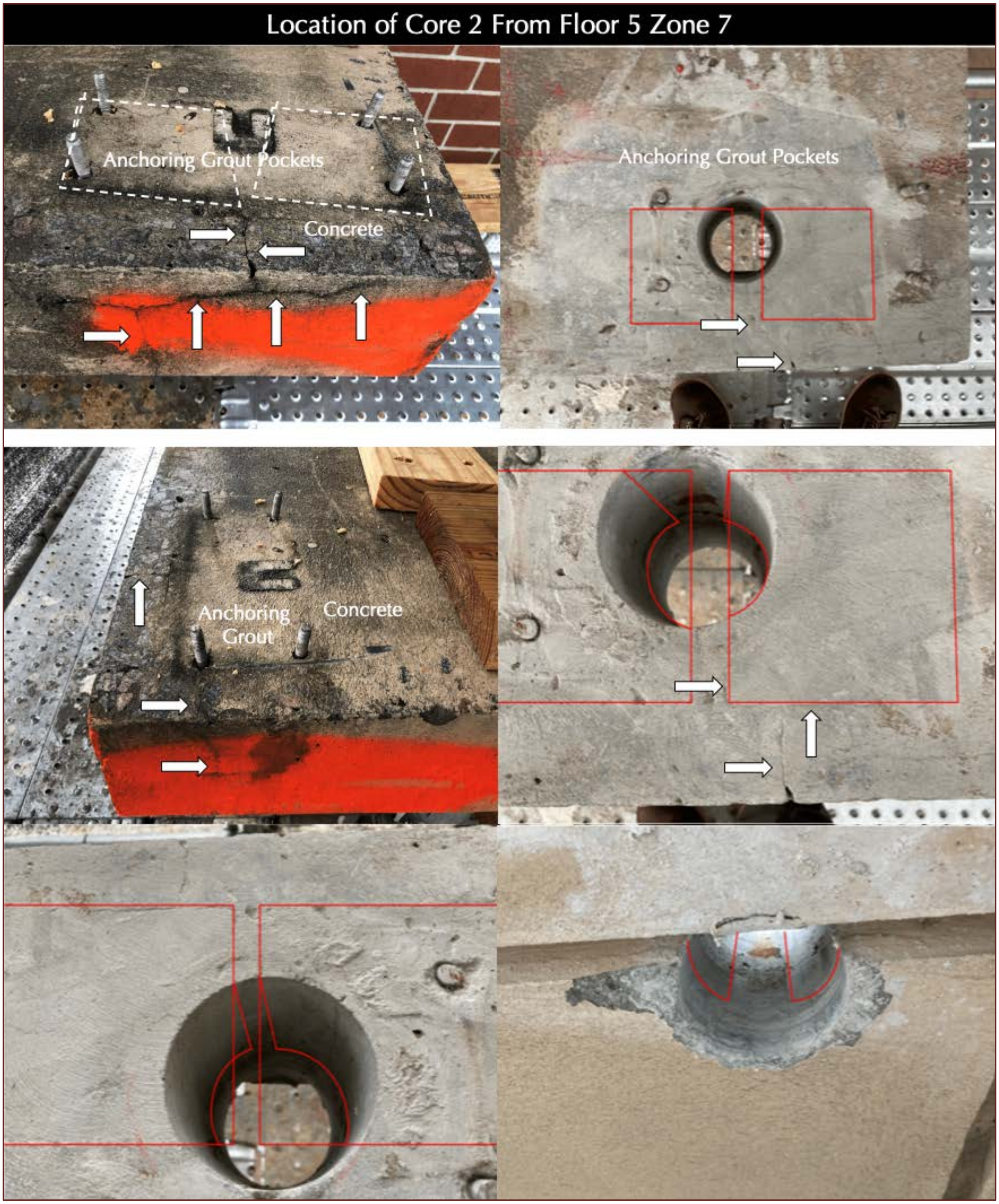

Figure 2: Field photographs showing cracking around the perimeter of the grout pocket indicated by arrows, which extend to the edges and face of the slab, and the location of Core 2 from Floor 5, Zone 7.

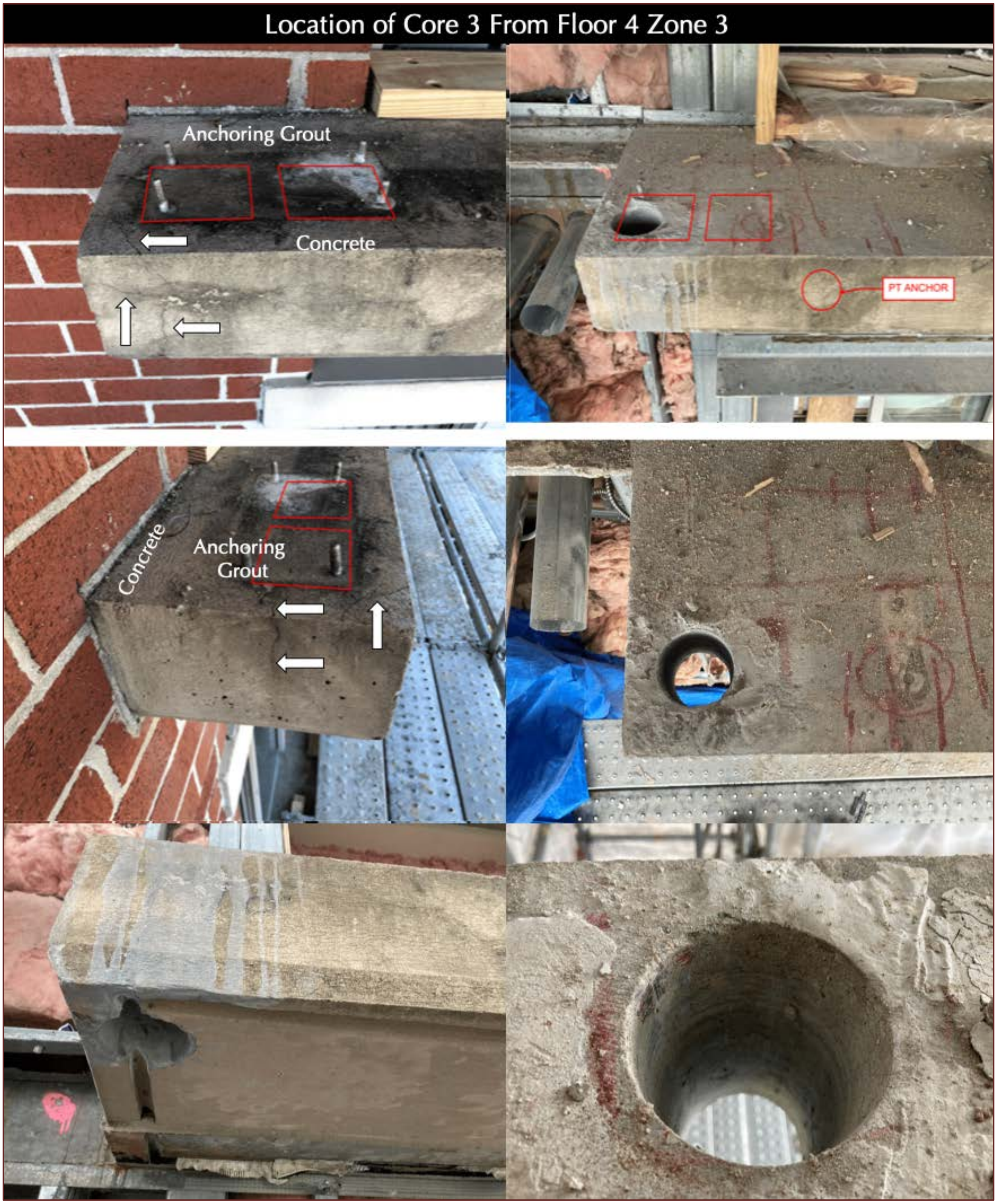

Figure 3: Field photographs showing cracking around the perimeter of the grout pocket indicated by arrows, which extend to the edges and face of the slab, and the location of Core 3 from Floor 4, Zone 3.

METHODOLOGIES

Common methodologies for evaluation of performance and durability of an anchoring grout system in the field include the following procedures, most of which are also applicable for evaluation of failure of such systems during service:

- Review of technical and safety data sheets to investigate possible compositions of binder, advertised intended application exposures (interior-only vs. both interior and exterior), setting time, water requirements, curing requirements, application methods, and manufacturer's test results (e.g., compressive strengths and expansion). Unfortunately, no technical data or specification of the grout used is available at the time of this investigation.
- Total sulfate contents – For evaluation of the presence of free calcium sulfate in the dry grout or hydrated in-place grout, which is the most common cause of distress when grout is exposed to moisture during service. For anchoring grouts, the binder usually constituents about half of the material by mass, so the sulfate contents for the material are about half of those for the binder alone. Materials with low sulfate content (<1.5% SO_3) are acceptable; materials with high sulfate content (> 15% SO_3) are unacceptable; and materials with moderate sulfate contents need to be evaluated further. For the present study, total sulfate contents of grout and concrete components in all three cores were determined by X-ray fluorescence studies, the details of which are described below.
- Mortar Bar Expansion - Particularly for evaluating performance of a grout in a moist environment. A modified ASTM C 157 test is appropriate to determine the 14-day and 28-day expansions of mortar bars prepared by following the manufacturer's recommended proportions (there is currently no ASTM test for expansion specific to rapid-hardening grout for use in moist exterior environments). Usually, if the measured expansion after 14 days is no more than 500 microstrain, the free calcium sulfate content of the grout is not likely to promote deleterious expansions during service. No laboratory test data is available for expansion of the grout used in the project.
- Petrographic Examinations, *a la* ASTM C 856, of the dry proprietary grout powder to characterize if the binder system is Portland-cement only, or gypsum-only, or Portland cement/gypsum blend, or Portland cement/calcium aluminate cement blend, as well as to determine the constituents in the binder that can cause deleterious expansions during service in a moist outdoor environment. Petrography is also routinely used to evaluate failure of hardened grout in service, as the present study, to evaluate the binder components and diagnose materials and microstructures that are indicative of grout failures. Details of petrographic examinations is described below.
- X-ray Diffraction – To determine the presence or absence of free calcium sulfate (e.g., gypsum) and/or sulfate-related distress compounds (e.g., ettringite) in the hydrated material, both of which are generally detectable by XRD when the binder SO_3 content is 1% or more. Details of XRD studies employed for evaluation of grout and concrete components of all three cores are described below.

PETROGRAPHIC EXAMINATIONS

The samples were examined by petrographic examinations by following the methods of ASTM C 856 "Standard Practice for Petrographic Examination of Hardened Concrete." Details of petrographic examinations and sample preparation are described in Jana (2006). The steps of petrographic examinations include (Jana 2006):

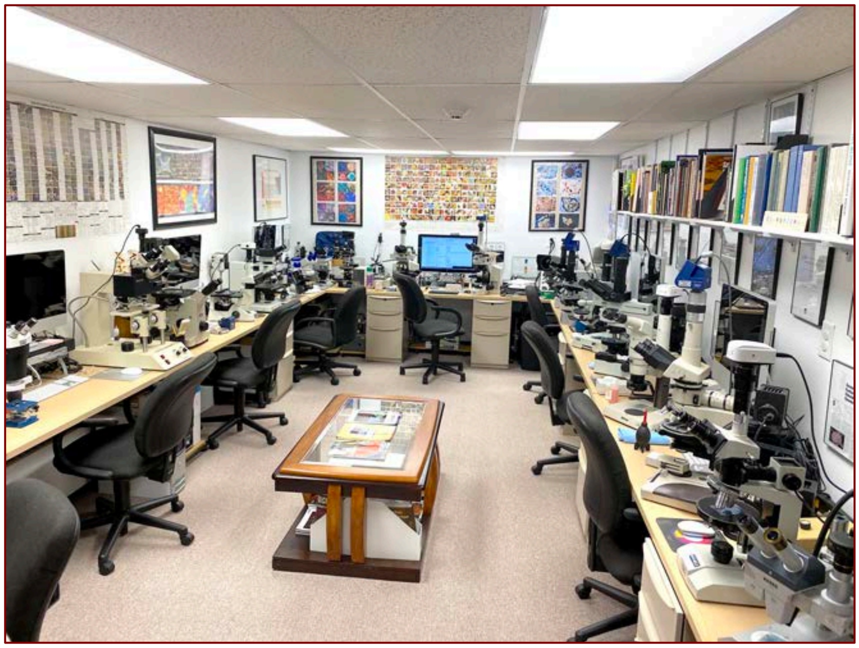

Figure 4: Optical microscopy laboratory in CMC that houses various stereo-microscopes, and petrographic microscopes used in this study.

i. Visual examinations of samples, as received;
ii. Low-power stereo microscopical examinations of as-received, saw-cut and freshly fractured sections, and lapped cross sections of samples for evaluation of textures, and composition;
iii. Low-power stereo microscopical examinations of air contents and air-void systems of grout and concrete in the samples;
iv. Examinations of oil immersion mounts in a petrographic microscope for mineralogical compositions of specific areas of interest;
v. Examinations of blue dye-mixed (to highlight open spaces, cracks, etc.) epoxy-impregnated large area (50 mm × 75 mm) thin sections of grout and concrete in a petrographic microscope for detailed compositional and microstructural analyses;
vi. Photographing samples, as received and at various stages of preparation with a digital camera and a flatbed scanner; and,
vii. Photomicrographs of lapped sections and thin sections of samples taken with stereomicroscope and petrographic microscope, respectively to provide detailed compositional and mineralogical information of grout and concrete.

The main purposes of optical microscopy are characterization of: (a) aggregates, e.g., type(s), chemical and mineralogical compositions, nominal maximum size, shape, angularity, grain-size distribution, soundness, alkali-aggregate reactivity, etc. (b) paste, e.g., compositions and microstructures to diagnose various type(s) of binder(s) used, (c) air, e.g., presence or absence of air entrainment, air content, etc., (d) alterations, e.g., lime leaching, carbonation, staining, etc. due to interactions with the environmental agents during service, and effects of such alterations on properties and performance; and (e) deteriorations, e.g., chemical and/or physical deteriorations during service, cracking from various mechanisms, salt attacks, possible reasons for the lack of bond if reported, etc. Portions selected from preliminary examinations for microscopy are sectioned, polished, and thin-sectioned (down to 25-30 micron thickness) preferably after encapsulating and impregnating with a dyed-epoxy to improve the overall integrity of the sample during precision sectioning and grinding, and to highlight porous areas, voids, and cracks. Prepared sections are then examined in a high-power (up to 100X) Stereozoom microscope having reflected and transmitted-light, and plane and crossed polarized-light facilities, and eventually in a high-power (up to 600X) petrographic microscope equipped with transmitted, reflected, polarized, and fluorescent-light facilities. Capturing high-resolution photomicrographs from these microscopes via digital microscope cameras with image analyses software are an integral part of documentations during petrographic examinations.

X-RAY DIFFRACTION (XRD)

X-ray diffraction (XRD) is a powerful method for: (a) determination of bulk mineralogical composition of sample, including its aggregate and binder mineralogies; (b) primary mineralogies and alteration products of aggregates and binder phases; (c) detection of any potentially deleterious constituents, e.g., deleterious salts, or efflorescence deposits; and (e) detection of components that are difficult to detect by microscopical methods.

For sample preparation, a Rocklab (Sepor Mini-Thor Ring) pulverizer is used to grind sample down to finer than 100 microns. Usually, a few drops of anhydrous alcohol are added to reduce decomposition of hydrous phases from the heat generated from grinding. Approximately 10 grams of sample is ground first in the pulverizer, from which about 8.0 grams of sample is selected, mixed with an appropriate binder (e.g., three Herzog grinding aid pellets from Oxford Instruments having a total binder weight of 0.6 gram for 8 grams of sample for a fixed binder proportion of 7.5 percent); the mixture is then further ground in Rocklab pulverizer and in a McCrone micronizing mill with anhydrous alcohol down to finer than 45-micron size. Approximately 7.0 grams of binder-mixed pulverized sample thus prepared is weighed into an aluminum sample cup and inserted in a stainless steel die press to prepare the sample pellet. A 25-ton Spex X-press is used to prepare 32 mm diameter pellet from the pulverized sample. The pressed pellet is then placed in a custom-made circular sample holder for XRD and excited with the copper radiation of 1.54 angstroms. Sample holders made with quartz or silicon are best for working with very small quantities of sample because these holders create no diffraction peaks between 2° and 90° 2θ.

Figure 5: Siemens D5000 X-ray diffractometer in CMC that is connected to PC through MDI Datascan to collect diffraction data. XRD results are analyzed with MDI Jade software with search-match, easy quant, and Rietveld modules. The bottom row shows sample preparation for XRD where a Sepor Ring pulverizer (2nd from left) followed by McCrone micronizing mill (leftmost one) pulverized the sample to finer than 45-micron size. The pulverized sample is mixed with an appropriate binder and pressed in a 25-ton Spex press to form a 32-mm diameter pellet. Small amount of sample (i.e. not enough to prepare a pellet) is pulverized and spread over a quartz plate coated with a thin film of Vaseline.

XRD is carried out in a Siemens D5000 Powder diffractometer (θ-2θ goniometer) employing a long line focus Cu X-ray tube, divergent and anti-scatter slits fixed at 1 mm, a receiving slit (0.6 mm), diffracted and incident beam Soller slits (0.04 rad), a curved graphite diffracted beam monochromator, and a sealed proportional counter. Siemens D5000 is equipped with (a) a horizontal stage (fixed), (b) an X-ray generator with CuKα, fine focus sealed tube source, (c) large diameter goniometer (600 mm), low divergence collimator, and Soller slits, (d) fixed detector slits 0.05, 0.2, 0.6, 1.0, 2.0, and 6.0, and (e) Scintillation detector. Generator settings used are 40 kV and 30 mA. Tests are usually run at 2θ from 4° to 64° with a step scan of 0.02° and a dwell time of one second. The resulting diffraction patterns are collected by DataScan 4 software of Materials Data, Inc. (MDI), analyzed by Jade software of MDI with ICDD PDF-4 (Minerals 2019) diffraction data. Phase identification, and quantitative analyses were carried out with MDI's Search/Match, Easy Quant, and Rietveld modules, respectively.

X-RAY FLUORESCENCE SPECTROSCOPY (XRF)

X-ray fluorescence (XRF) is used for determining: (a) major element oxide composition of sample, and (b) presence and amount of potentially deleterious constituents in the sample. A series of standards from Portland cements, lime, gypsum, to various rocks of certified compositions (e.g., from USGS, GSA, NIST, CCRL, Brammer, or measured by ICP) are used to calibrate the instrument for various oxides, and empirical calculations are done from such calibrations to determine oxide compositions of samples.

An energy-dispersive bench-top X-ray fluorescence unit from Rigaku Americas Corporation (NEX-CG) is used. Rigaku NEX CG delivers rapid qualitative and quantitative determination of major and minor atomic elements in a wide variety of sample types with minimal standards. Unlike conventional EDXRF analyzers, the NEX CG was engineered with a unique close-coupled Cartesian Geometry (CG) optical kernel that dramatically increases signal-to-noise. By using monochromatic secondary target excitation, instead of conventional direct excitation, sensitivity is further improved. The resulting dramatic reduction in background noise, and simultaneous increase in element peaks, result in a spectrometer capable of routine trace element analysis even in difficult sample types. The instrument is calibrated by using various certified (CCRL, NIST, GSA, and Brammer) reference standards of cements and rocks. The same pellet used for XRD for mineralogical compositions is used for XRF to determine the chemical composition.

Figure 6: Rigaku NEX-CG in CMC, which can perform analyses of up to 9 pressed pellets or fused beads of sample. Samples are prepared either as pressed pellet or can also accommodate fused bead with proper calibration of standard beads.

SAMPLES

PHOTOGRAPHS, IDENTIFICATION, INTEGRITY, AND DIMENSIONS

Figures 7 through 10, and Table 1 provide the overall dimensions and conditions of the grout-concrete composite cores received. Figures 11 through 16 show multiple parallel lapped cross sections of composite cores to reveal detailed internal features.

Core ID	Diameter	Length	End Surfaces	Distress/Condition
#1 Floor 7 Zone 1	$2^3/_4$ in. (70 mm)	$6^7/_8$ in. (175 mm)	Top – Finished Bottom – Formed, placed on metal decking	Top 4 in. (100 mm) grout, rest concrete; Intact
#2 Floor 5 Zone 7	$2^3/_4$ in. (70 mm)	7 in. (177 mm)	Top – Finished Bottom – Formed, placed on metal decking	Top 4 in. (100 mm) grout, rest concrete; Intact
#3 Floor 4 Zone 3	$2^3/_4$ in. (70 mm)	6 in. (150 mm)	Top – Finished, protruding threaded screw ($1^1/_4$ in.) Bottom – Formed, placed on metal decking	Top $2^3/_4$ in. (70 mm) grout, remaining $2^3/_4$ in. (70 mm) concrete Broken – grout completely debonded from concrete

Table 1: Overall dimensions and conditions of the grout-concrete composite cores received for laboratory examinations.

END SURFACES

All three cores showed finished top surfaces and formed bottom surfaces as seen in Figures 7 through 10.

CRACKING & OTHER VISIBLE DISTRESS, IF ANY

Core 3 was received broken into two portions due to debonding at the grout-concrete interface. There are no large voids or other visible distress in the three cores received.

EMBEDDED ITEMS

Core 3 contains a $1^1/_4$ in. threaded screw embedded in and protruding from the top finished surface. No other wire mesh, reinforcing steel, fiber, or other embedded items are found in the cores.

RESONANCE

The cores have a ringing resonance, when hammered.

TESTING STRATEGY

The cores were first examined in detail in as received condition and photographed with a digital camera. Preliminary examinations were followed by sectioning of cores in multiple longitudinal sections to obtain full-length slices of grout-concrete so that the internal structures of cores can be revealed. Longitudinal slices of composite cores were then lapped on a rotating iron lapping wheel with various successively finer metal and resin-bonded diamond abrasives with water as coolant. Separate slices were used for preparing blue dye-mixed epoxy-impregnated thin sections of composite cores. Remaining pieces were used for pulverization for XRD and XRF studies.

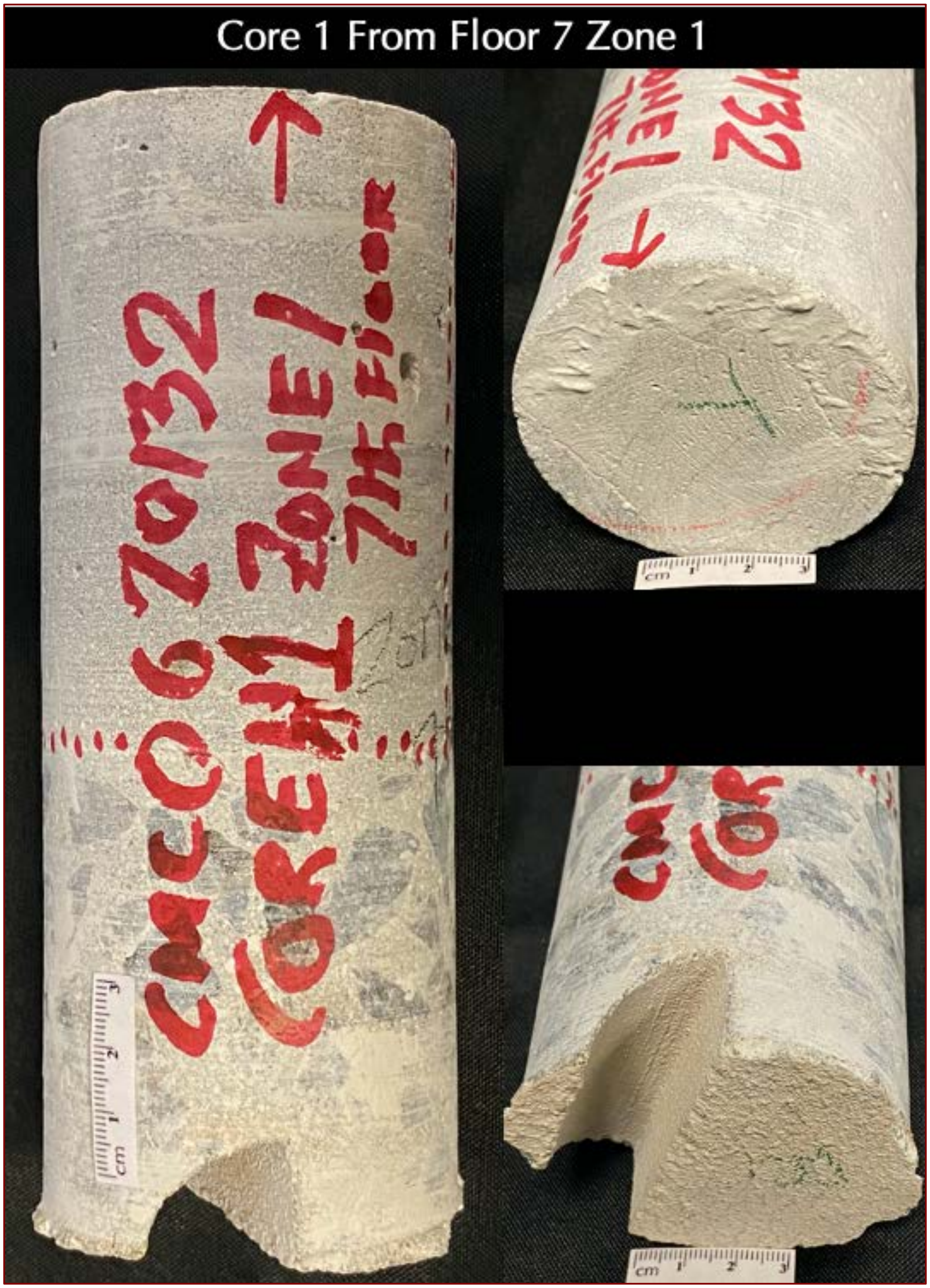

Figure 7: Core 1 from Zone 1 7th floor showing:

(a) A finished exposed surface of grout which is seen in sound condition;

(b) A formed base of concrete at the core bottom with a thin cream-colored paint coat on concrete; indicating placement of slab on a metal decking followed by painting of the concrete base,

(c) A good bond between the gray grout and concrete components of core which is marked as dotted line on the cylindrical surface of core;

(d) Overall intact condition of the grout-concrete composite core;

(e) Crushed granite coarse aggregate particles in concrete; and,

(f) Dense and well-consolidated natures of both grout and concrete components.

Figure 8: Core 2 showing:

(a) A good bond between the gray grout and concrete components of core, which is marked as dotted red line on the cylindrical surface of core;

(b) Overall intact condition of the grout-concrete composite core;

(c) Crushed granite coarse aggregate particles in concrete; and,

(d) Dense and well-consolidated natures of both grout and concrete components.

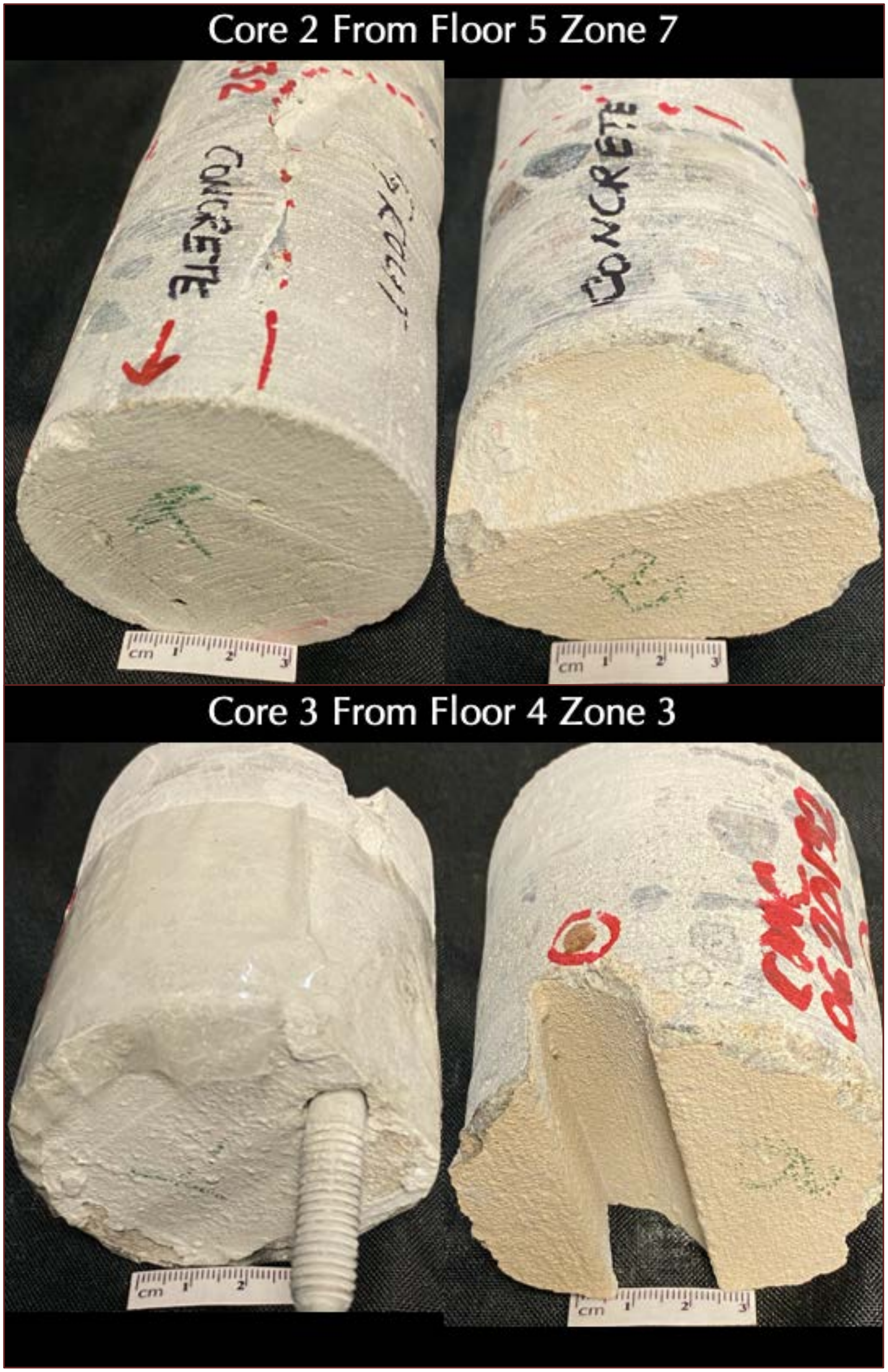

Figure 9: Exposed finished surfaces of grouts in Cores 2 and 3, and opposite formed surfaces of concretes in both cores showing placement of concrete slab on metal decking. Notice a cream-colored paint coat present on the concrete base in both cores (also seen in Core 1).

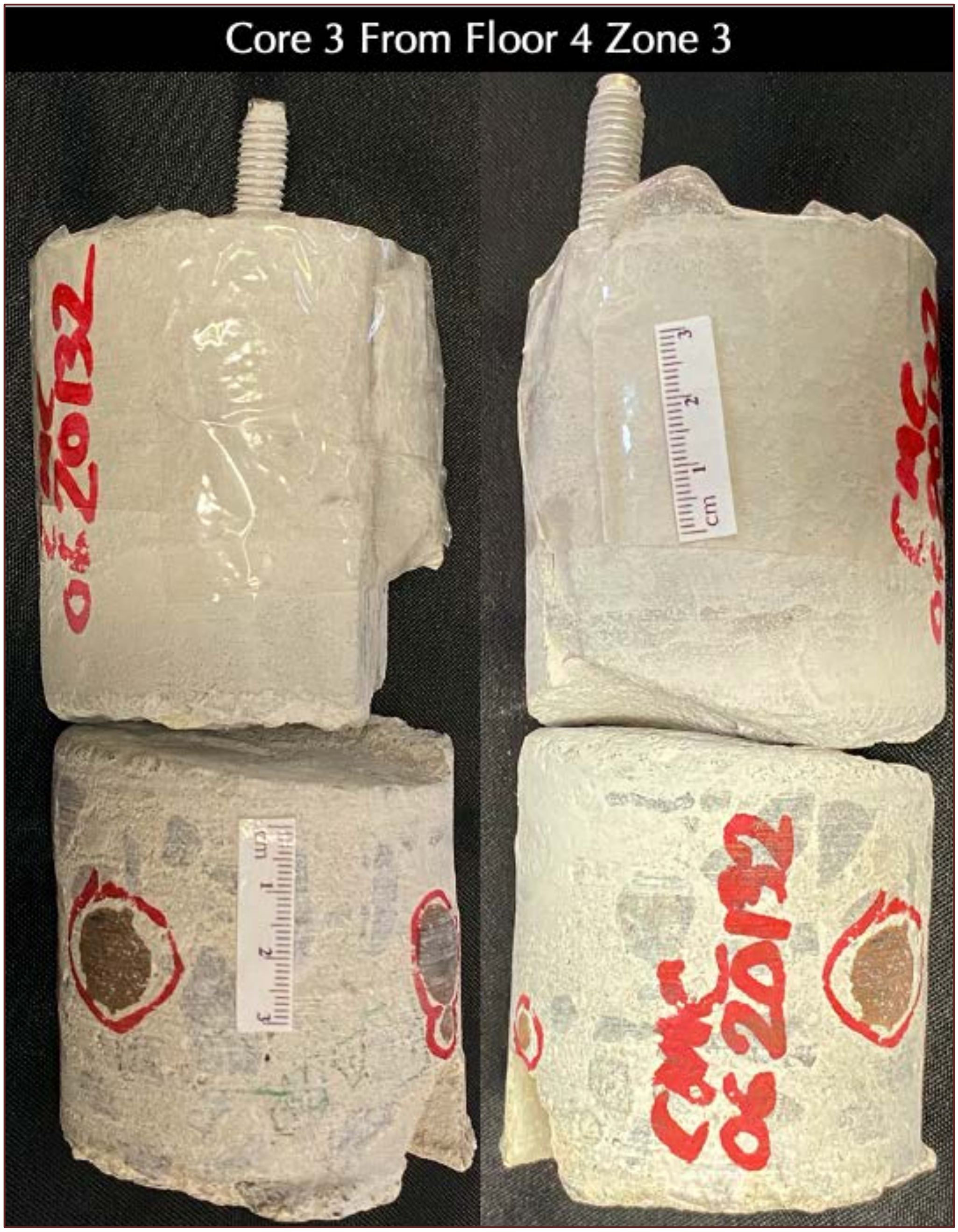

Figure 10: Core 3 showing:

(a) Completely de-bonded nature of grout at the top from concrete at the bottom half of core;

(b) A screw protruding from the grout;

(c) A No. 4 reinforcing steel and a wire mesh in the concrete at the mid-depth location of the concrete component, about an inch above the formed base of concrete;

(d) Overall intact condition of the grout and concrete components in the composite core despite complete debonding;

(e) Crushed granite coarse aggregate particles in concrete; and,

(f) Dense and well-consolidated natures of both grout and concrete components.

LABORATORY STUDIES

SAW-CUT CROSS SECTIONS

Figure 11: Saw-cut sections of Core 1 showing: (a) the dark gray grout and medium gray concrete components, (b) crushed granite coarse aggregate particles in concrete that are poorly graded due to the deficiency of some finer and intermediate-size particles, as well as poor distribution with some settlement of coarser fractions of coarse aggregate particles towards the bottom concrete portion of the core (concrete adjacent to the grout lacks coarser particles of crushed granite coarse aggregate), (c) good bond between the grout and concrete components, (d) a thin cream-colored paint coat at the formed bottom of concrete, (e) a thin light beige discolored carbonated concrete at the bottom end, indicating a period of atmospheric carbonation of concrete at its formed base prior to the installation of paint coat.

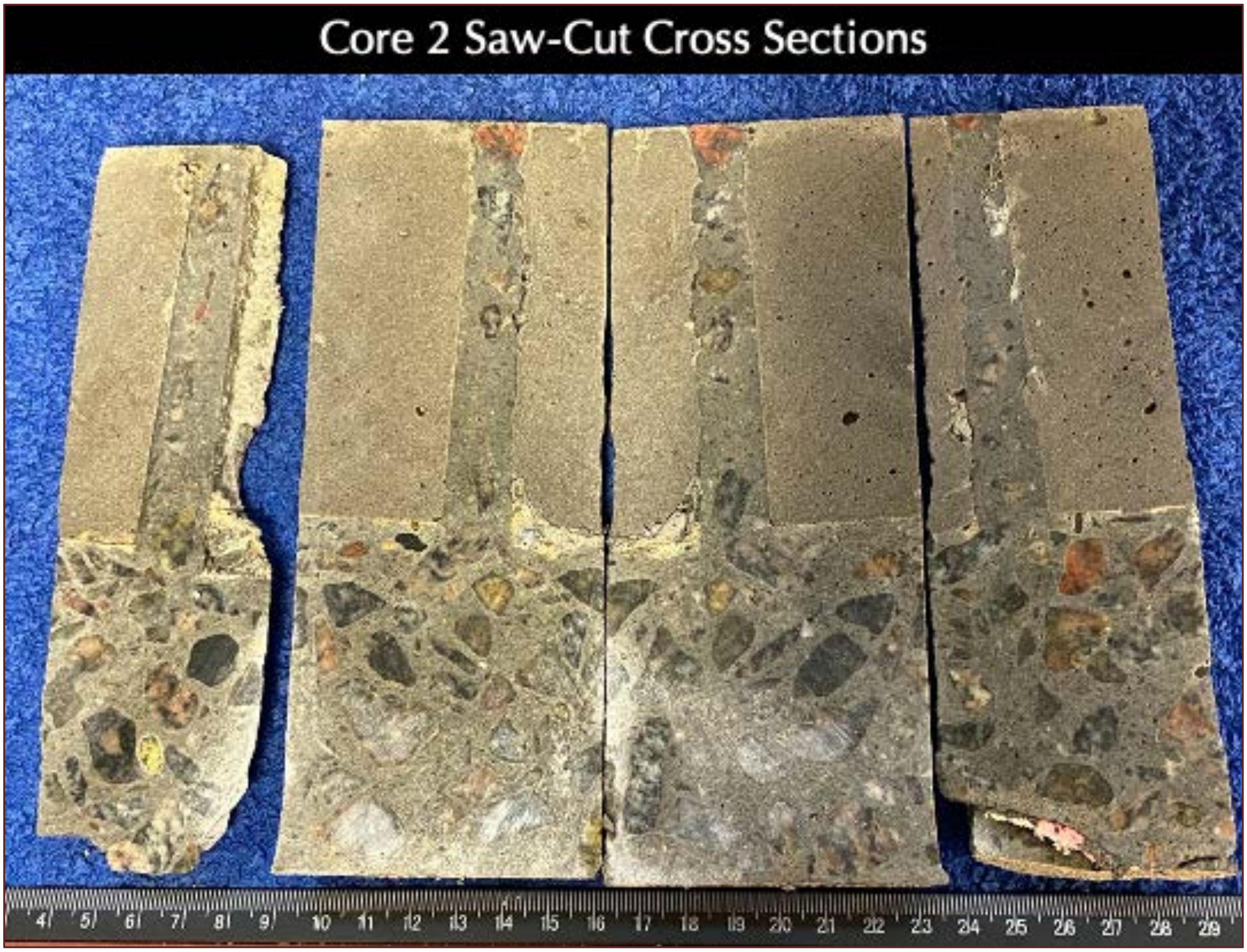

Figure 12: Saw-cut sections of Core 2 showing: (a) the dark gray grout and medium gray concrete components, (b) crushed granite coarse aggregate particles in concrete that are poorly graded due to the deficiency of some finer and intermediate-size particles, as well as poor distribution with some settlement of coarser fractions of coarse aggregate particles towards the bottom concrete portion of the core (concrete sandwiched between lacks coarser particles of crushed granite coarse aggregate), (c) good bond between the grout and concrete components, (d) a thin cream-colored paint coat at the formed bottom of concrete, (e) a thin light beige discolored carbonated concrete at the bottom end, indicating a period of atmospheric carbonation of concrete at its formed base prior to the installation of paint coat.

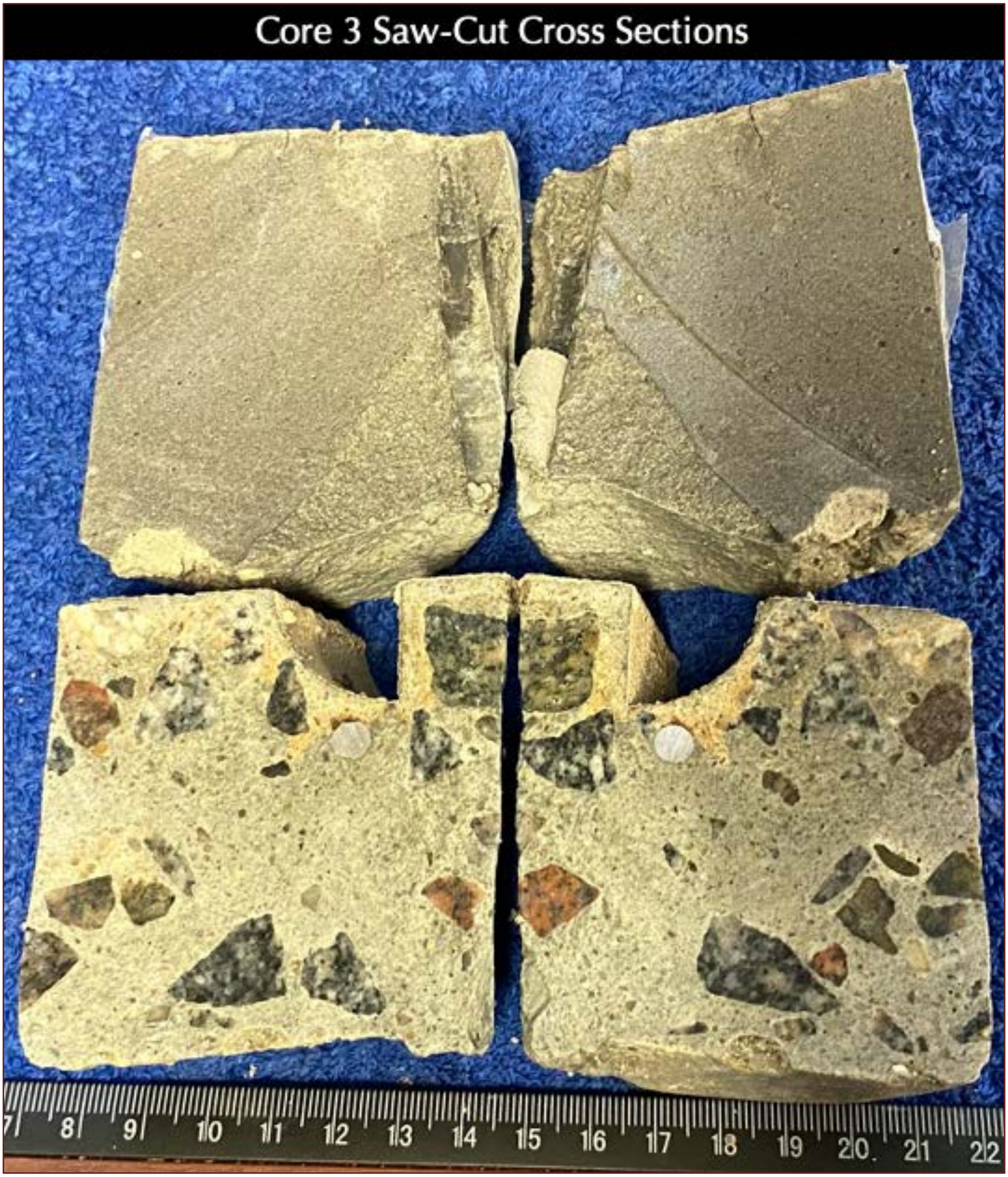

Figure 13: Saw-cut sections of Core 3 showing: (a) the dark gray grout and medium gray concrete components that are completely de-bonded, (b) crushed granite coarse aggregate particles in concrete that are poorly graded due to the deficiency of some finer and intermediate-size particles, and (c) a thin cream-colored paint coat at the formed bottom of concrete.

LAPPED CROSS SECTIONS

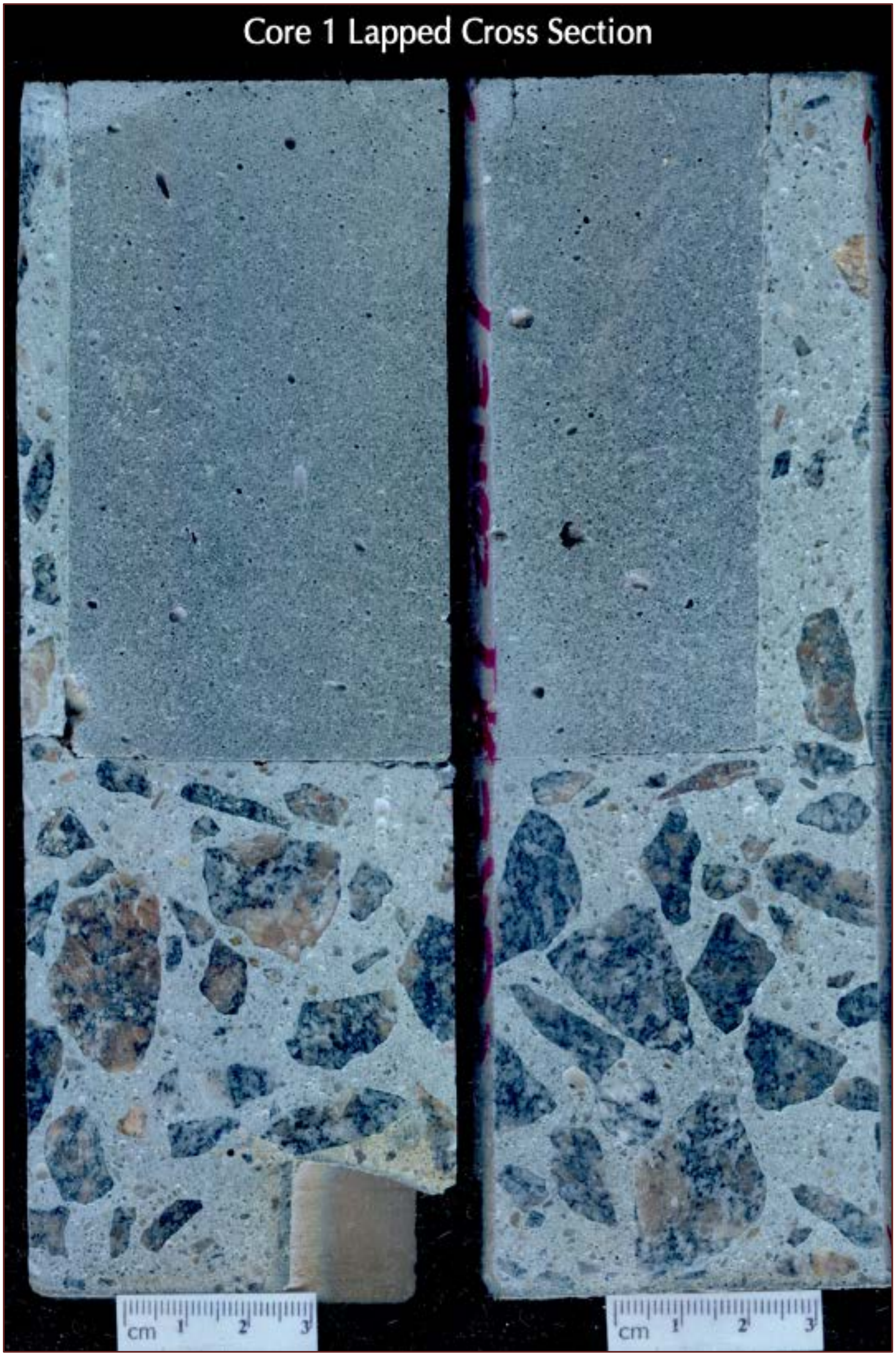

Figure 14: Lapped cross section of Core 1 showing:

(a) The dark gray grout and medium gray concrete components,

(b) Crushed granite coarse aggregate particles in concrete that are poorly graded due to the deficiency of some finer and intermediate-sized particles as well as poor distribution with some settlement of coarser fractions of coarse aggregate particles towards the bottom concrete portion of the core (concrete adjacent to the grout lacks coarser particles of crushed granite coarse aggregate),

(c) Good bond between the grout and concrete components,

(d) a thin cream-colored paint coat at the formed bottom of concrete,

(e) a thin light beige discolored carbonated concrete at the bottom end, indicating a period of atmospheric carbonation of concrete at its formed base prior to the installation of paint coat.

Figure 15: Lapped cross section of Core 2 showing:

(a) The dark gray grout and medium gray concrete components,

(b) Crushed granite coarse aggregate particles in concrete that are poorly graded due to the deficiency of some finer and intermediate-sized particles as well as poor distribution with some settlement of coarser fractions of coarse aggregate particles towards the bottom concrete portion of the core (concrete sandwiched between lacks coarser particles of crushed granite coarse aggregate),

(c) Good bond between the grout and concrete components, (the crack in the middle developed during the lapping process);

(d) A thin cream-colored paint coat at the formed bottom of concrete,

(e) A thin light beige discolored carbonated concrete at the bottom end, indicating a period of atmospheric carbonation of concrete at its formed base prior to the installation of paint coat.

Figure 16: Lapped cross section of Core 3 showing:

(a) The dark gray grout and medium gray concrete components that are completely de-bonded,

(b) Crushed granite coarse aggregate particles in concrete that are poorly graded due to the deficiency of some finer and intermediate-size particles, and

(c) A thin cream-colored paint coat at the formed bottom of concrete.

MICROGRAPHS OF LAPPED CROSS SECTIONS

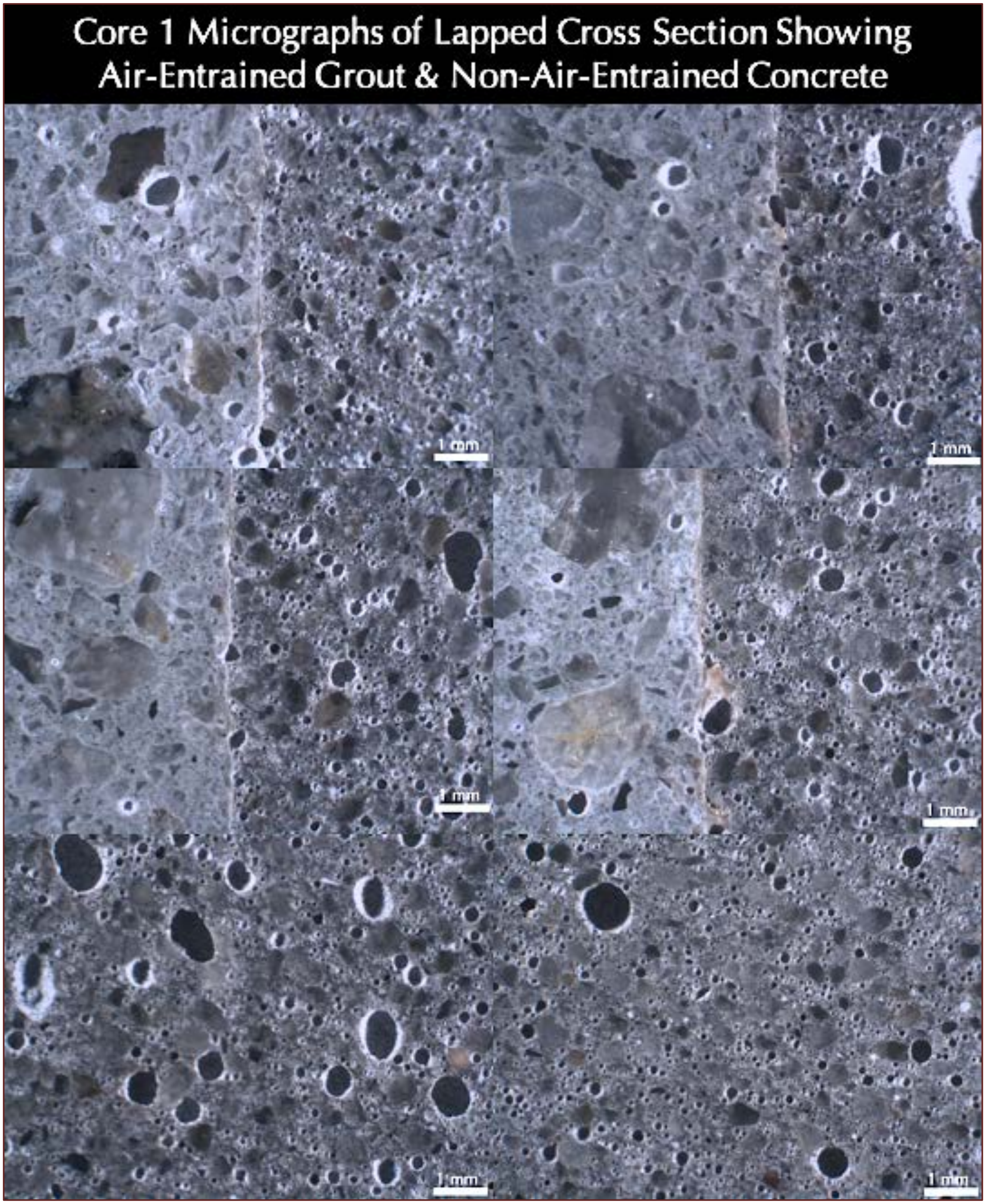

Figure 17: Micrographs of lapped cross section of Core 1 showing: (a) excessively air-entrained dark gray grout and non-air-entrained medium gray concrete; (b) good grading and well-distribution of crushed siliceous sand particles in dark gray grout; (c) poor grading of crushed granite coarse aggregate particles in concrete; and (d) good bond between the grout and concrete despite a marked difference in air content and air entrainment between the two components. Scale bars are 1 mm.

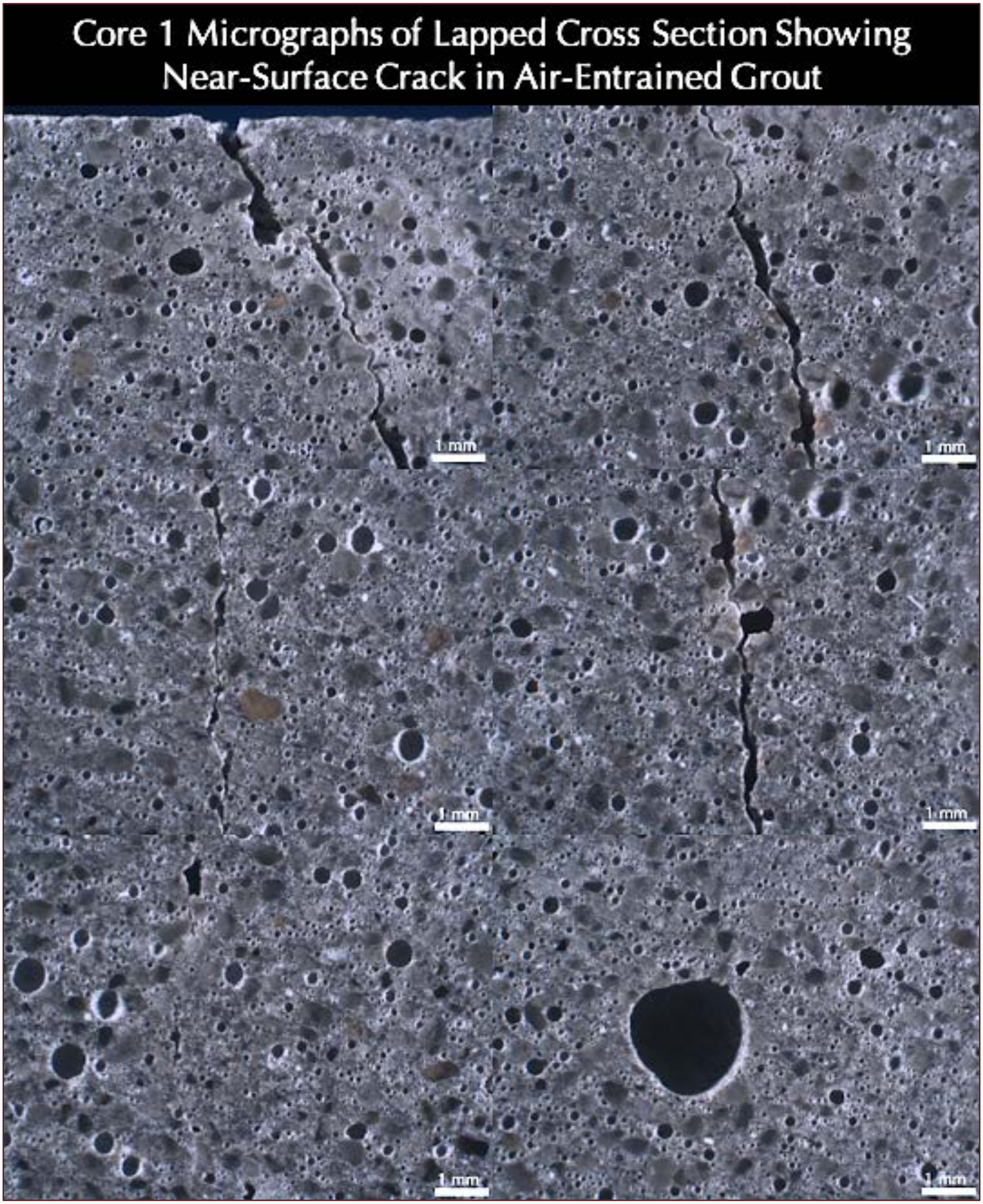

Figure 18: Micrographs of lapped cross section of Core 1 showing: (a) excessively air-entrained dark gray grout; and (b) a vertical shrinkage microcrack at the exposed surface of grout that has extended to a depth of 15 mm (micrographs have followed the crack path towards the interior until the crack disappeared). Scale bars are 1 mm.

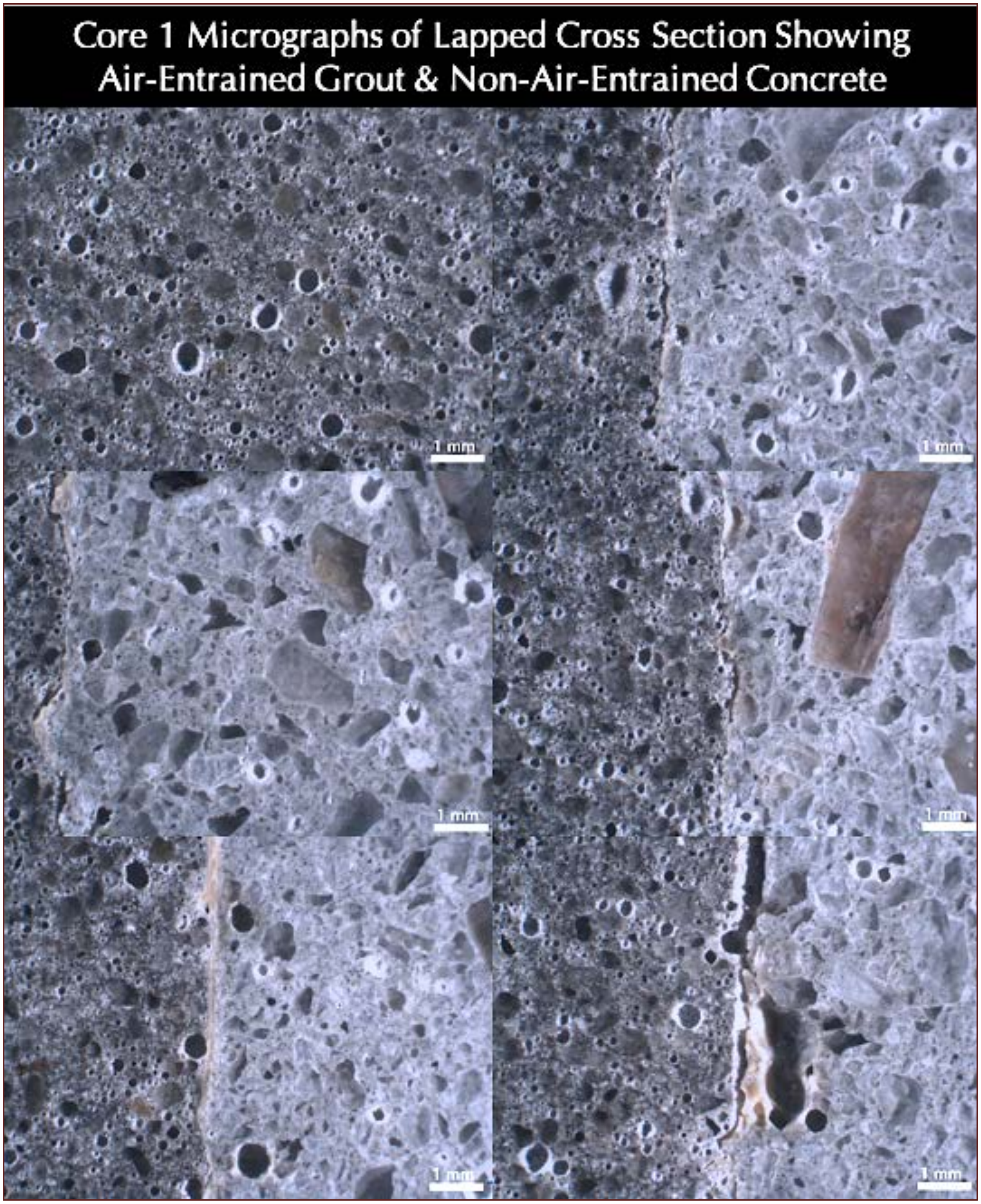

Figure 19: Micrographs of lapped cross section of Core 1 showing: (a) excessively air-entrained dark gray grout and non-air-entrained medium gray concrete; (b) good grading and well-distribution of crushed siliceous sand particles in dark gray grout; (c) poor grading of crushed granite coarse aggregate particles, but good grading and distribution of crushed silica sand fine aggregate in concrete; (d) good bond between the grout and concrete despite a marked difference in air content and air entrainment between the two components; and (e) secondary ettringite deposits lining the walls of some air voids in concrete. Scale bars are 1 mm.

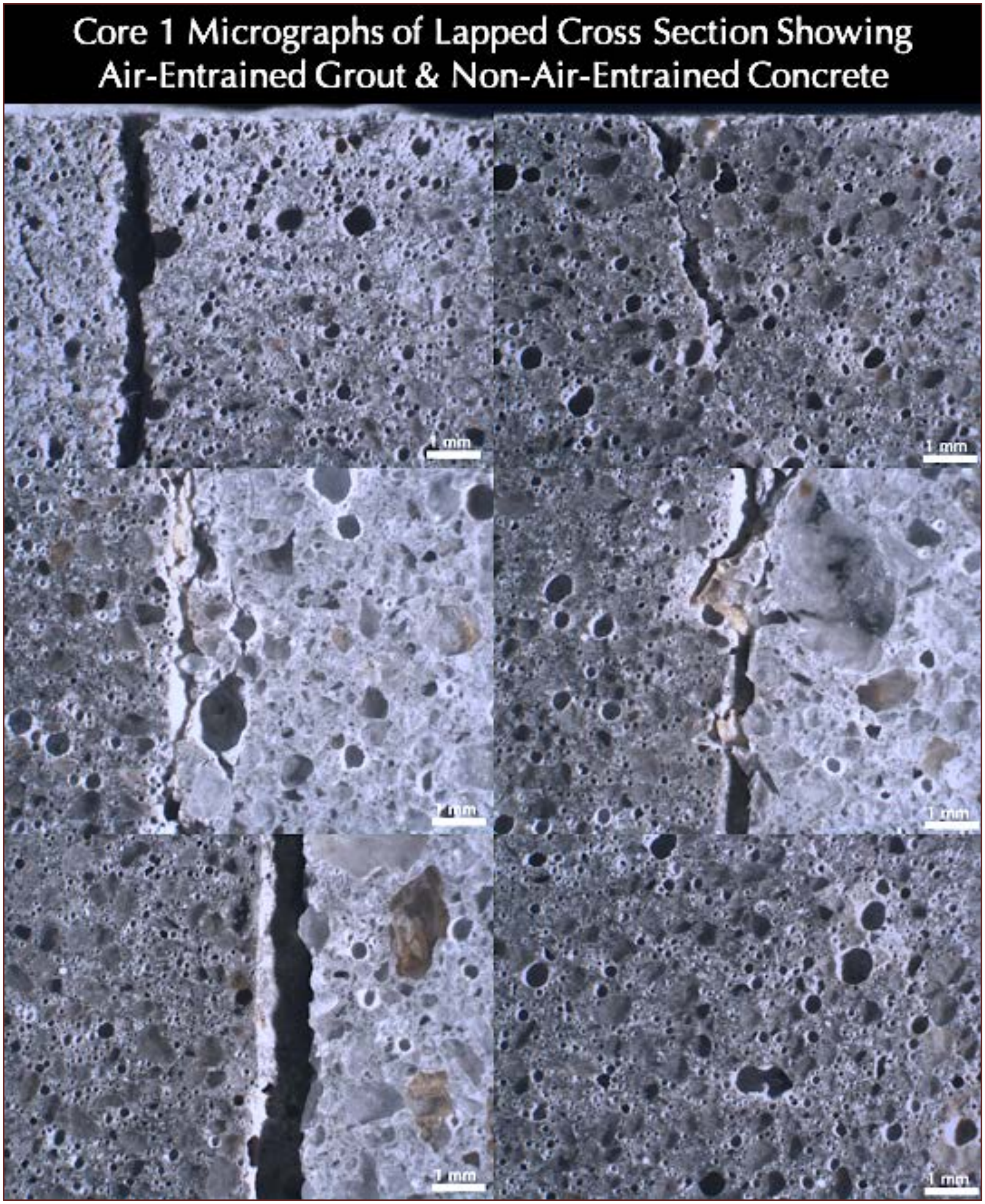

Figure 20: Micrographs of lapped cross section of Core 1 showing: (a) excessively air-entrained dark gray grout and non-air-entrained medium gray concrete; (b) good grading and well-distribution of crushed siliceous sand particles in dark gray grout; (c) poor grading of crushed granite coarse aggregate particles, but good grading and distribution of crushed silica sand fine aggregate in concrete; and (d) good bond between the grout and concrete despite a marked difference in air content and air entrainment between the two components. Scale bars are 1 mm.

Figure 21: Micrographs of lapped cross section of Core 2 showing: (a) excessively air-entrained dark gray grout and non-air-entrained medium gray concrete; (b) good grading and well-distribution of crushed siliceous sand particles in dark gray grout; (c) poor grading of crushed granite coarse aggregate particles, but good grading and distribution of crushed silica sand fine aggregate in concrete; (d) good bond between the grout and concrete despite a marked difference in air content and air entrainment between the two components; and (e) secondary ettringite deposits lining the walls of some air voids in concrete. Scale bars are 1 mm.

Figure 22: Micrographs of lapped cross section of Core 2 showing: (a) excessively air-entrained dark gray grout and non-air-entrained medium gray concrete; (b) good grading and well-distribution of crushed siliceous sand particles in dark gray grout; (c) poor grading of crushed granite coarse aggregate particles, but good grading and distribution of crushed silica sand fine aggregate in concrete; (d) good bond between the grout and concrete despite a marked difference in air content and air entrainment between the two components; and (e) secondary ettringite deposits lining the walls of some air voids in concrete. Scale bars are 1 mm.

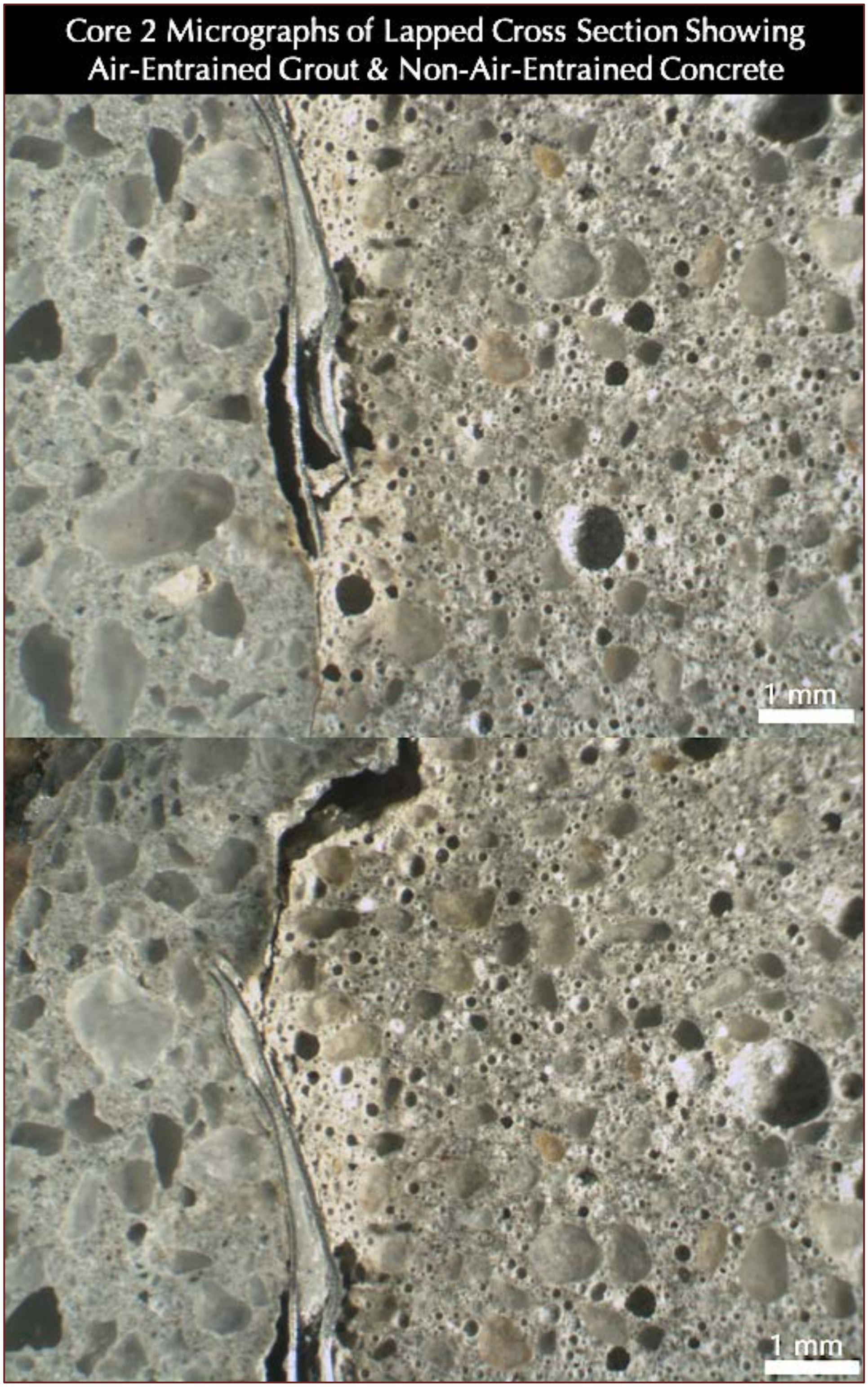

Figure 23: Micrographs of lapped cross section of Core 2 showing: (a) excessively air-entrained dark gray grout and non-air-entrained medium gray concrete; (b) good grading and well-distribution of crushed siliceous sand particles in dark gray grout; (c) poor grading of crushed granite coarse aggregate particles, but good grading and distribution of crushed silica sand fine aggregate in concrete; (d) good bond between the grout and concrete despite a marked difference in air content and air entrainment between the two components; (e) evidence of some beige discoloration in concrete adjacent to grout possibly due to some exposure to air before coming into contact with grout; and (f) presence of a sheet-like material at the grout-concrete interface. Scale bars are 1 mm.

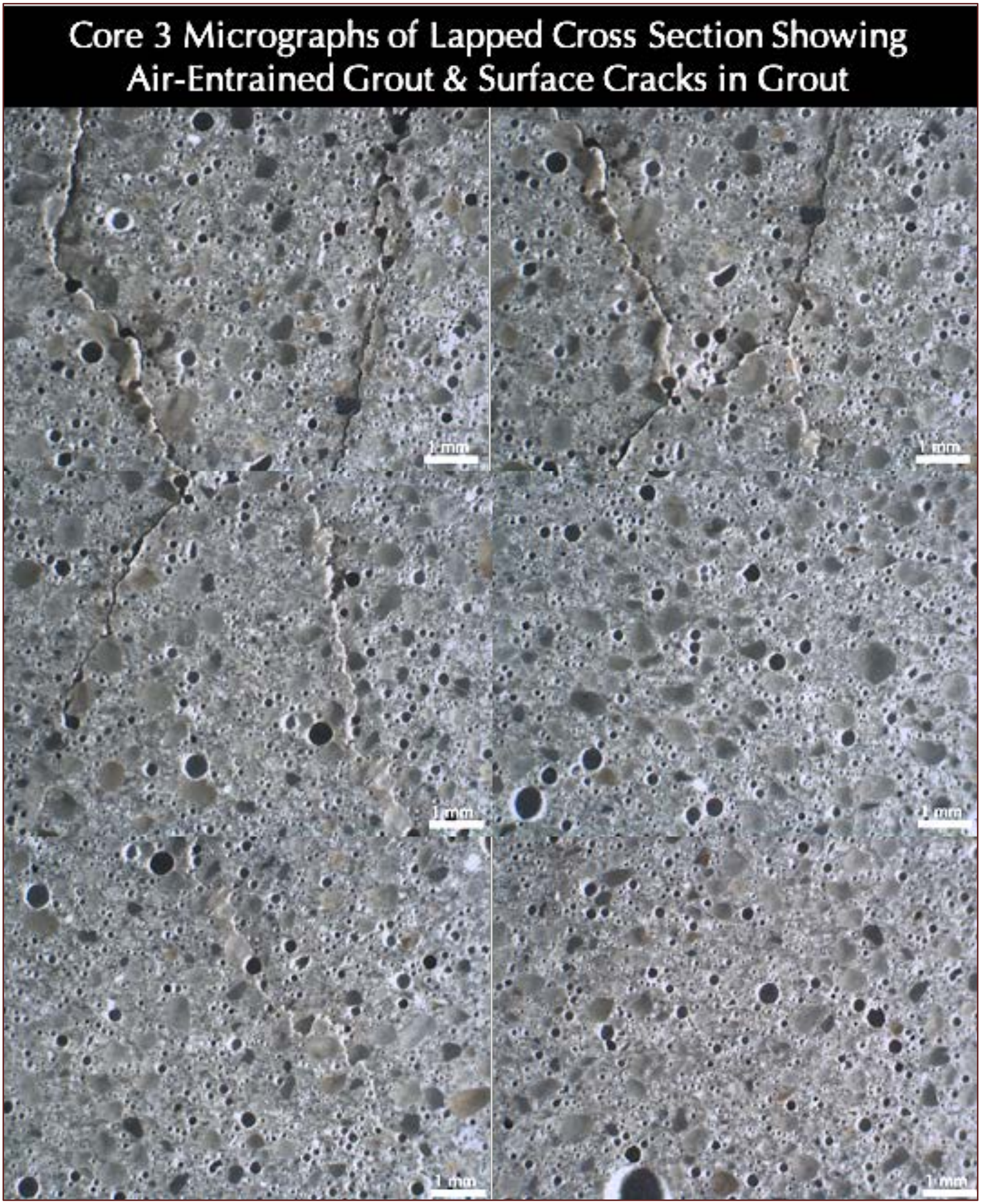

Figure 24: Micrographs of lapped cross section of Core 3 showing: (a) excessively air-entrained dark gray grout; and (b) two vertical shrinkage microcracks at the exposed surface of grout that extend to a depth of 20 mm (micrographs have followed the crack path towards the interior until the crack disappeared). Scale bars are 1 mm.

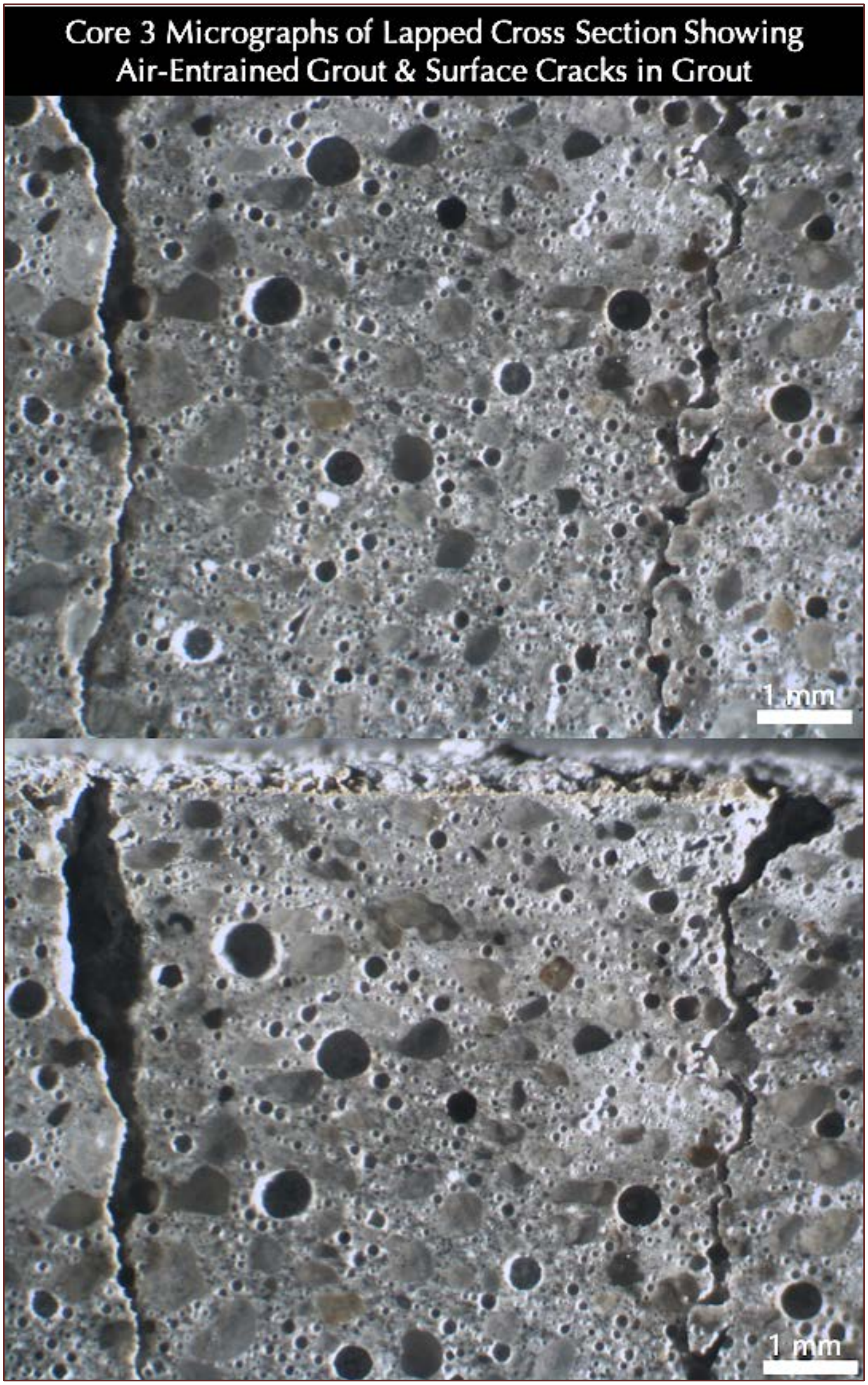

Figure 25: Micrographs of lapped cross section of Core 3 showing:

(a) Excessively air-entrained dark gray grout; and,

(b) Two vertical shrinkage microcracks at the exposed surface of grout that extend to a depth of 20 mm.

Scale bars are 1 mm.

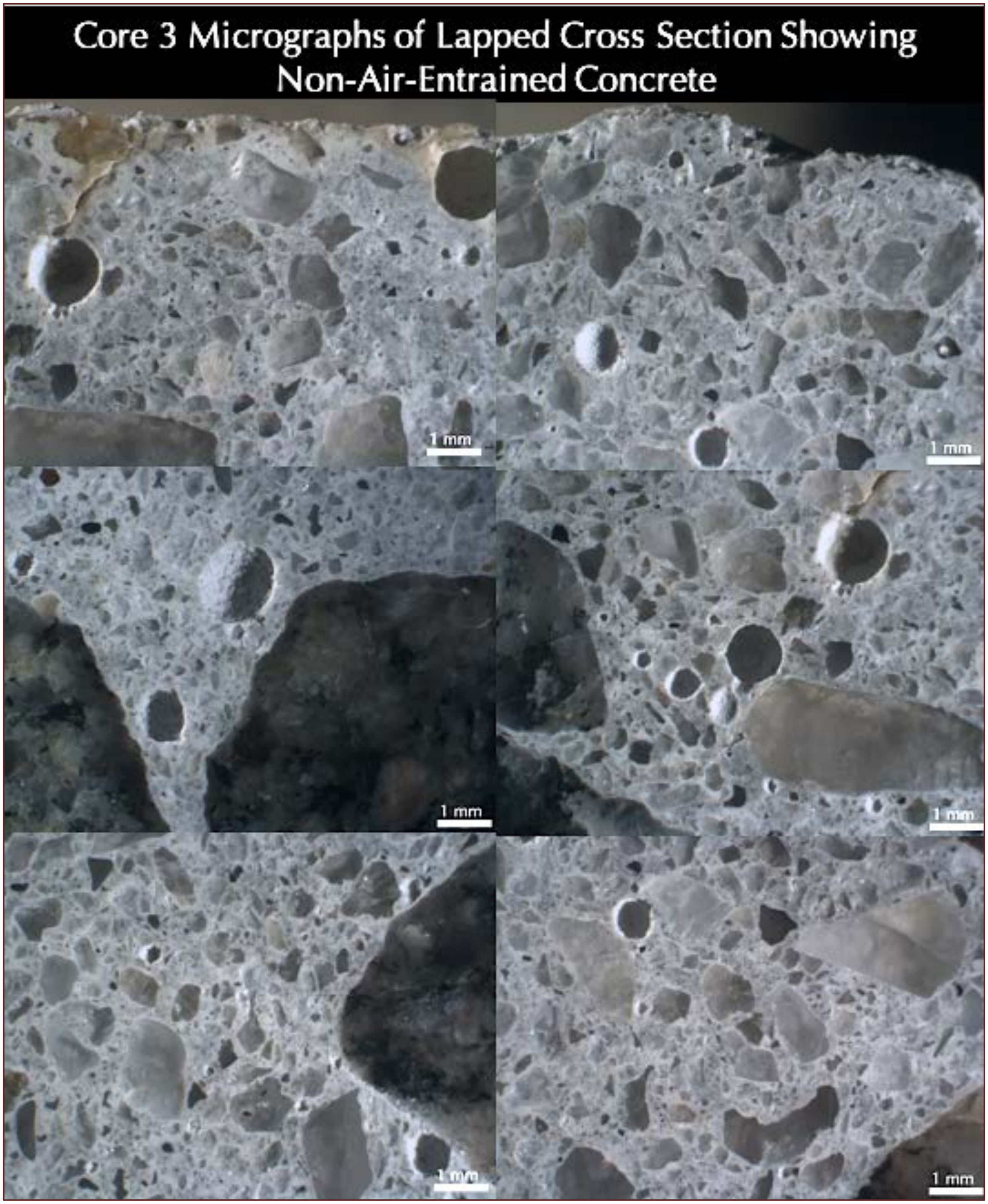

Figure 26: Micrographs of lapped cross section of Core 3 showing: (a) non-air-entrained medium gray concrete having a few coarse near-spherical and irregular-shaped entrapped air voids; (b) a fine shrinkage microcrack at the top end of concrete in the top left photo; (c) poor grading of crushed granite coarse aggregate particles, but good grading and well-distribution of siliceous sand fine aggregate particles in concrete; and (d) overall dense and well-consolidated nature of concrete. Scale bars are 1 mm.

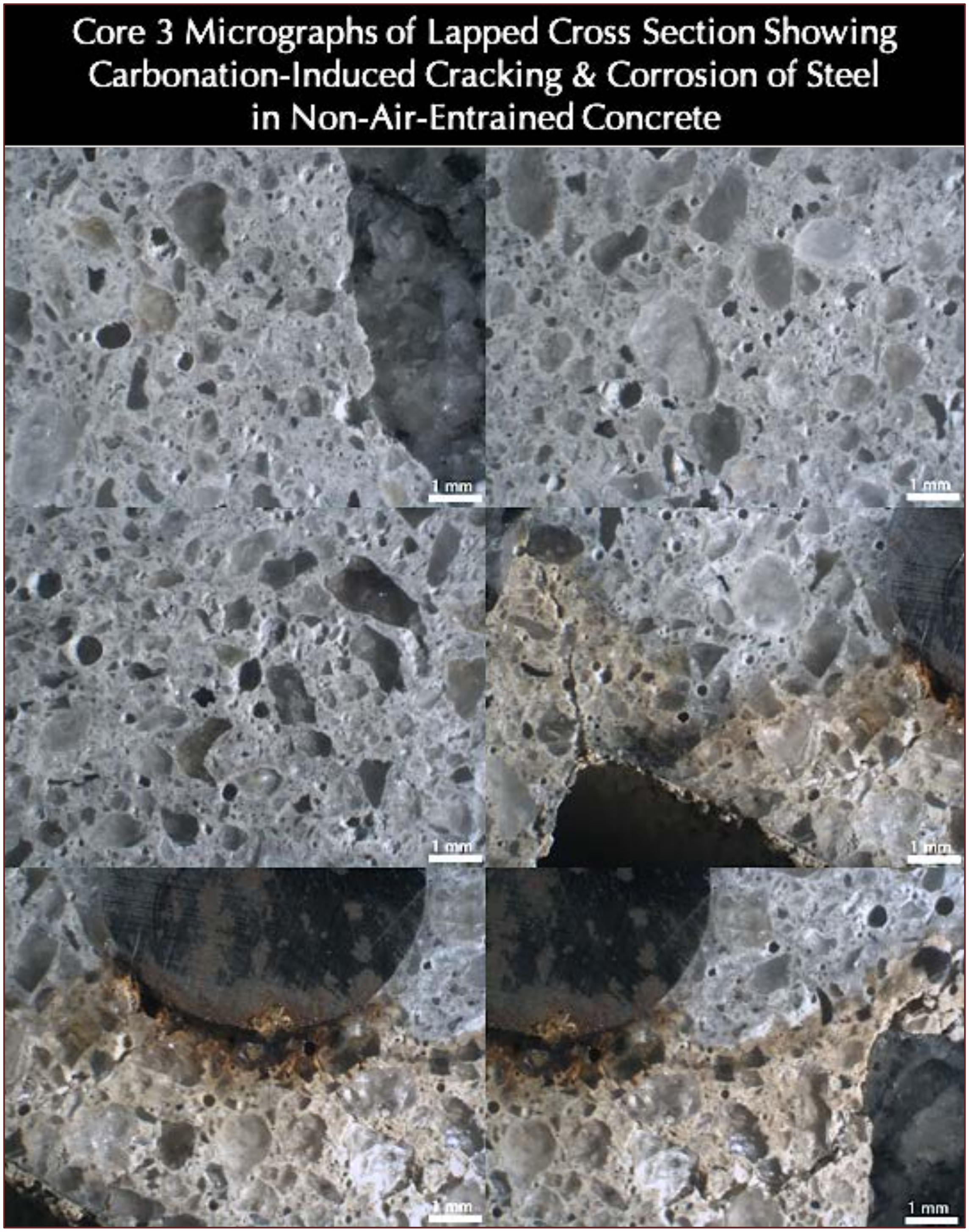

Figure 27: Micrographs of lapped cross section of Core 3 showing: (a) non-air-entrained medium gray concrete having a few coarse near-spherical and irregular-shaped entrapped air voids but overall dense and well-consolidated nature; and (b) carbonation-induced corrosion of a wire mesh situated at mid-depth location in concrete, about an inch above the formed concrete base. The mesh shows reddish-brown corrosion products and cracking associated with corrosion. The beige discoloration of concrete base from atmospheric carbonation has reached the level of wire mesh and hence caused carbonation-induced de-passivation of the protective oxide film around the mesh to initiate corrosion in the presence of moisture and oxygen. Cracks formed from corrosion of steel have opened up pathways for migration of carbon dioxide deep inside the concrete as seen by the V-shaped carbonation front along a radial crack from corroded steel in the middle right photo.

THIN SECTIONS

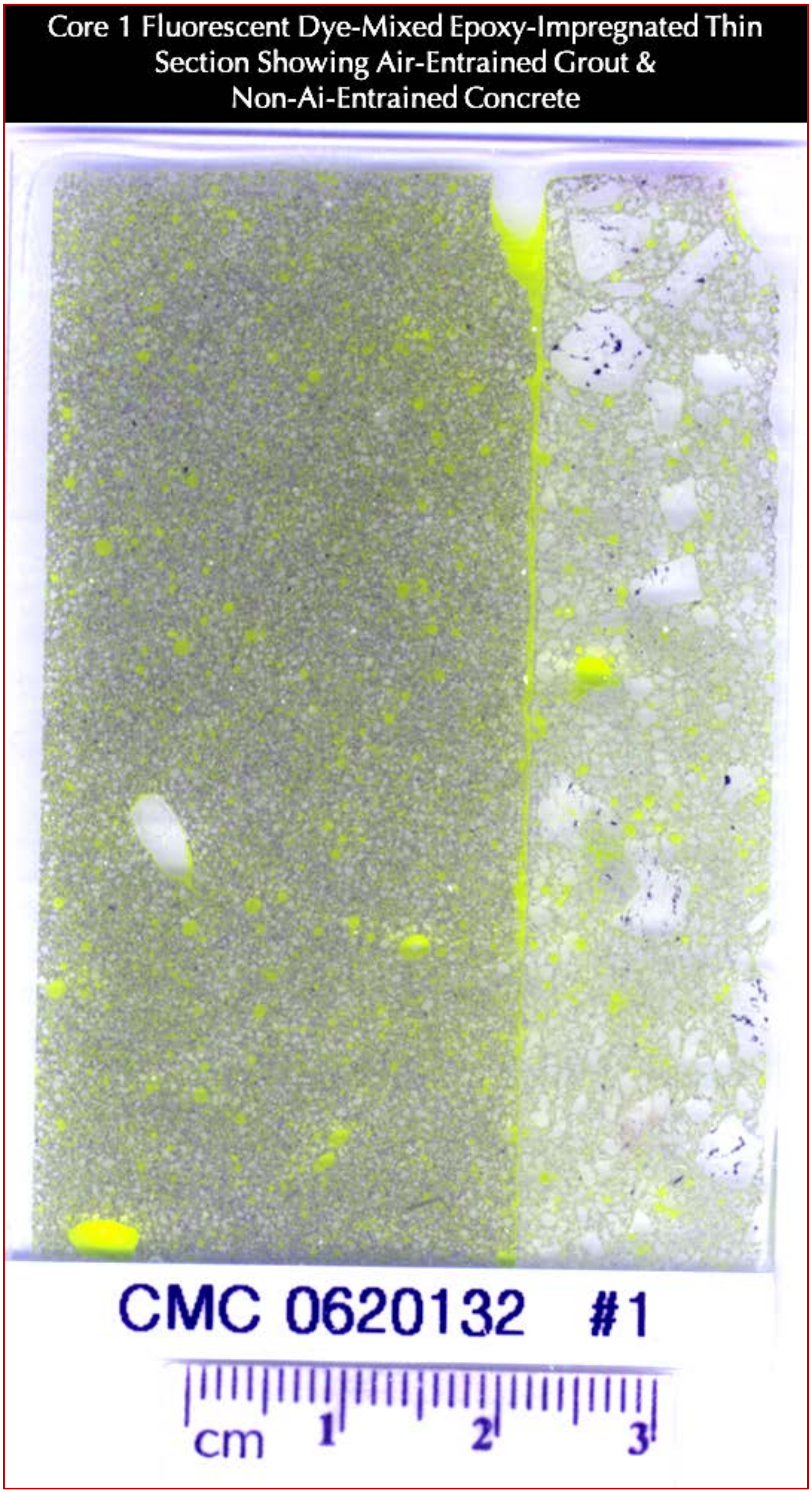

Figure 28: Fluorescent dye-mixed epoxy-impregnated thin section of grout and concrete in Core 1 showing:

(a) Overall denser nature of grout relative to concrete;

(b) Excessively air-entrained nature of grout as opposed to non-air-entrained nature of concrete;

(c) Crushed granite coarse aggregate and siliceous sand fine aggregate particles in concrete;

(d) Good bond between grout and concrete; and,

(e) Overall dense and well-consolidated nature of grout and concrete.

Thin section is approximately 30 microns (0.03 mm) in thickness and transparent to polarized-light.

Core 2 Fluorescent Dye-Mixed Epoxy-Impregnated Thin Section Showing Air-Entrained Grout & Non-Ai-Entrained Concrete

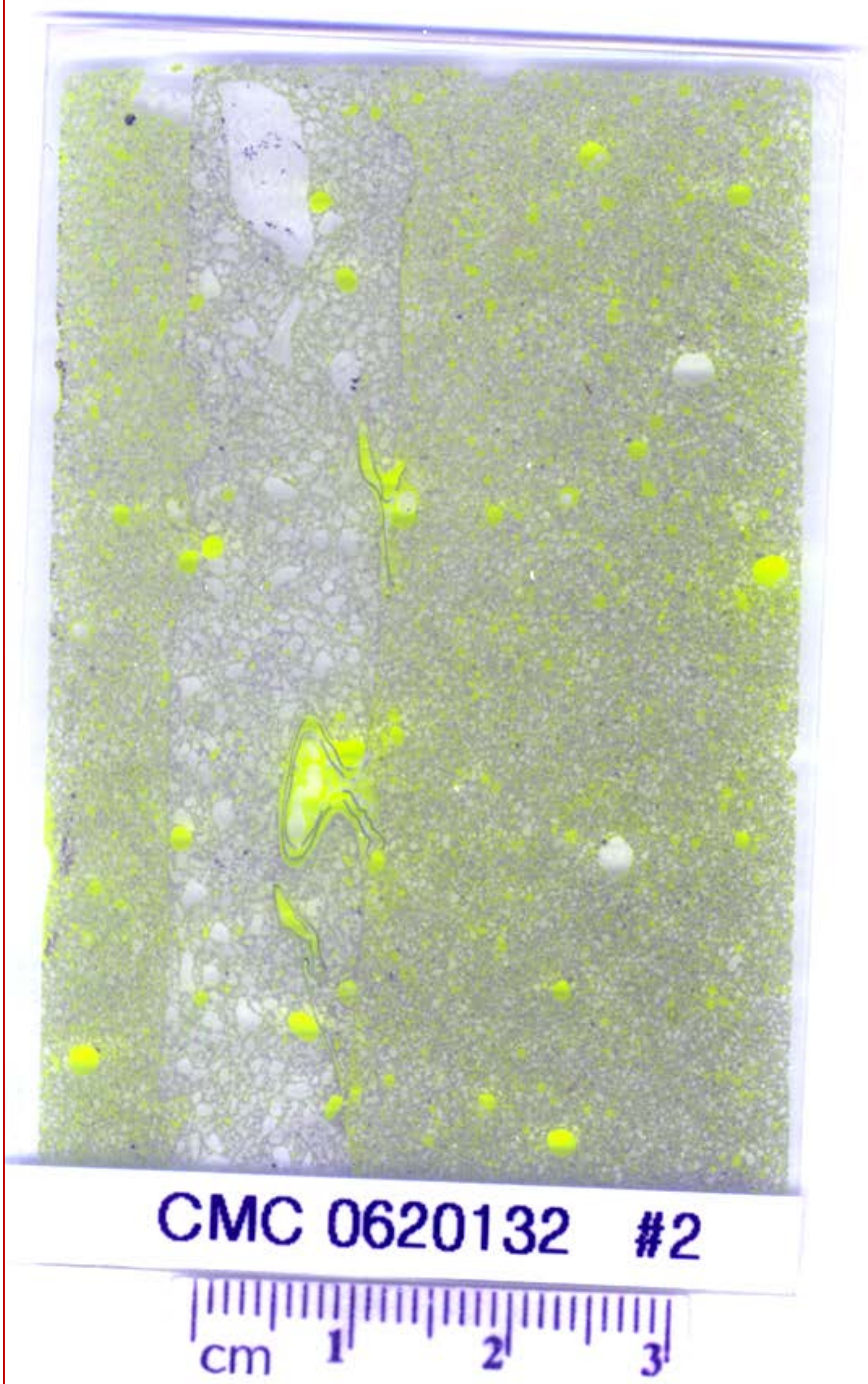

Figure 29: Fluorescent dye-mixed epoxy-impregnated thin section of grout and concrete in Core 2 showing:

(a) Overall denser nature of grout relative to concrete;

(b) Excessively air-entrained nature of grout as opposed to non-air-entrained nature of concrete;

(c) Crushed granite coarse aggregate and siliceous sand fine aggregate particles in concrete;

(d) Good bond between grout and concrete; and,

(e) Overall dense and well-consolidated nature of grout and concrete.

Thin section is approximately 30 microns (0.03 mm) in thickness and transparent to polarized-light.

Figure 30: Fluorescent dye-mixed epoxy-impregnated thin section of grout and concrete in Core 3 showing:

(a) Overall denser nature of grout relative to concrete;

(b) Excessively air-entrained nature of grout as opposed to non-air-entrained nature of concrete;

(c) Crushed granite coarse aggregate and siliceous sand fine aggregate particles in concrete;

(d) Complete de-bonding of grout from concrete;

(e) Overall dense and well-consolidated nature of grout and concrete; and,

(f) A fine vertical shrinkage microcrack in grout from the exposed surface that extended to a depth of 20 mm.

Thin section is approximately 30 microns (0.03 mm) in thickness and transparent to polarized-light.

MICROGRAPHS OF THIN SECTIONS OF GROUTS

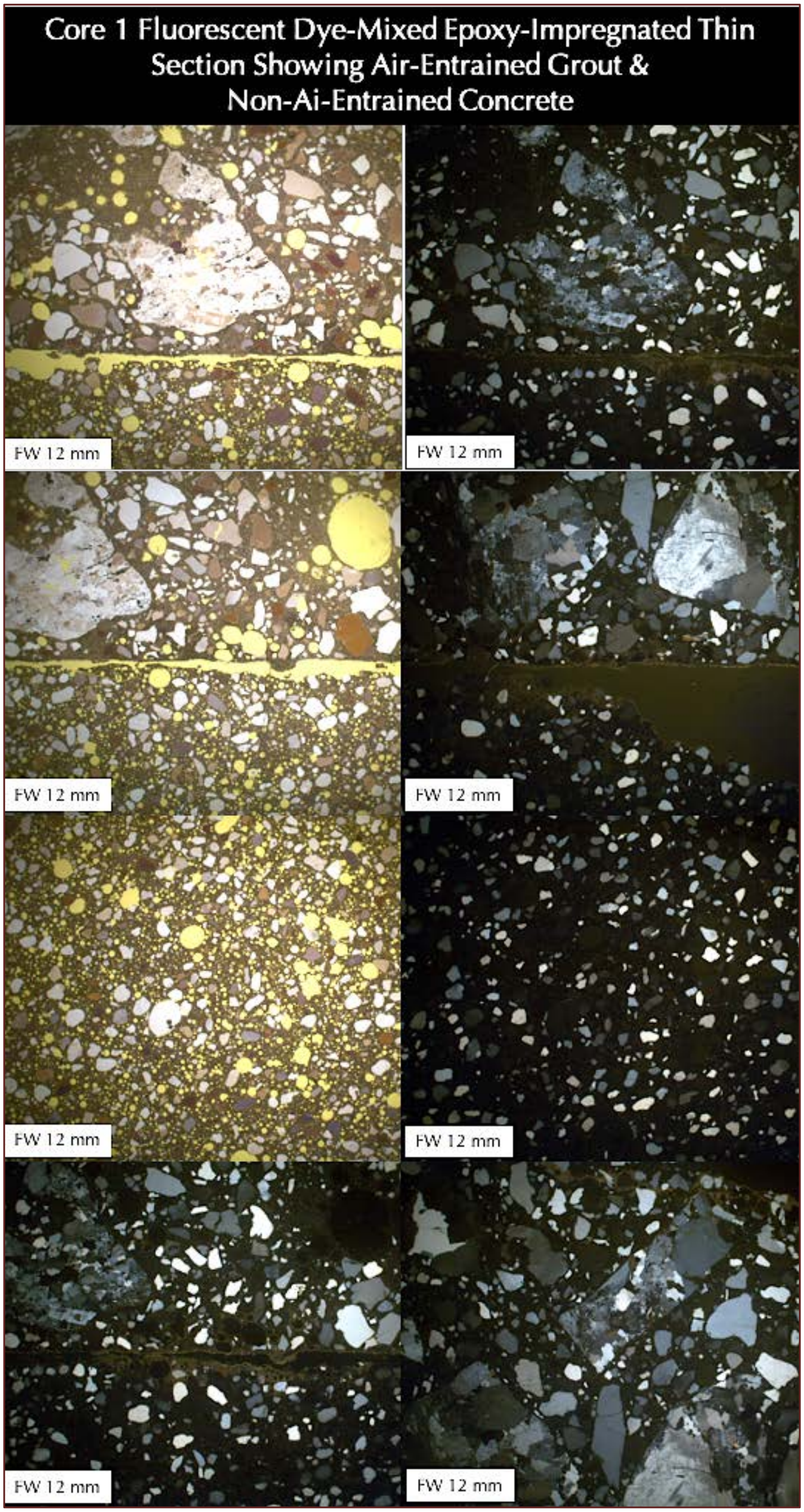

Figure 31: A mosaic of eight micrographs of thin section of Core 1 taken in plane and crossed-polarized light modes with an Olympus SZX12 stereozoom fluorescent-light microscope with attachments for polarized light showing:

(a) Excessively air-entrained nature of grout as opposed to non-air-entrained nature of concrete where air voids are highlighted by fluorescent epoxy; and,

(b) Size, shape, angularity, sphericity, grading, and, distribution of crushed silica sand particles in grout, crushed granite coarse aggregate particles in concrete, and natural siliceous sand (quartz-quartzite) particles in fine aggregate in concrete.

Photos were taken with a 2X objective to cover the maximum area and show distribution of air voids and aggregates in grout and concrete. Field width of each photo is 12 mm.

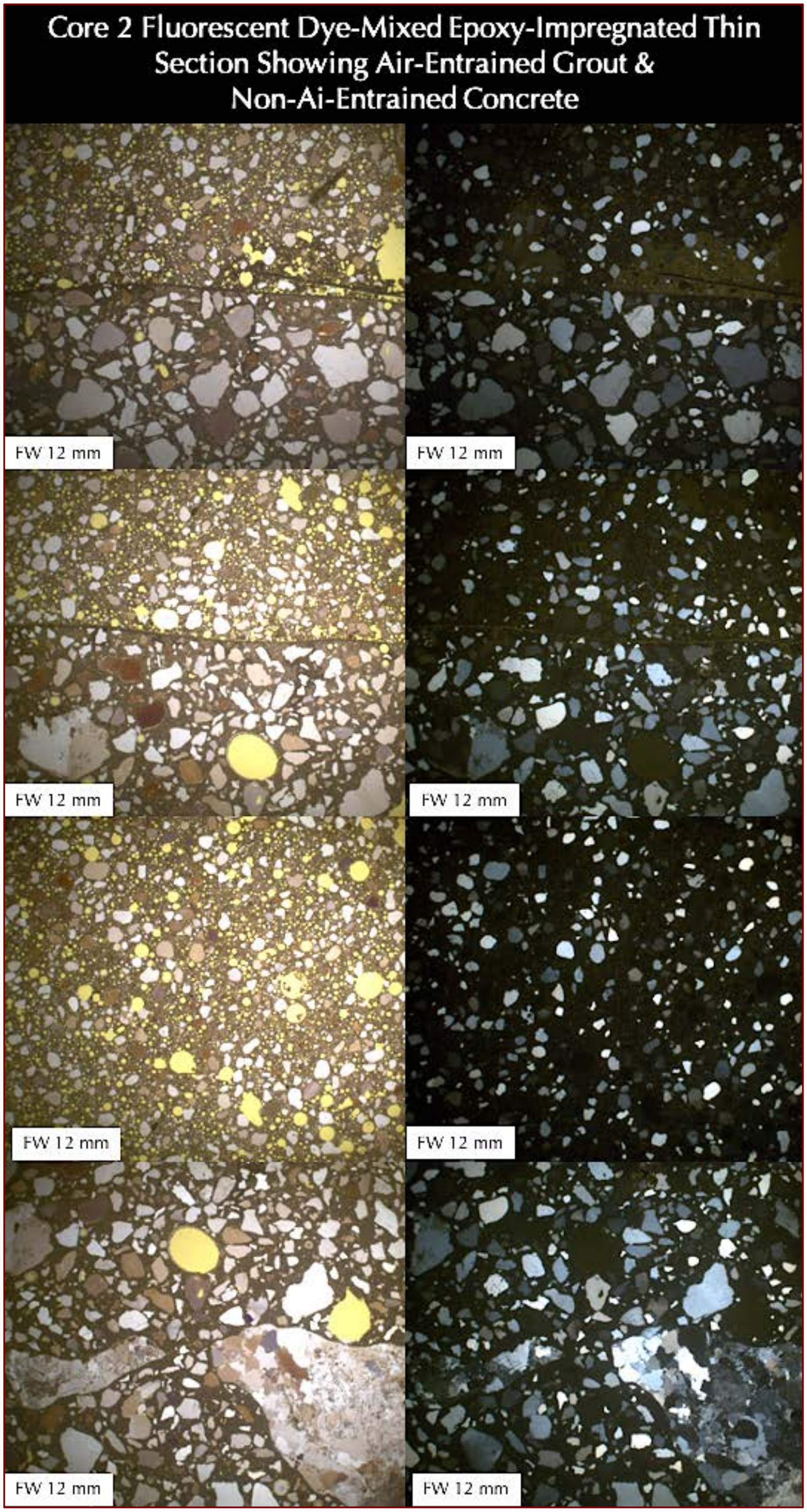

Figure 32: A mosaic of eight micrographs of thin section of Core 2 taken in plane and crossed-polarized light modes with an Olympus SZX12 stereozoom fluorescent-light microscope with attachments for polarized light showing:

(a) Excessively air-entrained nature of grout as opposed to non-air-entrained nature of concrete where air voids are highlighted by fluorescent epoxy; and,

(b) Size, shape, angularity, sphericity, grading, and, distribution of crushed silica sand particles in grout, crushed granite coarse aggregate particles in concrete, and natural siliceous sand (quartz-quartzite) particles in fine aggregate in concrete.

Photos were taken with a 2X objective to cover the maximum area and show distribution of air voids and aggregates in grout and concrete. Field width of each photo is 12 mm.

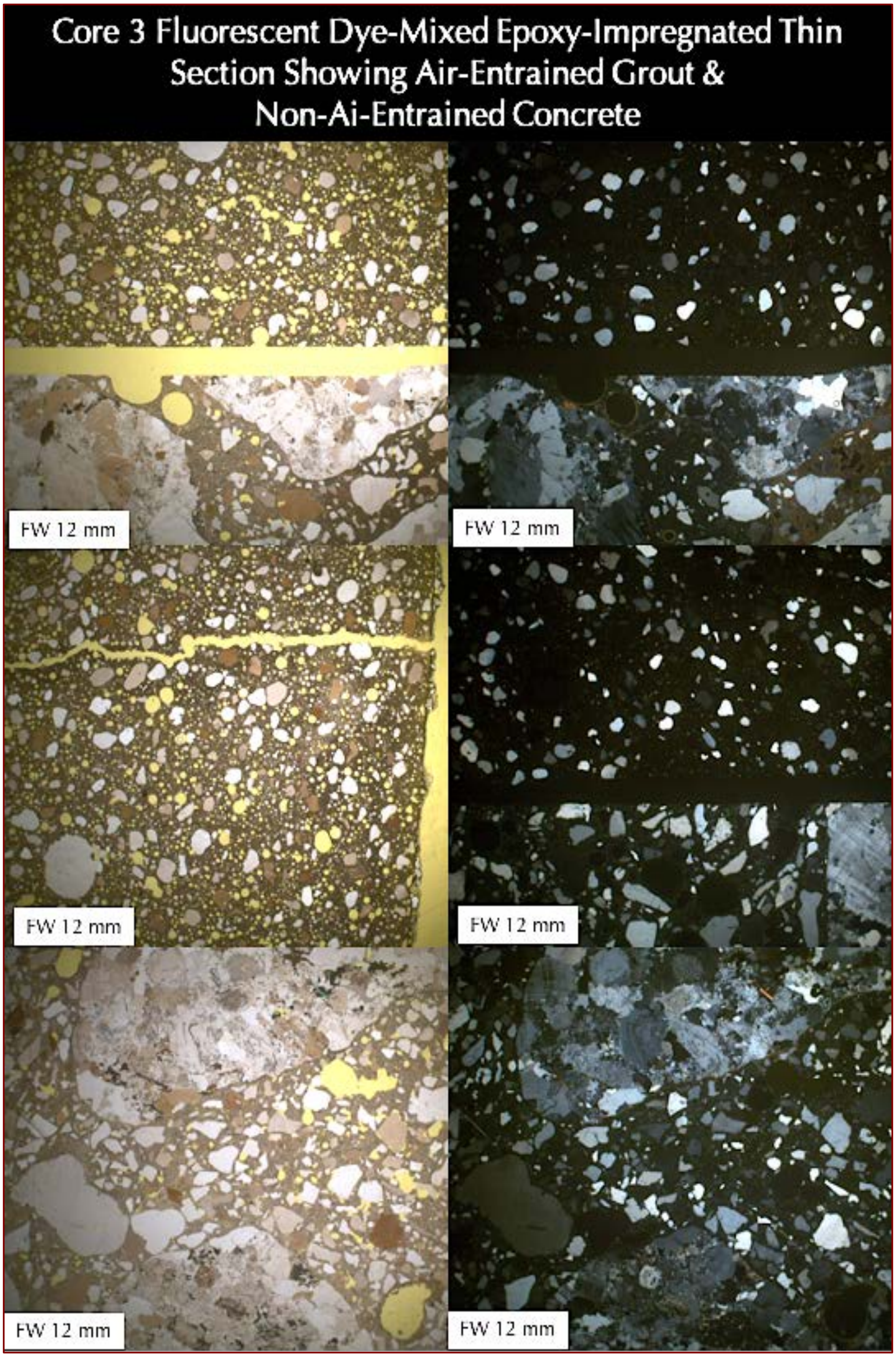

Figure 33: A mosaic of six micrographs of thin section of Core 3 taken in plane and crossed-polarized light modes with an Olympus SZX12 stereozoom fluorescent-light microscope with attachments for polarized light showing:

(a) Excessively air-entrained nature of grout as opposed to non-air-entrained nature of concrete where air voids are highlighted by fluorescent epoxy; and,

(b) Size, shape, angularity, sphericity, grading, and, distribution of crushed silica sand particles in grout, crushed granite coarse aggregate particles in concrete, and natural siliceous sand (quartz-quartzite) particles in fine aggregate in concrete.

Photos were taken with a 2X objective to cover the maximum area and show distribution of air voids and aggregates in grout and concrete. Field width of each photo is 12 mm.

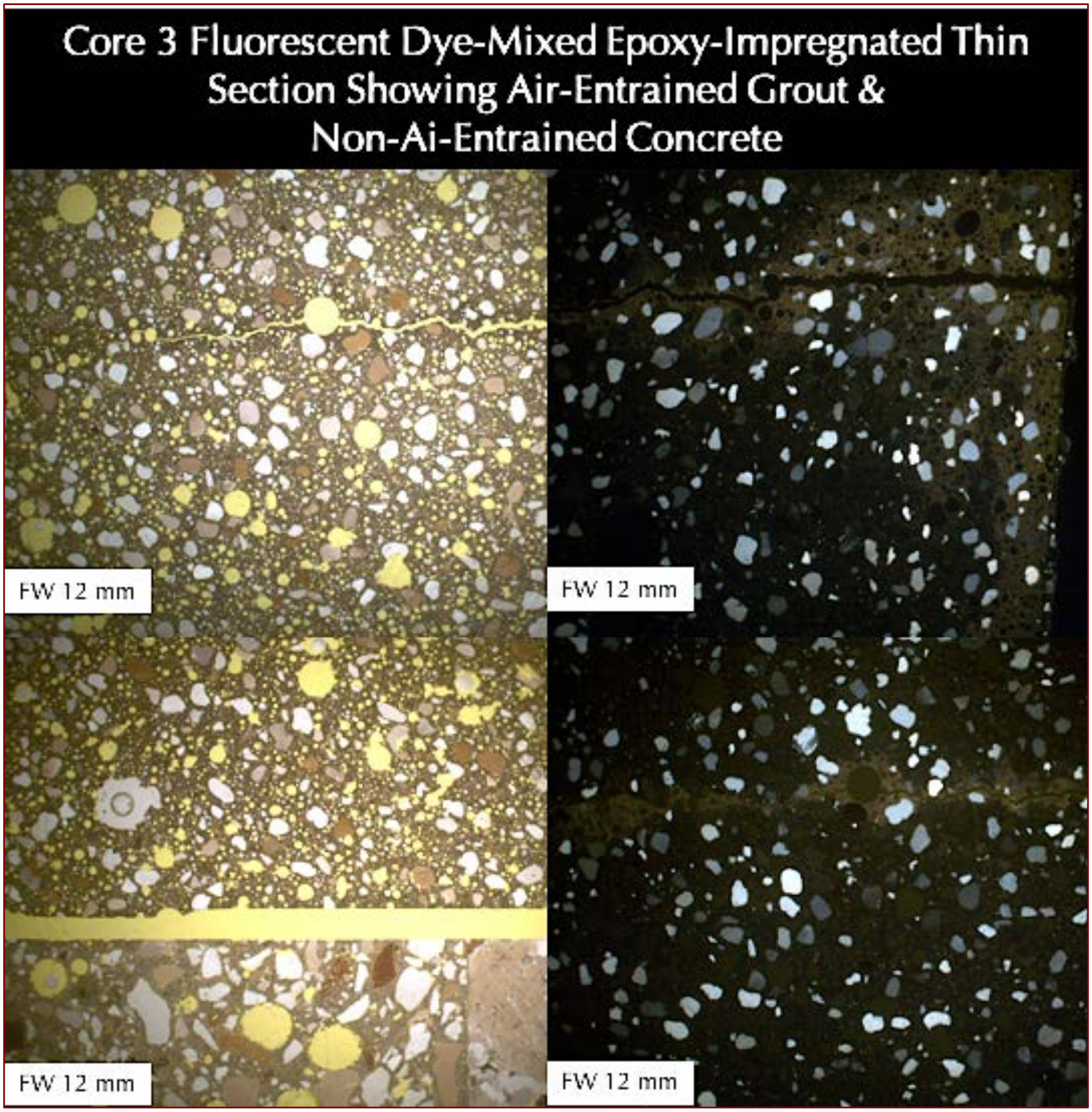

Figure 34: A mosaic of four micrographs of thin section of Core 3 taken in plane and crossed-polarized light modes with an Olympus SZX12 stereozoom fluorescent-light microscope with attachments for polarized light showing:

(a) Excessively air-entrained nature of grout as opposed to non-air-entrained nature of concrete where air voids are highlighted by fluorescent epoxy; and,

(b) Size, shape, angularity, sphericity, grading, and, distribution of crushed silica sand particles in grout, crushed granite coarse aggregate particles in concrete, and natural siliceous sand (quartz-quartzite) particles in fine aggregate in concrete.

Photos were taken with a 2X objective to cover the maximum area and show distribution of air voids and aggregates in grout and concrete. Field width of each photo is 12 mm.

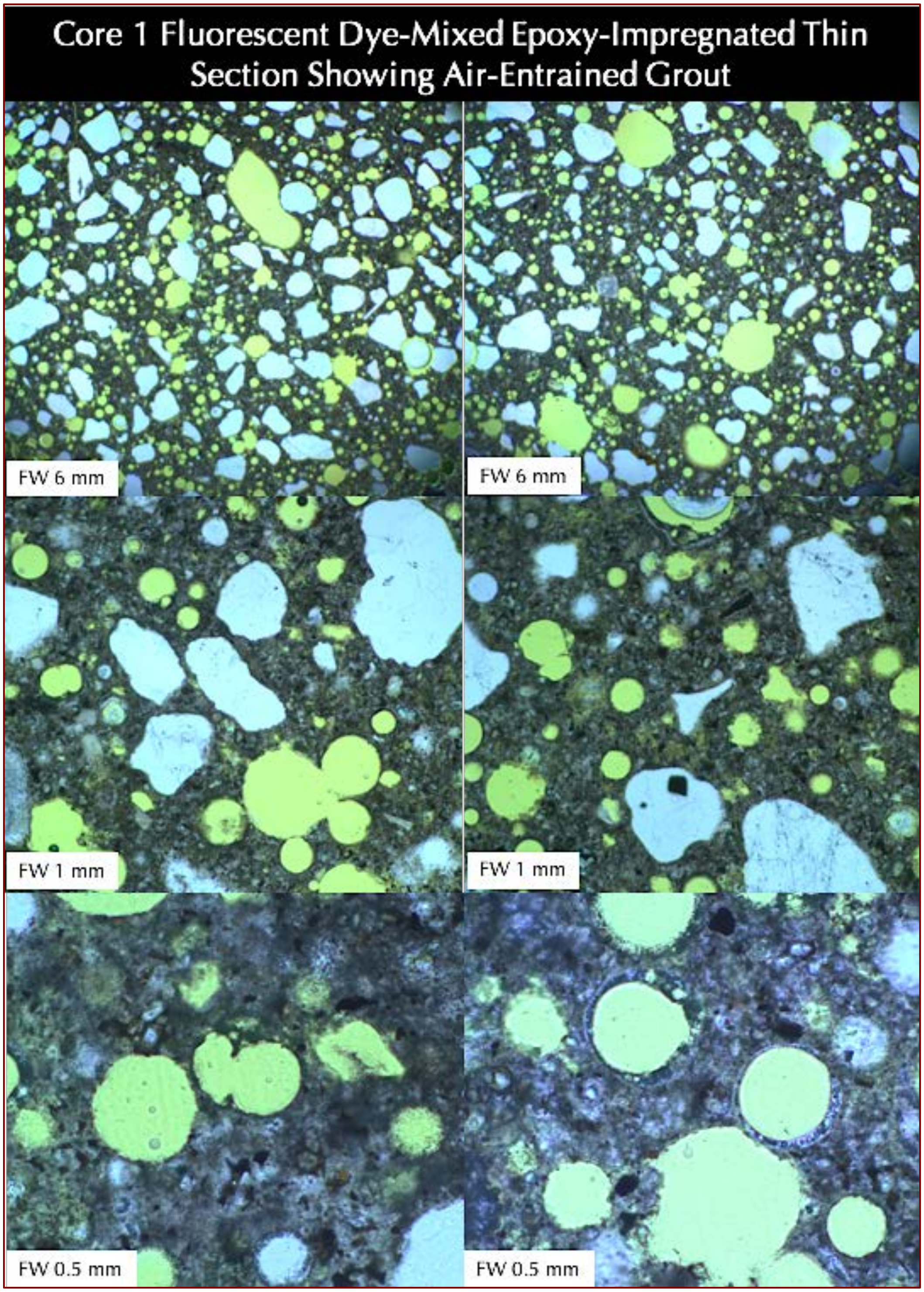

Figure 35: A mosaic of six micrographs of thin section of Core 1 taken in plane-polarized light mode with a Nikon Eclipse E600 fluorescent-light microscope with attachments for polarized light showing:

(a) Excessively air-entrained nature of grout where air voids are highlighted by fluorescent epoxy;
(b) Size, shape, angularity, gradation, and distirbution of lightly crushed quartz sand paticles in grout;
(c) Overall dense and well-conslidated nature of grout; and,
(d) Dense paste of grout having abundant residual Portland cement particles, cement hydration products, and potential addition of other pozzolanic and/or cementitious materials to create a dense paste microstructure which is relevant in the bottom two photos.

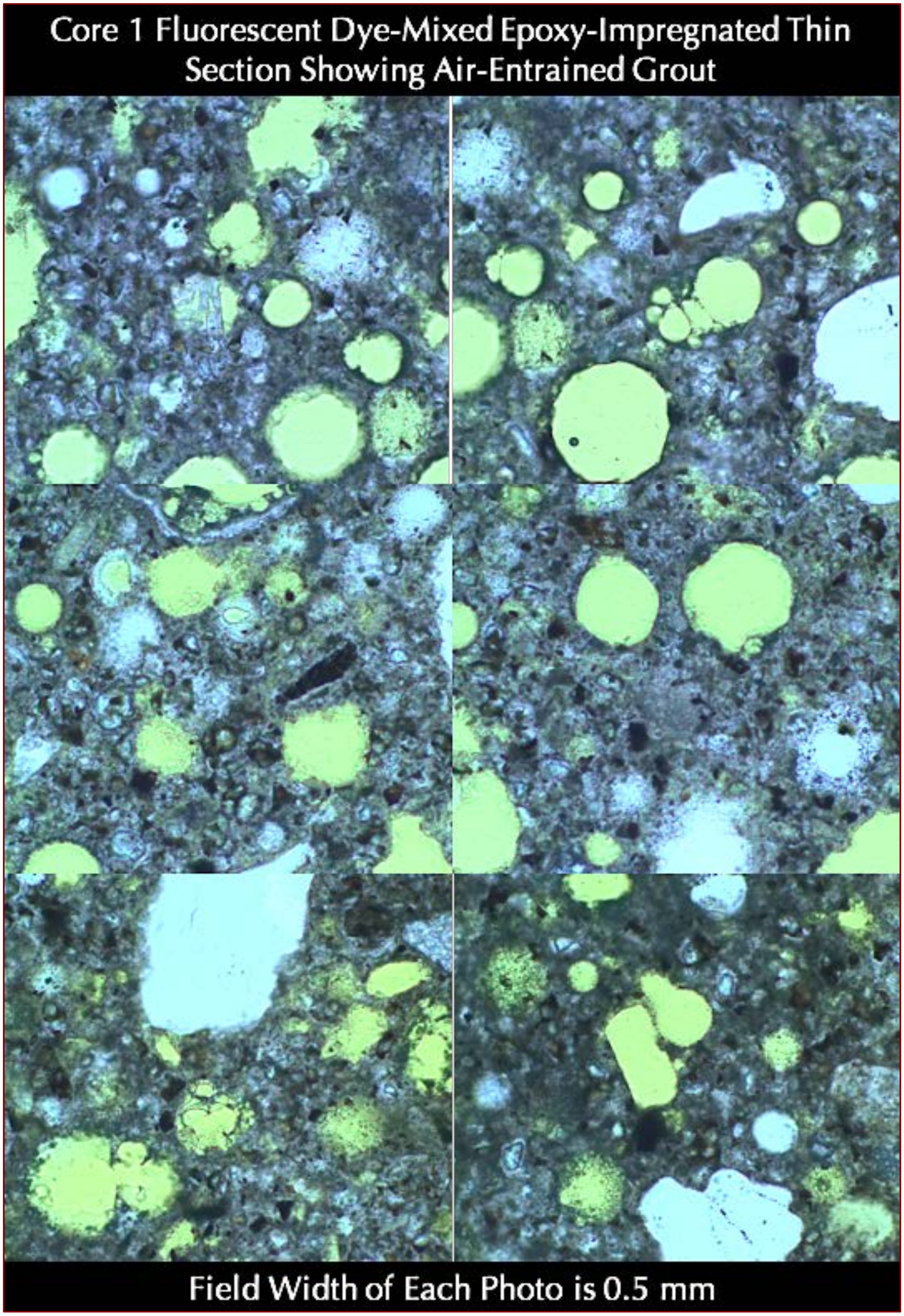

Figure 36: A mosaic of six micrographs of thin section of Core 1 taken in plane-polarized light mode with a Nikon Eclipse E600 fluorescent-light microscope with attachments for polarized light showing a dense paste of grout having abundant residual Portland cement particles, cement hydration products, and potential addition of other pozzolanic and/or cementitious materials to create a dense paste microstructure.

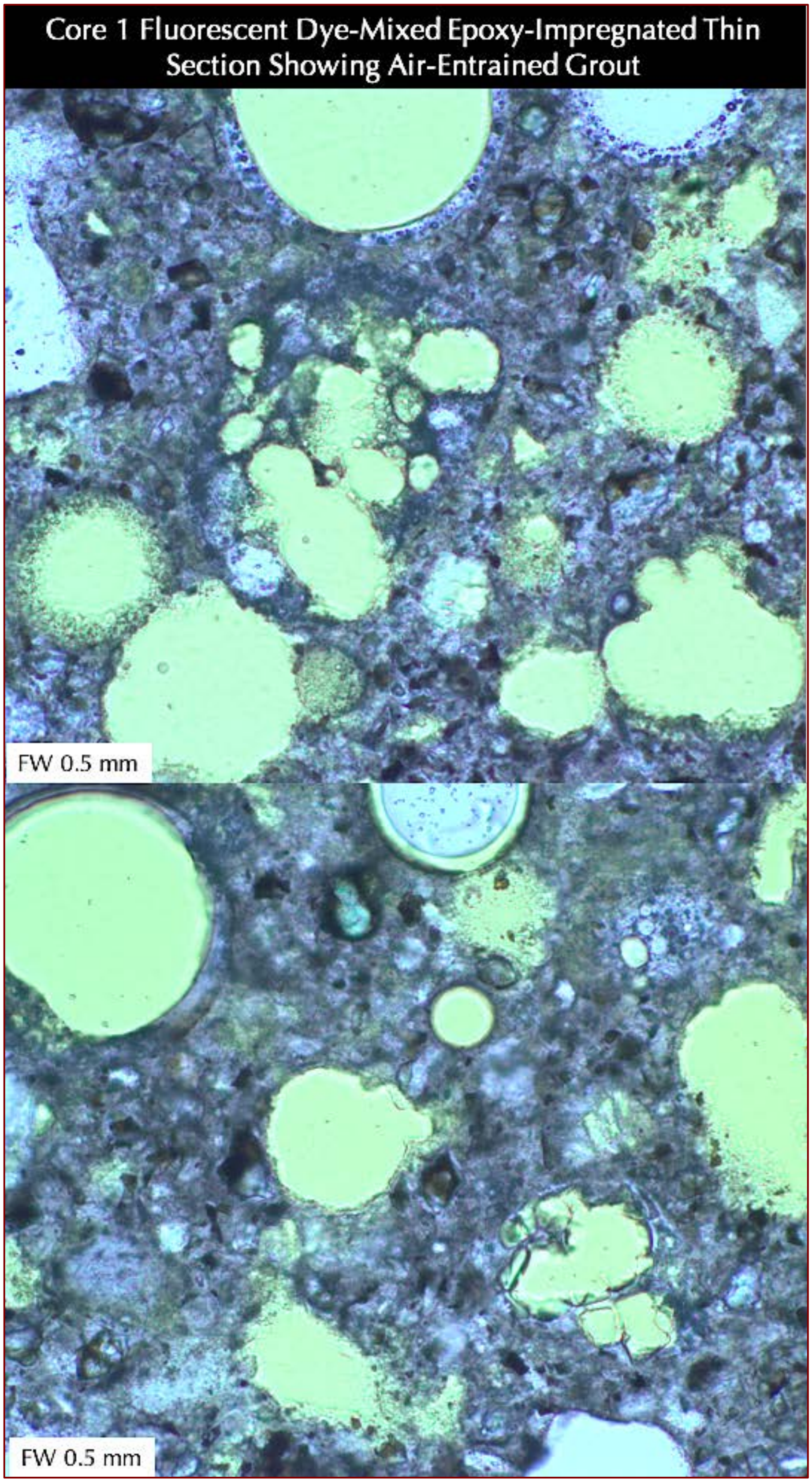

Figure 37: Two micrographs of thin section of Core 1 taken in plane-polarized light mode with a Nikon Eclipse E600 fluorescent-light microscope with attachments for polarized light showing a dense paste of grout having abundant residual Portland cement particles, cement hydration products, and potential addition of other pozzolanic and/or cementitious materials to create a dense paste microstructure.

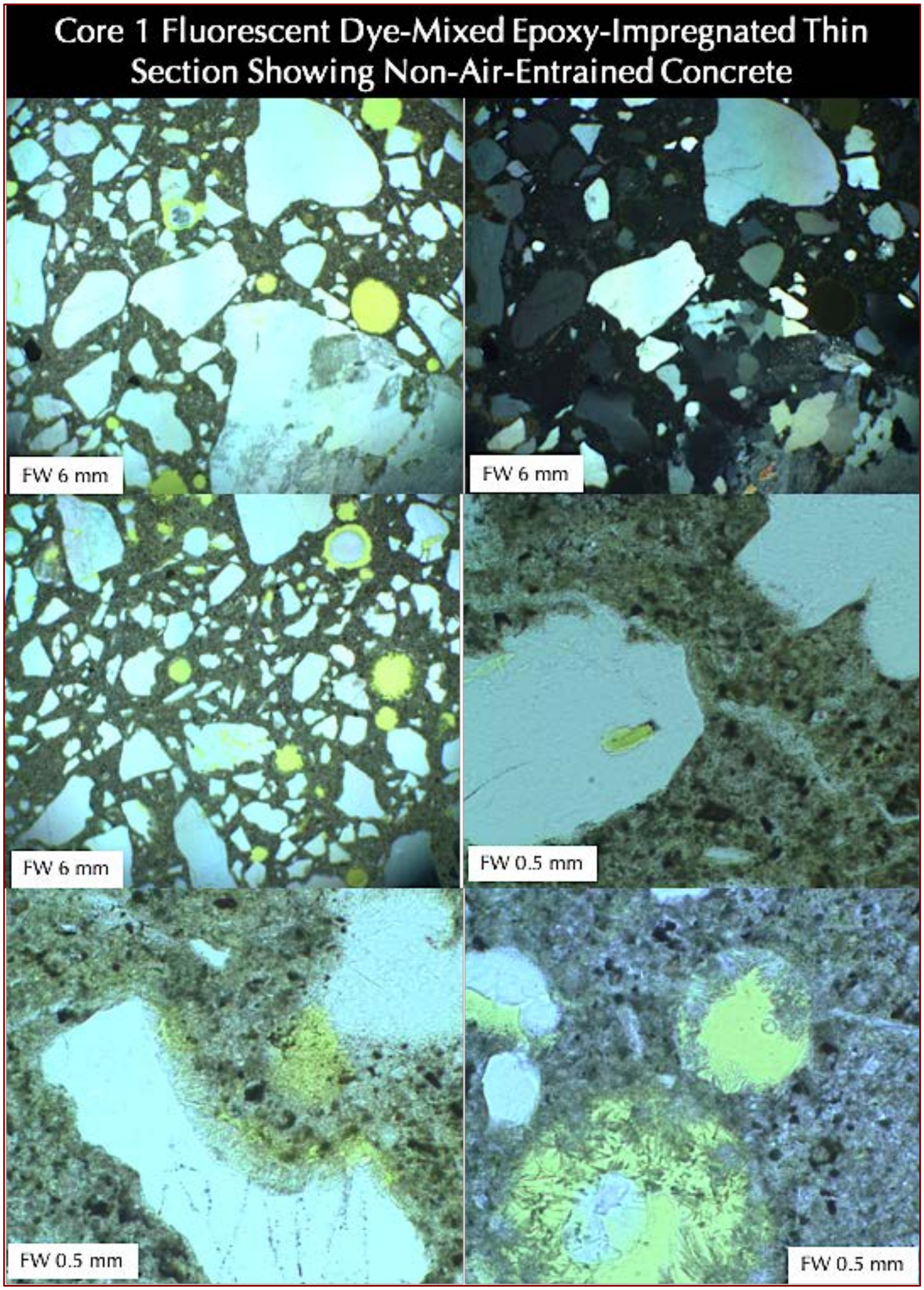

Figure 38: Micrographs of thin section of Core 1 taken in plane-polarized light mode with a Nikon Eclipse E600 fluorescent-light microscope with attachments for polarized light showing:

(a) Crushed granite coarse aggregate and crushed silica (quartz>quartzite) sand fine aggregate particles in concrete;

(b) A dense Portland cement paste of concrete having a few residual Portland cement particles, and cement hydration products;

(c) Non-air-entrained nature of concrete where a few near-spherical and irregular-shaped entrapped air voids are highlighted by fluorescent epoxy; and,

(d) Fine, acicular secondary ettringite deposits lining the walls of some air voids (bottom two photos) that are also seen in micrographs of lapped cross sections of concrete.

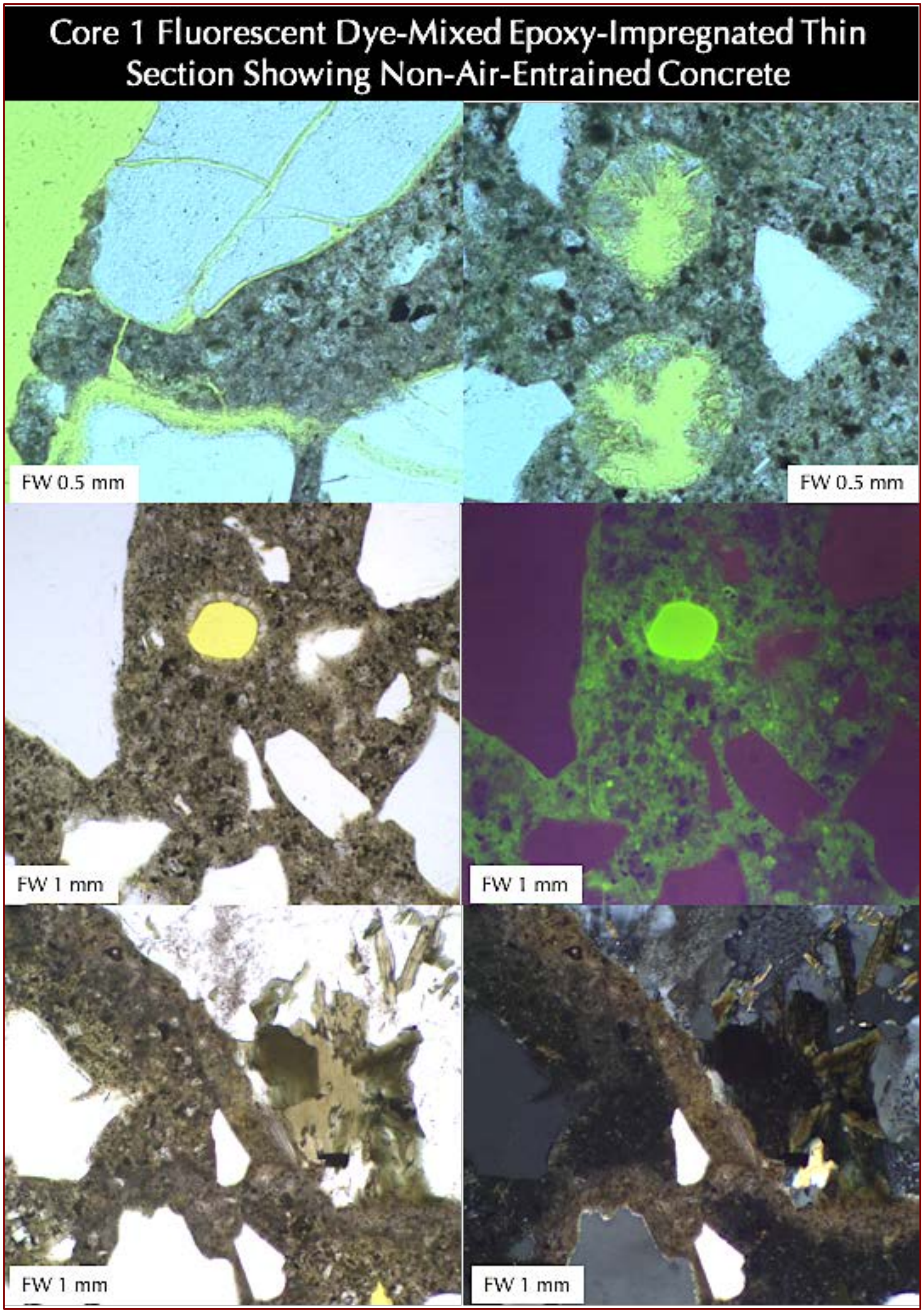

Figure 39: Micrographs of thin section of Core 1 taken in plane-polarized light mode with a Nikon Eclipse E600 fluorescent-light microscope with attachments for polarized light showing:

(a) Crushed granite coarse aggregate and crushed silica (quartz>quartzite) sand fine aggregate particles in concrete;

(b) A dense Portland cement paste of concrete having a few residual Portland cement particles, and cement hydration products;

(c) Non-air-entrained nature of concrete where a few near-spherical and irregular-shaped entrapped air voids are highlighted by fluorescent epoxy; and,

(d) Fine, acicular secondary ettringite deposits lining the walls of some air voids (top two photos) that are also seen in micrographs of lapped cross sections of concrete.

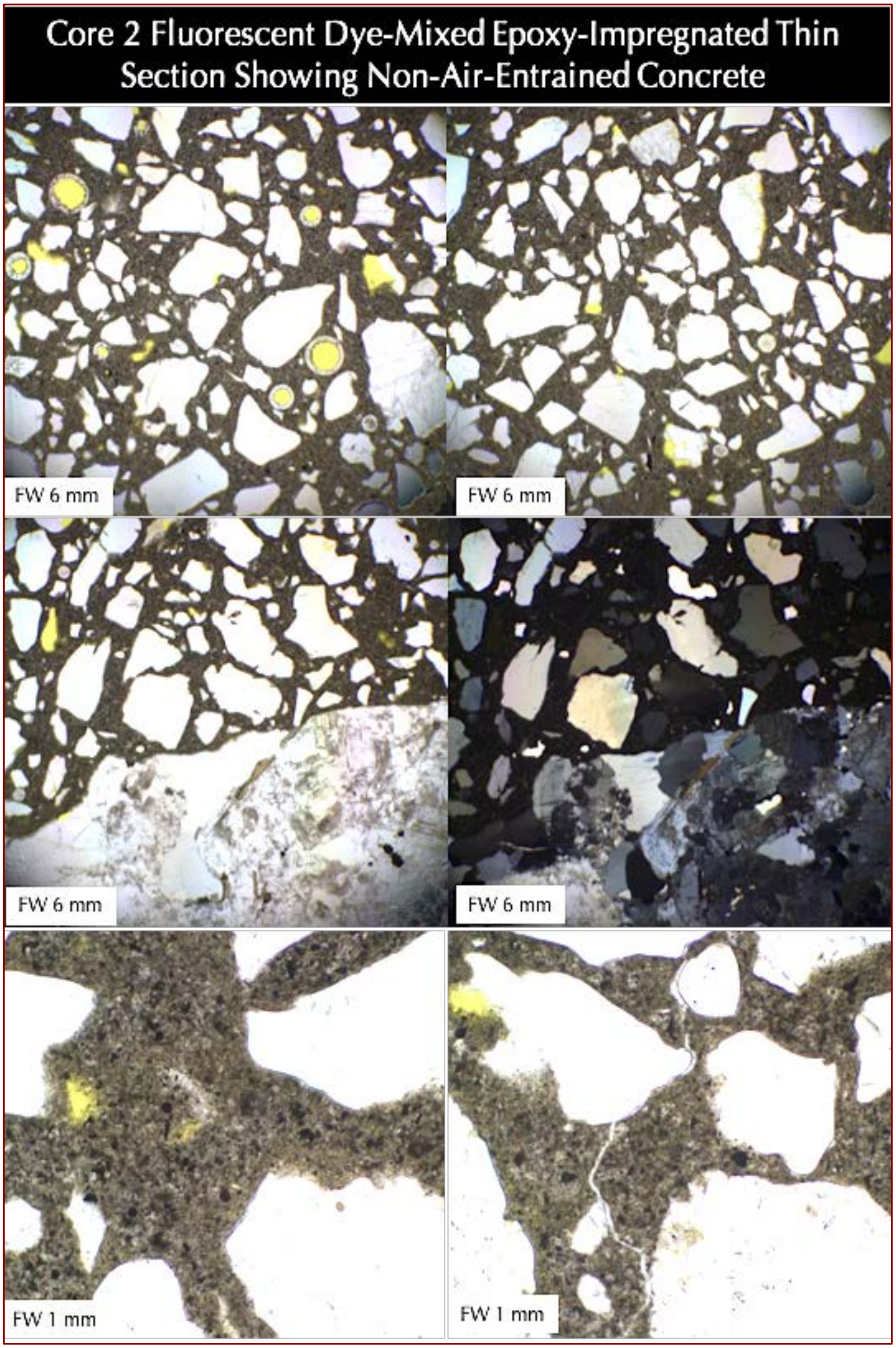

Figure 40: Micrographs of thin section of Core 2 taken in plane-polarized light mode with a Nikon Eclipse E600 fluorescent-light microscope with attachments for polarized light showing:

(a) Crushed granite coarse aggregate and crushed silica (quartz>quartzite) sand fine aggregate particles in concrete;

(b) A dense Portland cement paste of concrete having a few residual Portland cement particles, and cement hydration products;

(c) Non-air-entrained nature of concrete where a few near-spherical and irregular-shaped entrapped air voids are highlighted by fluorescent epoxy;

(d) Fine, acicular secondary ettringite deposits lining the walls of some air voids that are also seen in micrographs of lapped cross sections of concrete; and,

(e) A few fine hair-line shrinkage microcracks in the paste fraction of concrete (bottom right photo).

Core 2 Fluorescent Dye-Mixed Epoxy-Impregnated Thin Section Showing Non-Air-Entrained Concrete

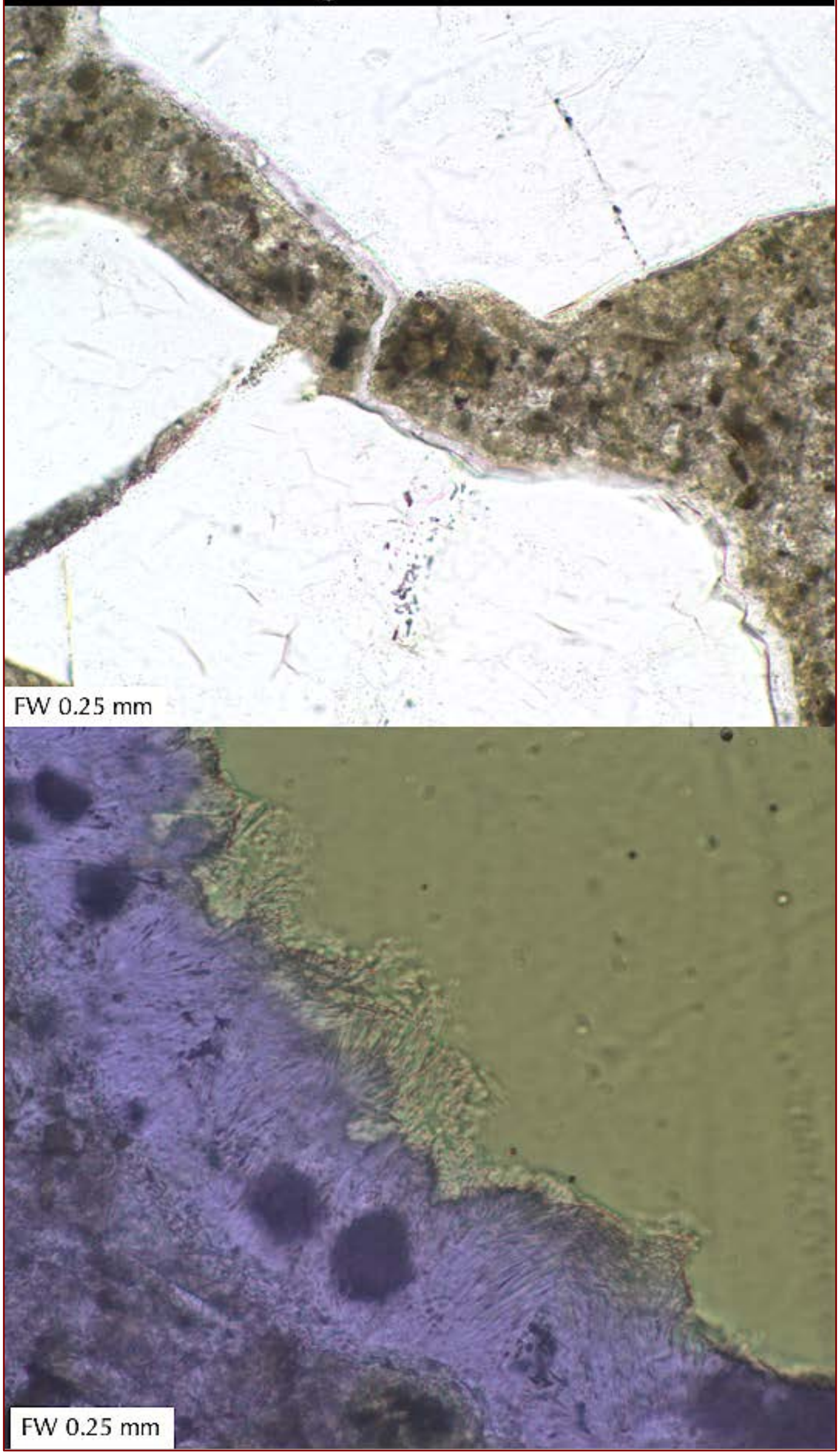

Figure 41: Micrographs of thin section of Core 2 taken in plane-polarized light mode with a Nikon Eclipse E600 fluorescent-light microscope with attachments for polarized light showing:

(a) A dense Portland cement paste of concrete having a few residual Portland cement particles, and cement hydration products; and,

(b) Fine, acicular secondary ettringite deposits lining the walls of a crack (bottom photo) that are also seen in micrographs of lapped cross sections of concrete.

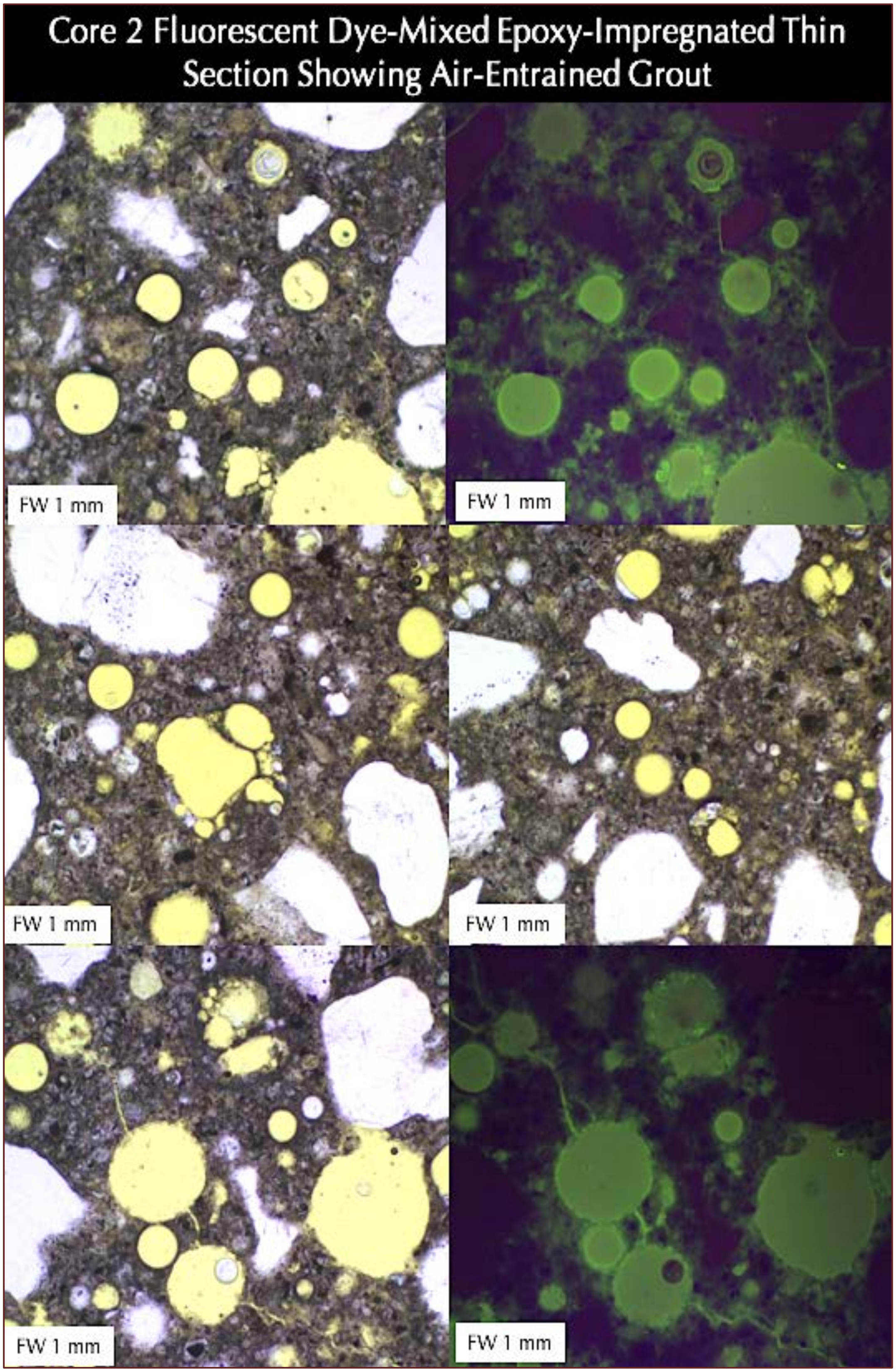

Figure 42: Micrographs of thin section of Core 2 taken in plane-polarized light mode with a Nikon Eclipse E600 fluorescent-light microscope with attachments for polarized light showing:

(a) Excessively air-entrained nature of grout where air voids are highlighted by fluorescent epoxy;

(b) Size, shape, angularity, gradation, and distribution of lightly crushed quartz sand particles in grout;

(c) Overall dense and well-consolidated nature of grout; and,

(d) Dense paste of grout having abundant residual Portland cement particles, cement hydration products, and potential addition of other pozzolanic and/or cementitious materials to create a dense paste microstructure.

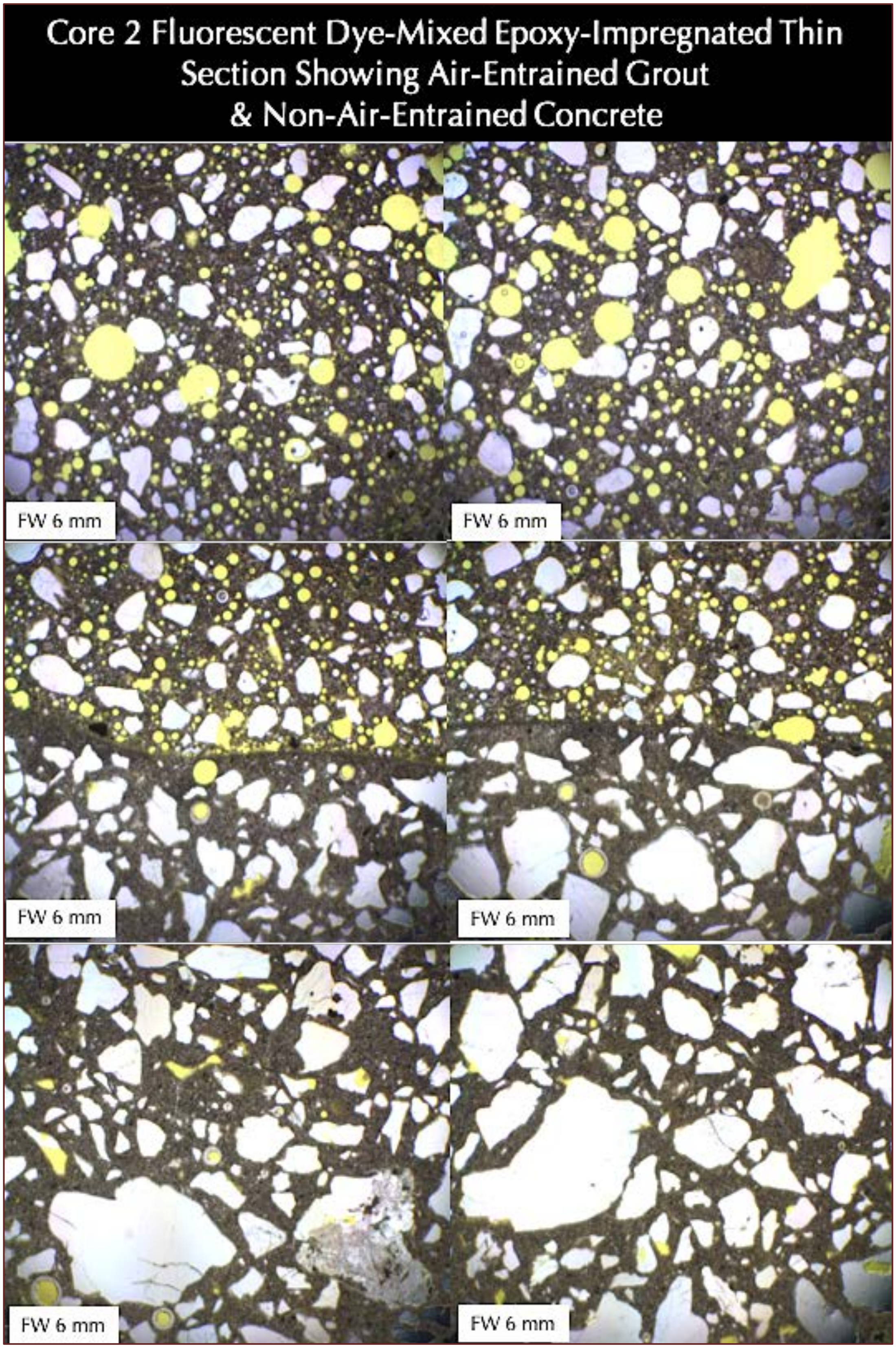

Figure 43: Micrographs of thin section of Core 2 taken in plane polarized light mode with a Nikon Eclipse E600 fluorescent-light microscope showing:

(a) Excessively air-entrained nature of grout as opposed to non-air-entrained nature of concrete where air voids are highlighted by fluorescent epoxy; and,

(b) Size, shape, angularity, sphericity, grading, and, distribution of crushed silica sand particles in grout, crushed granite coarse aggregate particles in concrete, and crushed and natural siliceous sand (quartz-quartzite) particles in fine aggregate in concrete.

Photos were taken with a 2X objective to cover the maximum area and show distribution of air voids and aggregates in grout and concrete. Field width of each photo is 6 mm.

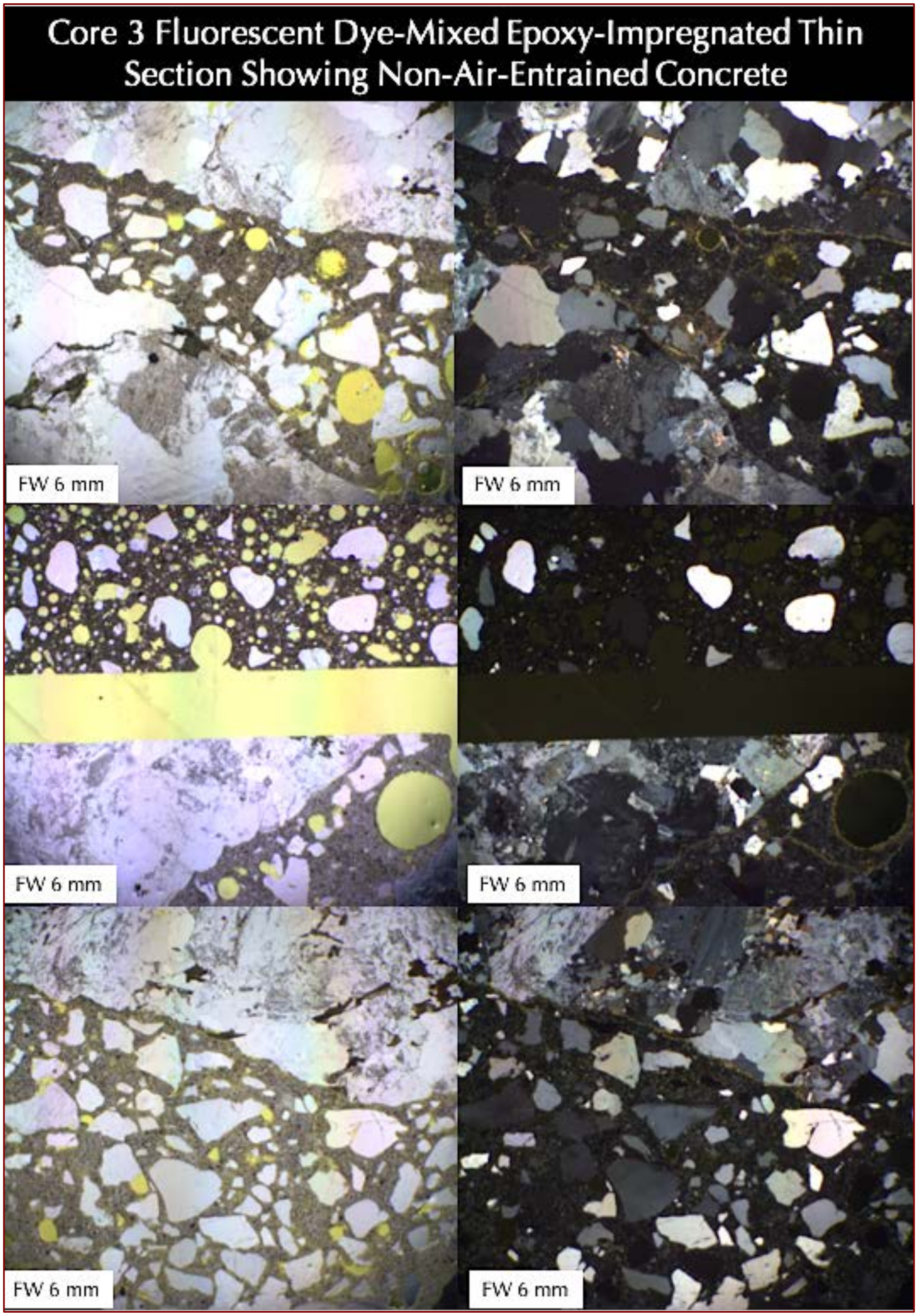

Figure 44: Micrographs of thin section of Core 3 taken in plane polarized light mode with a Nikon Eclipse E600 fluorescent-light microscope with attachments for polarized light showing:

(a) Crushed granite coarse aggregate and crushed silica (quartz>quartzite) sand fine aggregate particles in concrete;

(b) A dense Portland cement paste of concrete having a few residual Portland cement particles, and cement hydration products; and,

(c) Non-air-entrained nature of concrete where a few near-spherical and irregular-shaped entrapped air voids are highlighted by fluorescent epoxy.

Photos were taken with a 2X objective to cover the maximum area and show distribution of air voids and aggregates in grout and concrete. Field width of each photo is 6 mm.

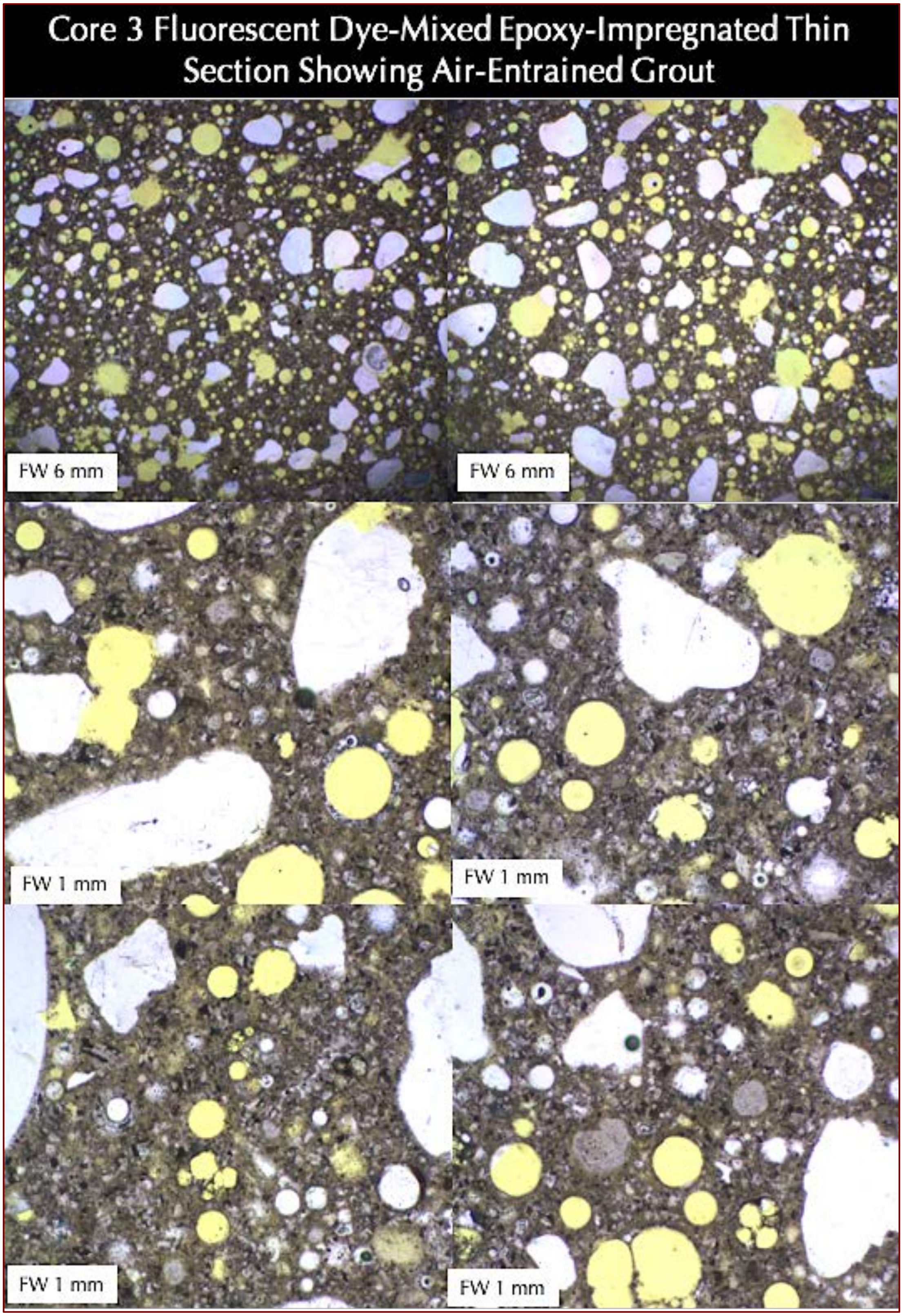

Figure 45: Micrographs of thin section of Core 3 taken in plane-polarized light mode with a Nikon Eclipse E600 fluorescent-light microscope with attachments for polarized light showing:

(a) Excessively air-entrained nature of grout where air voids are highlighted by fluorescent epoxy;

(b) Size, shape, angularity, gradation, and distribution of lightly crushed quartz sand particles in grout;

(c) Overall dense and well-consolidated nature of grout; and,

(d) Dense paste of grout having abundant residual Portland cement particles, cement hydration products, and potential addition of other pozzolanic and/or cementitious materials to create a dense paste microstructure.

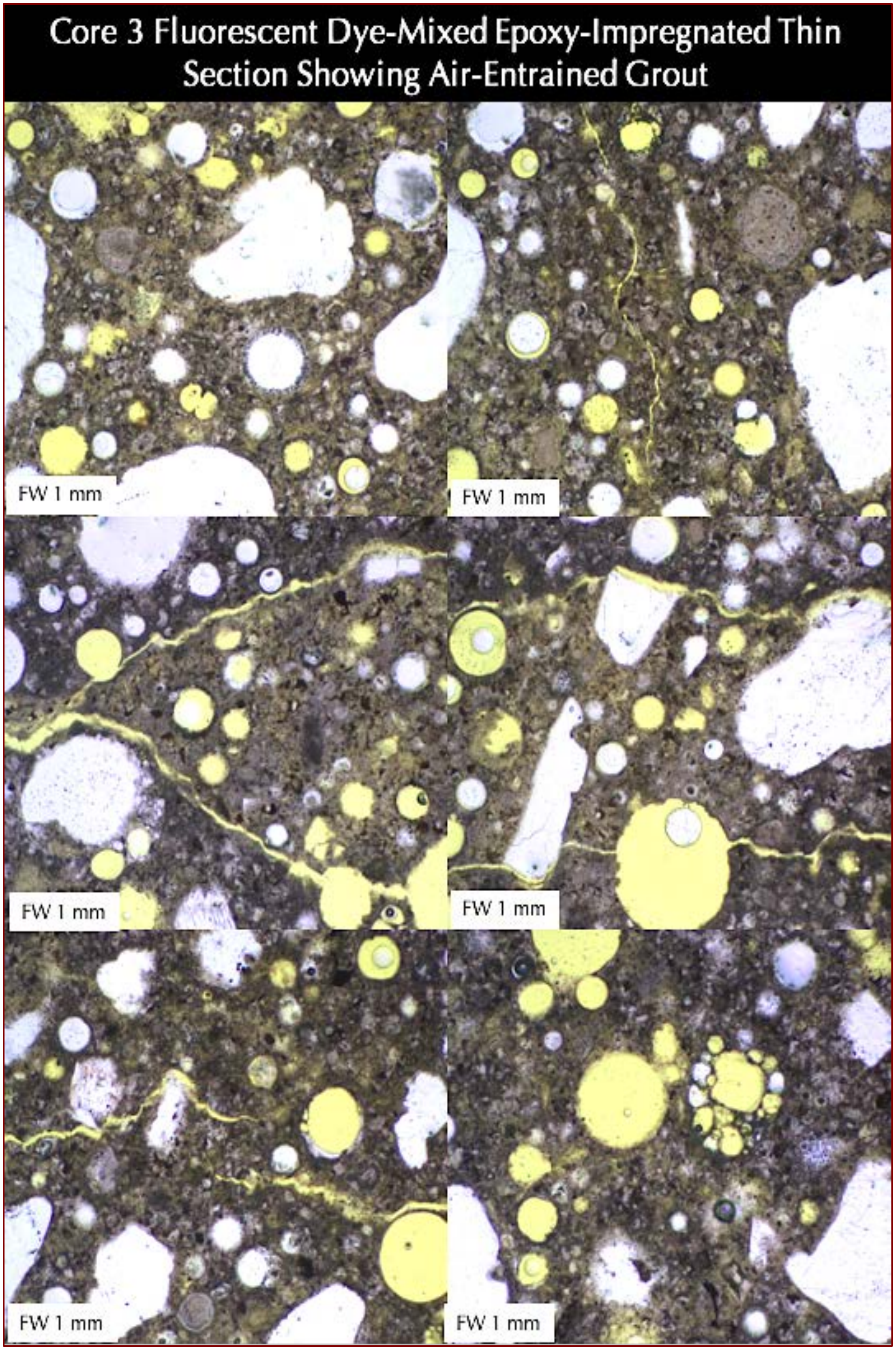

Figure 46: Micrographs of thin section of Core 3 taken in plane-polarized light mode with a Nikon Eclipse E600 fluorescent-light microscope with attachments for polarized light showing:

(a) Excessively air-entrained nature of grout where air voids are highlighted by fluorescent epoxy;

(b) Size, shape, angularity, gradation, and distribution of lightly crushed quartz sand particles in grout;

(c) Overall dense and well-consolidated nature of grout; and,

(d) Dense paste of grout having abundant residual Portland cement particles, cement hydration products, and potential addition of other pozzolanic and/or cementitious materials to create a dense paste microstructure.

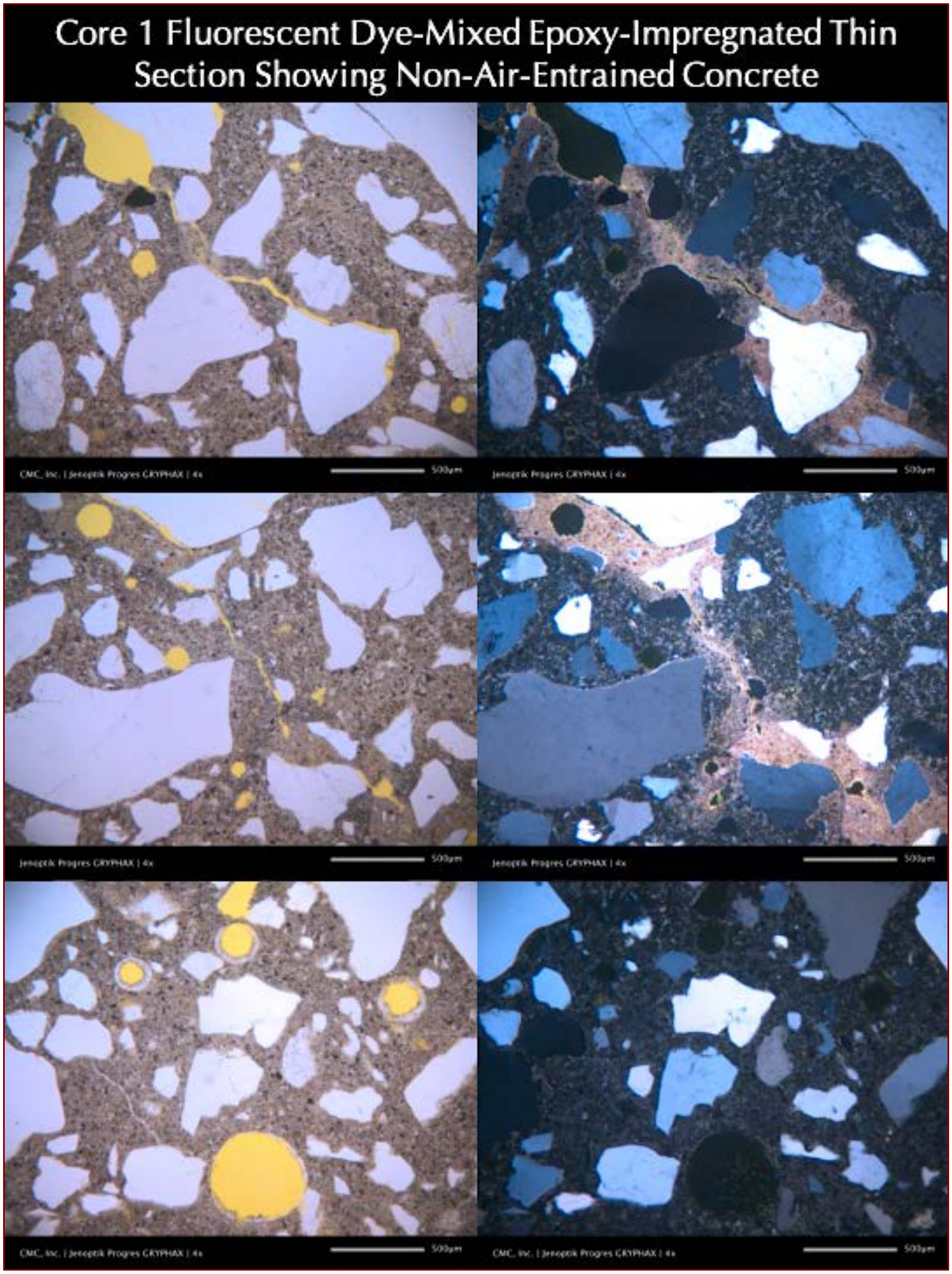

Figure 47: Micrographs of thin section of concrete portion of Core 1 taken with a Nikon Eclipse E600 POL petrographic microscope in plane (left column) and crossed (right column) polarized light modes showing: (a) crushed silica sand fine aggregate particles, (b) a dense Portland cement paste having a few residual Portland cement particles in cement hydration products, (c) a few entrapped air voids highlighted by fluorescent epoxy; (d) fine acicular secondary ettringite deposits lining walls of some air voids; and (d) shrinkage microcrack in paste and carbonation of paste along the walls of microcrack (top and bottom right photos).

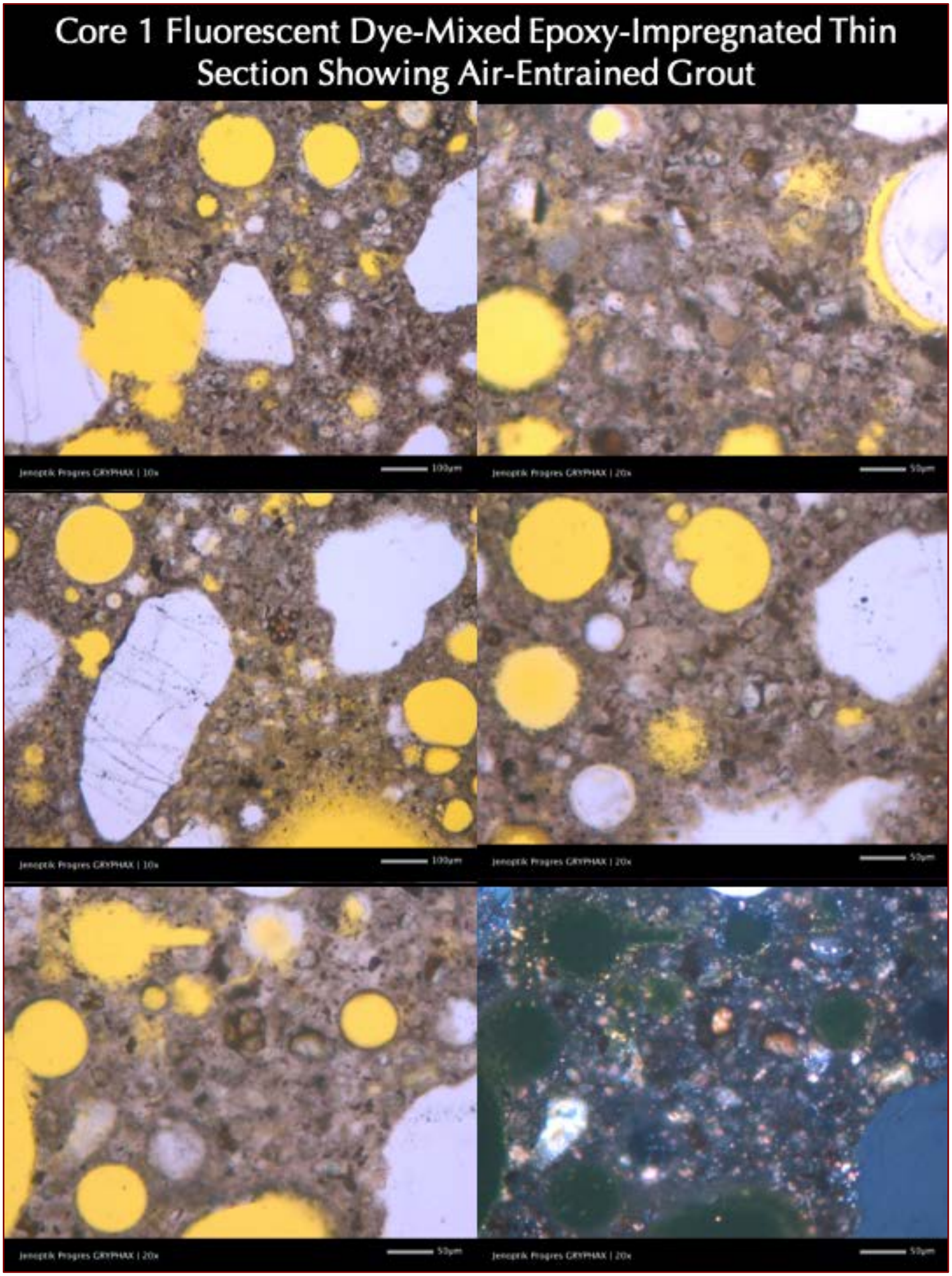

Figure 48: Micrographs of thin section of grout portion of Core 1 taken with a Nikon Eclipse E600 POL petrographic microscope in plane and crossed (bottom right photo) polarized light modes showing: (a) lightly crushed silica sand fine aggregate particles, (b) a dense paste having abundant residual Portland cement particles and evidence of addition of some other pozzolanic and cementitious materials distributed in cement hydration products, and (c) spherical entrained air voids highlighted by fluorescent epoxy.

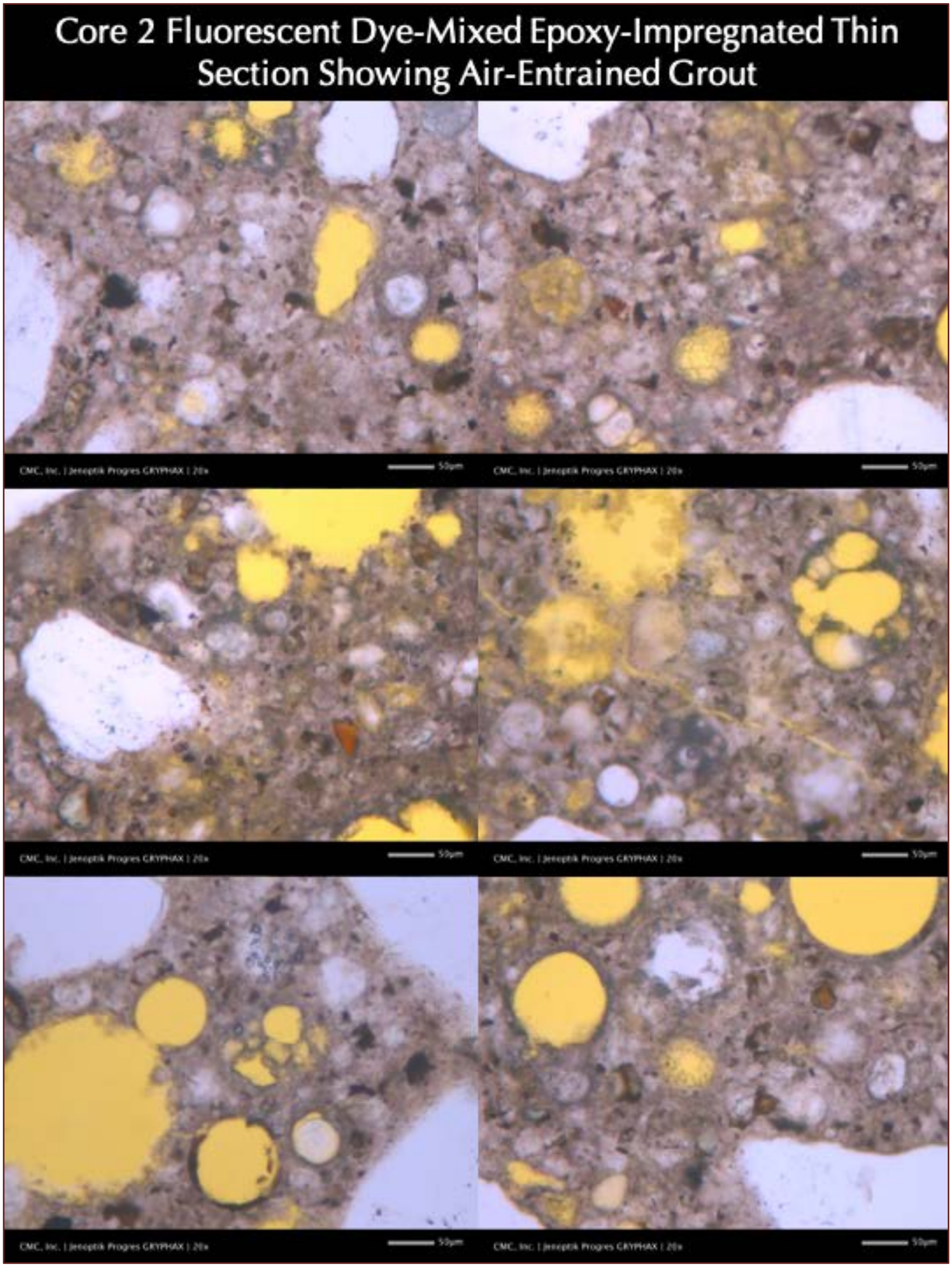

Figure 49: Micrographs of thin section of grout portion of Core 2 taken with a Nikon Eclipse E600 POL petrographic microscope in plane polarized light mode showing: (a) lightly crushed silica sand fine aggregate particles, (b) a dense paste having abundant residual Portland cement particles and evidence of addition of some other pozzolanic and cementitious materials distributed in cement hydration products, and (c) spherical entrained air voids highlighted by fluorescent epoxy.

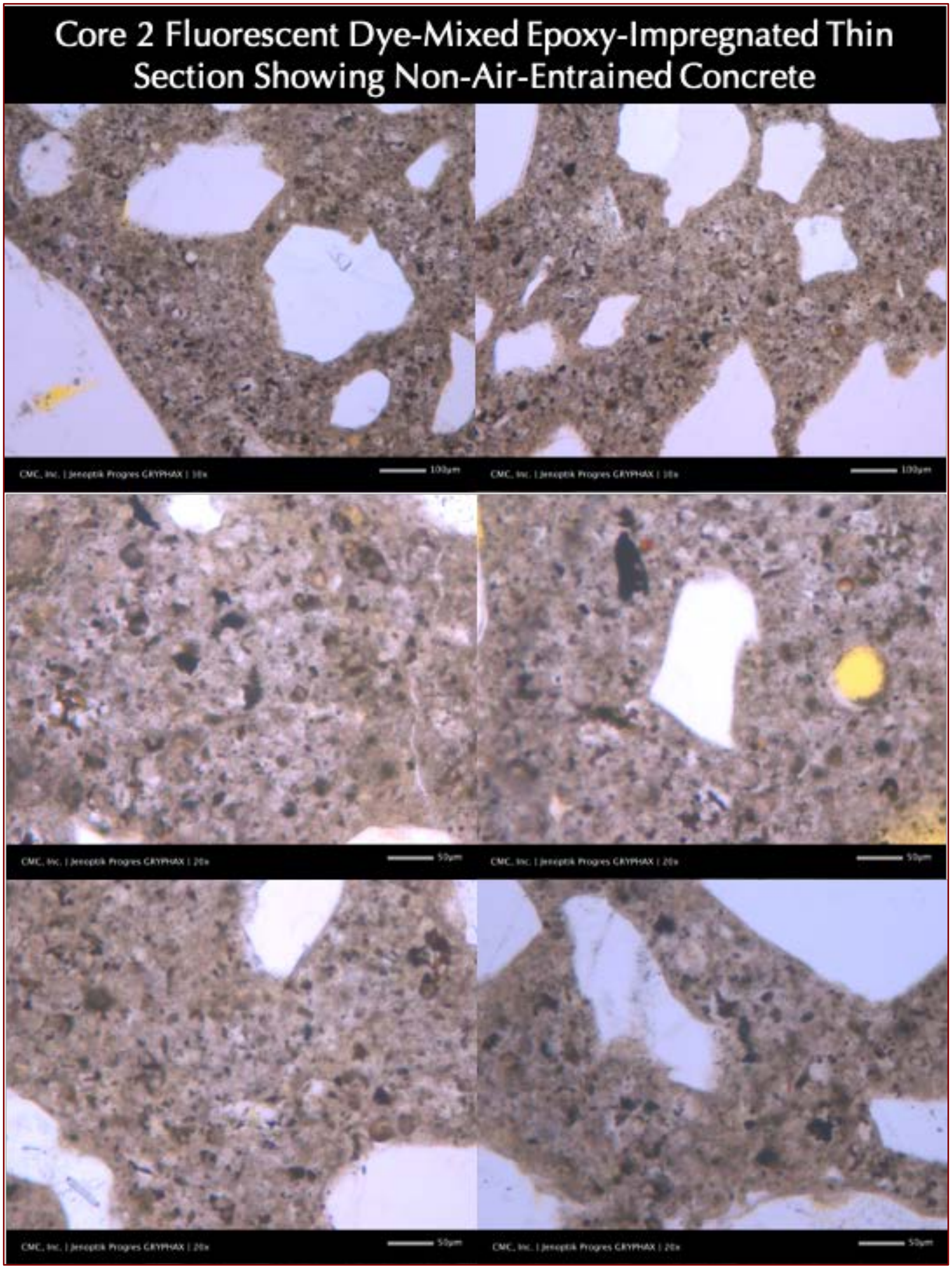

Figure 50: Micrographs of thin section of concrete portion of Core 2 taken with a Nikon Eclipse E600 POL petrographic microscope in plane polarized light mode showing: (a) crushed silica sand fine aggregate particles, (b) a dense Portland cement paste having a few residual Portland cement particles in cement hydration products, and (c) a few entrapped air voids highlighted by fluorescent epoxy.

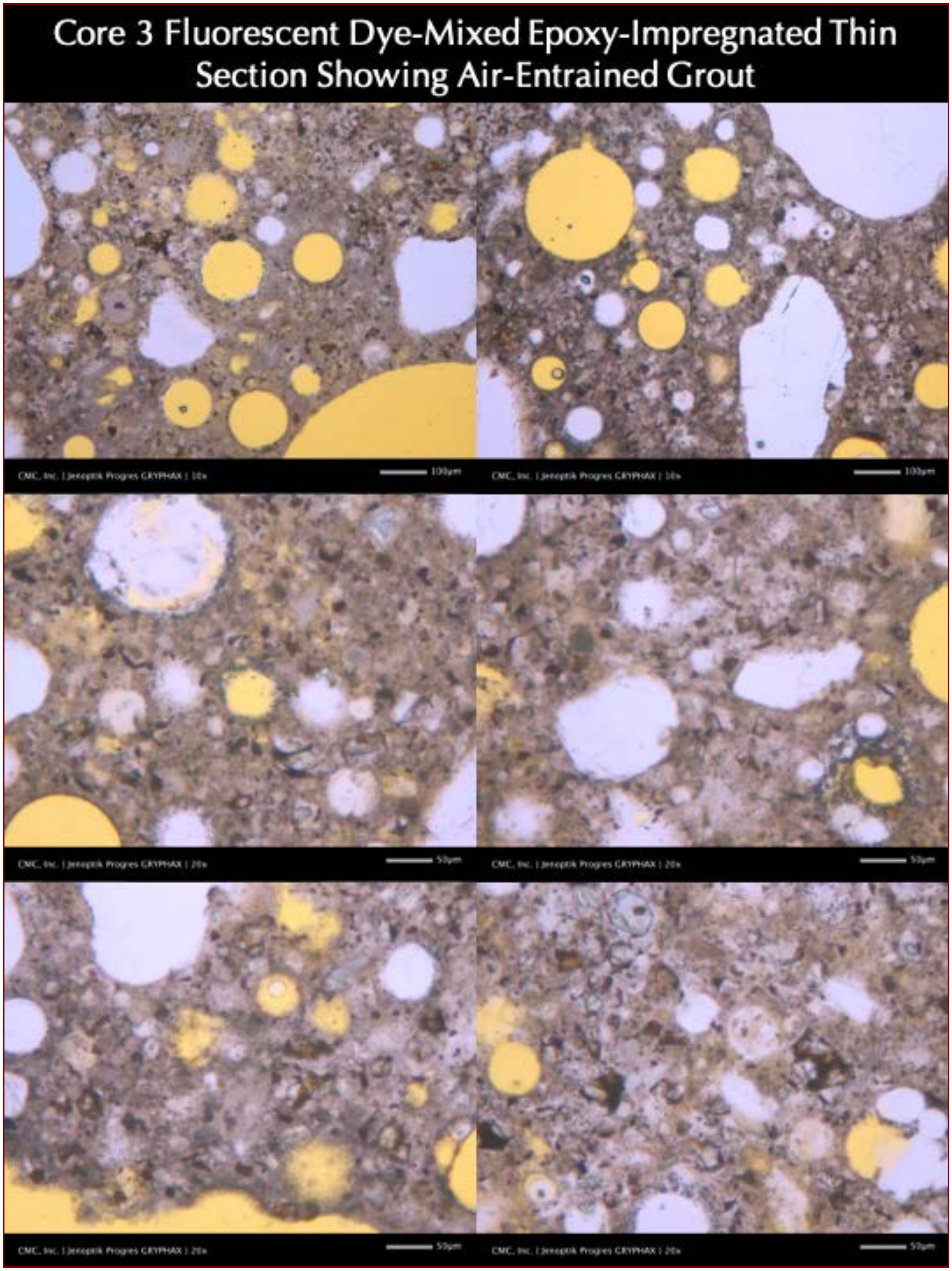

Figure 51: Micrographs of thin section of grout portion of Core 3 taken with a Nikon Eclipse E600 POL petrographic microscope in plane polarized light mode showing: (a) lightly crushed silica sand fine aggregate particles, (b) a dense paste having abundant residual Portland cement particles and evidence of addition of some other pozzolanic and cementitious materials distributed in cement hydration products, and (c) spherical entrained air voids highlighted by fluorescent epoxy.

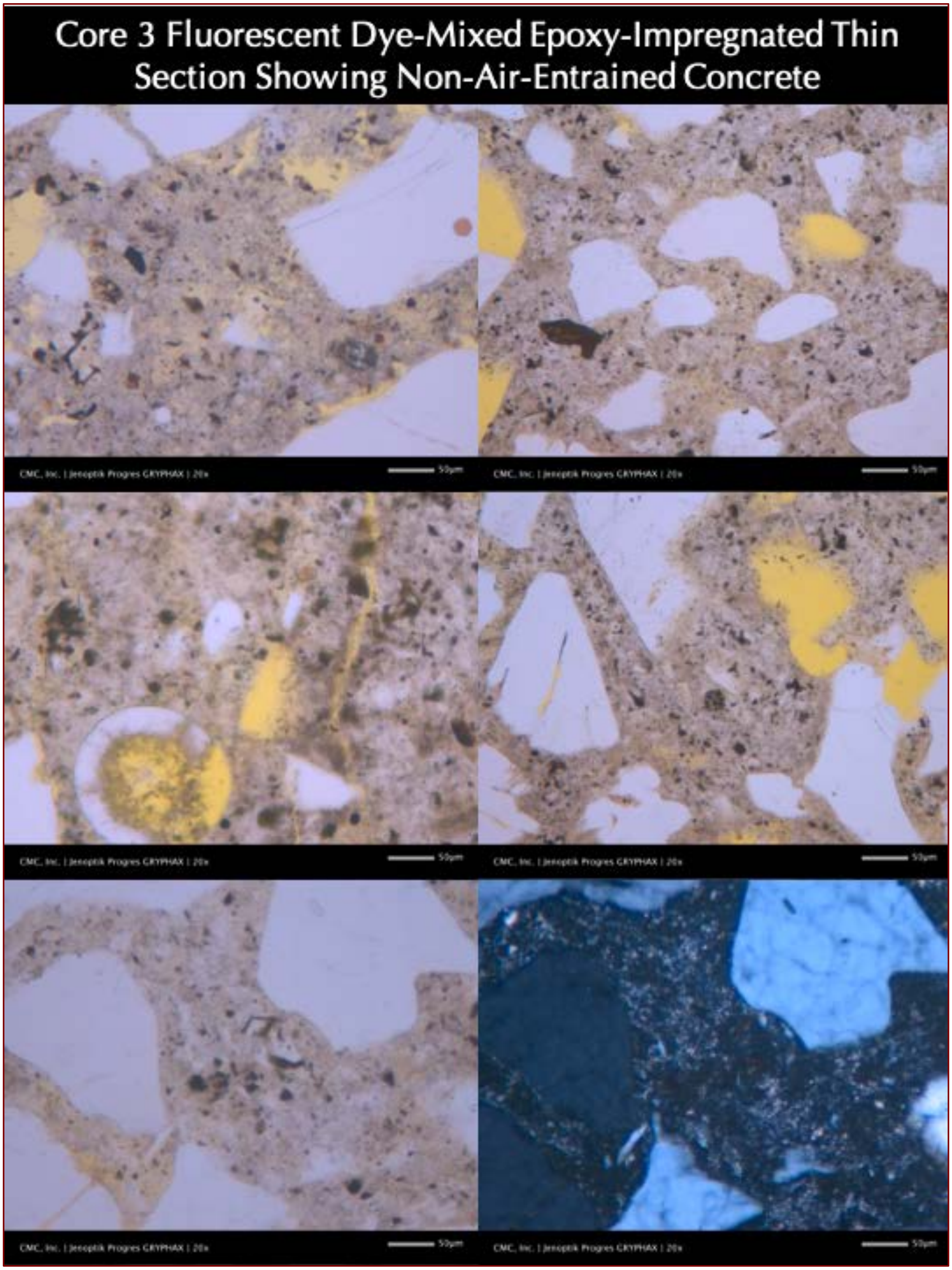

Figure 52: Micrographs of thin section of concrete portion of Core 3 taken with a Nikon Eclipse E600 POL petrographic microscope in plane and crossed (bottom right photo) polarized light modes showing: (a) crushed silica sand fine aggregate particles, (b) a dense Portland cement paste having a few residual Portland cement particles in cement hydration products, (c) a few entrapped air voids highlighted by fluorescent epoxy, and (d) fine acicular secondary ettringite deposits lining walls of some air voids.

X-RAY DIFFRACTION (XRD) STUDIES OF GROUTS AND CONCRETES

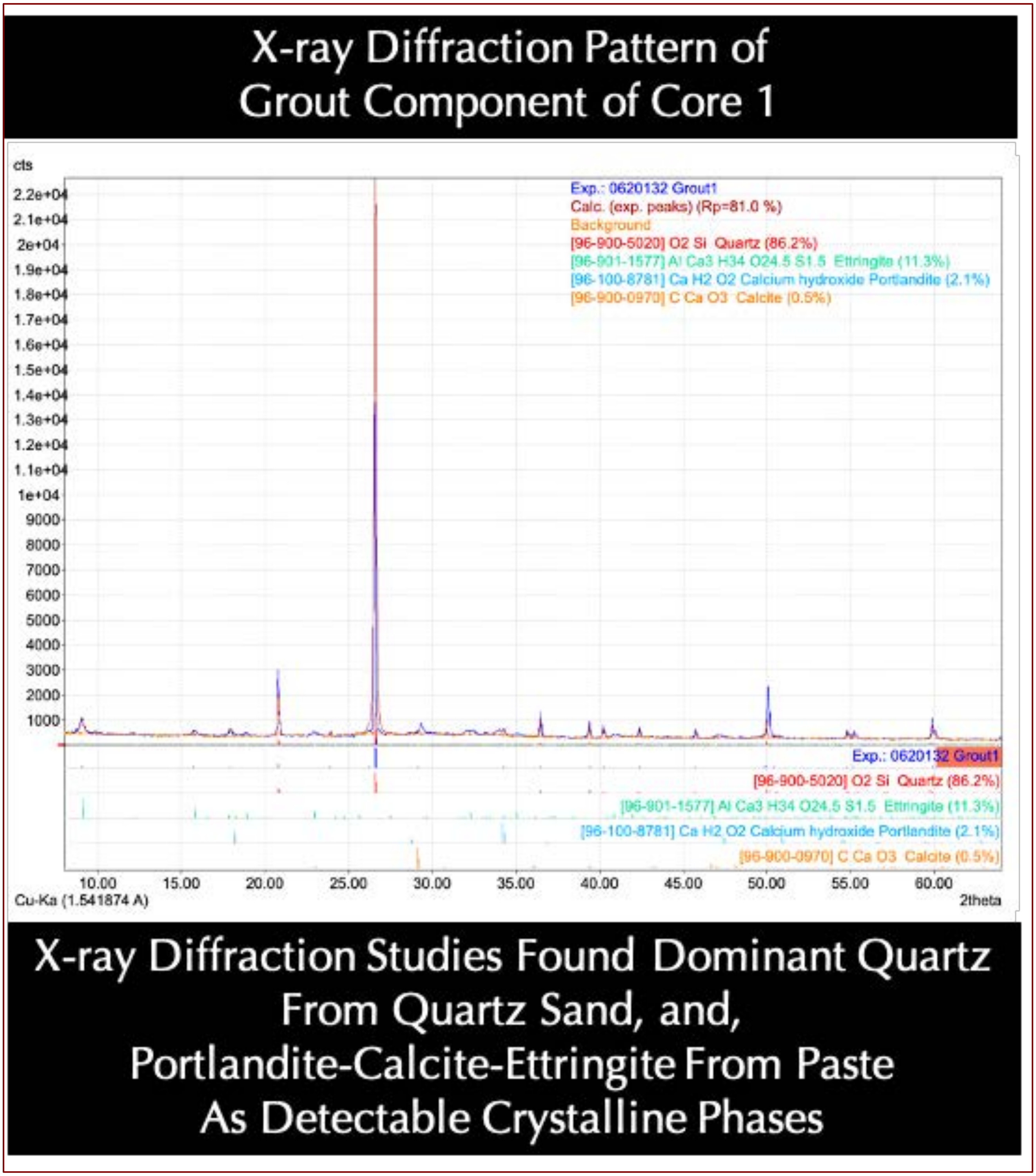

Figure 53: X-ray diffraction pattern of grout component of Core 1.

X-ray Diffraction Pattern of Concrete Component of Core 1

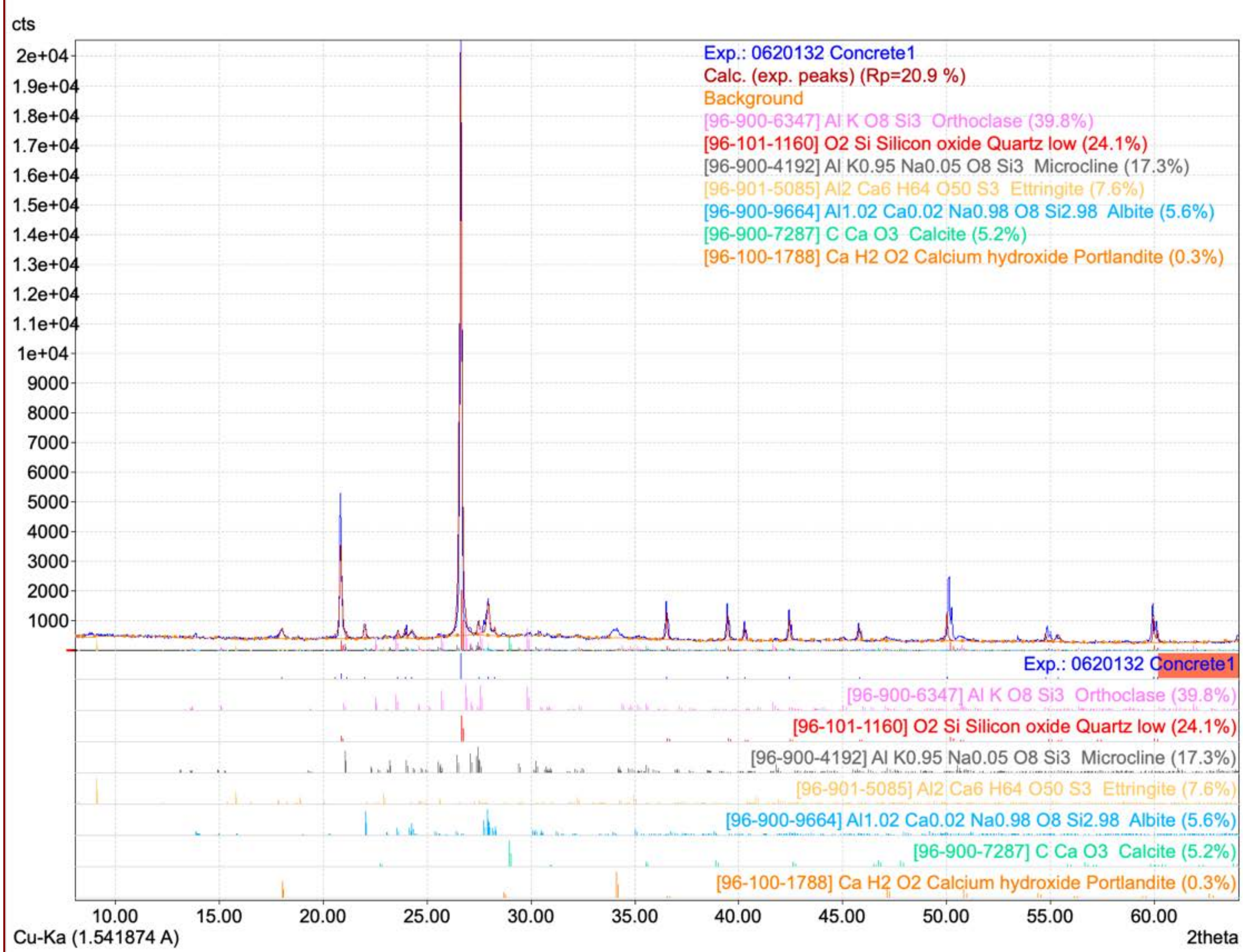

X-ray Diffraction Studies Found Dominant Quartz And Feldspar Albite-Orthoclase-Microcline) From Crushed Granite Coarse Aggregate and Quartz Sand Fine Aggregate, and, Portlandite-Calcite-Ettringite From Paste As Detectable Crystalline Phases

Figure 54: X-ray diffraction pattern of concrete component of Core 1.

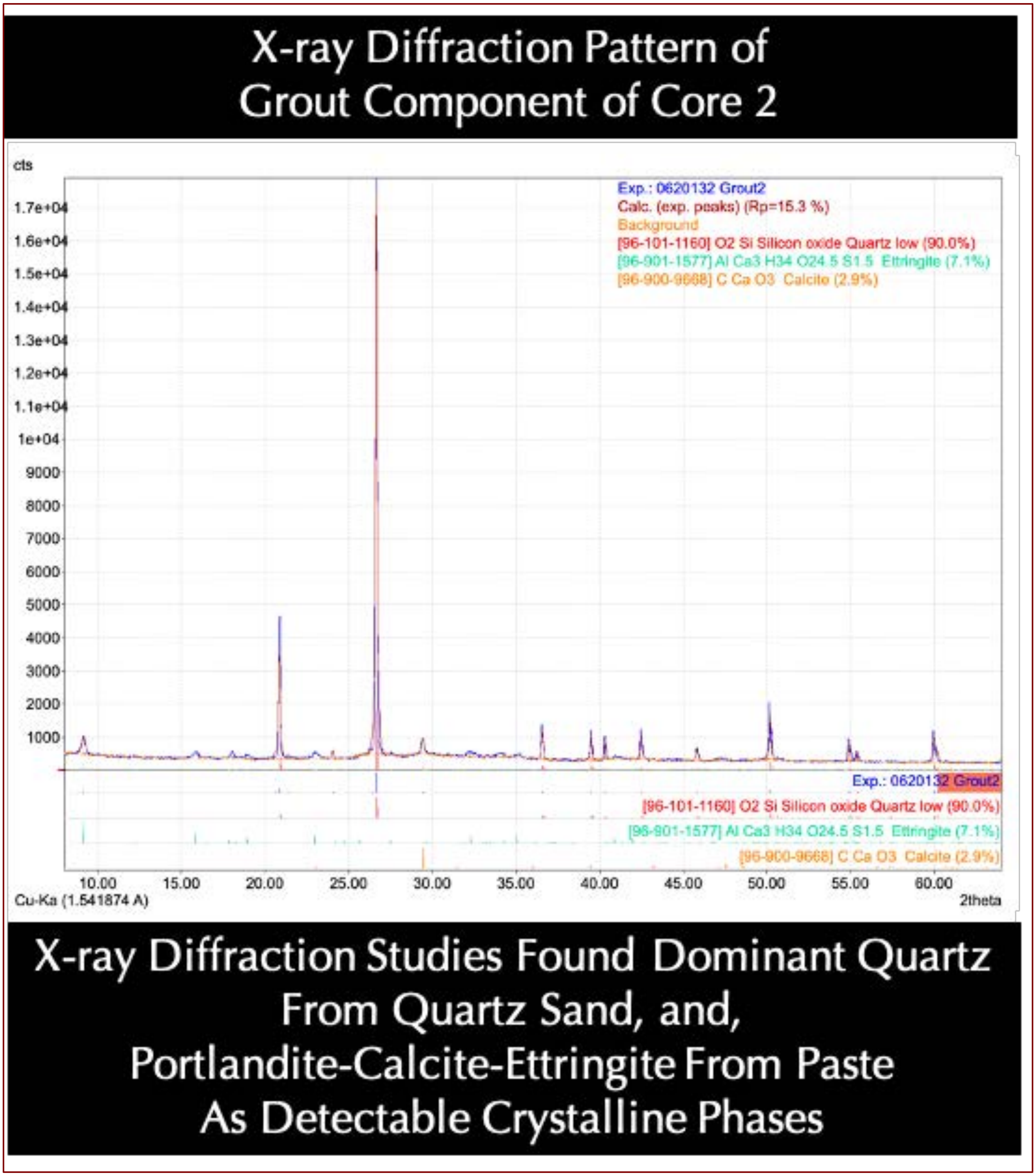

Figure 55: X-ray diffraction pattern of grout component of Core 2.

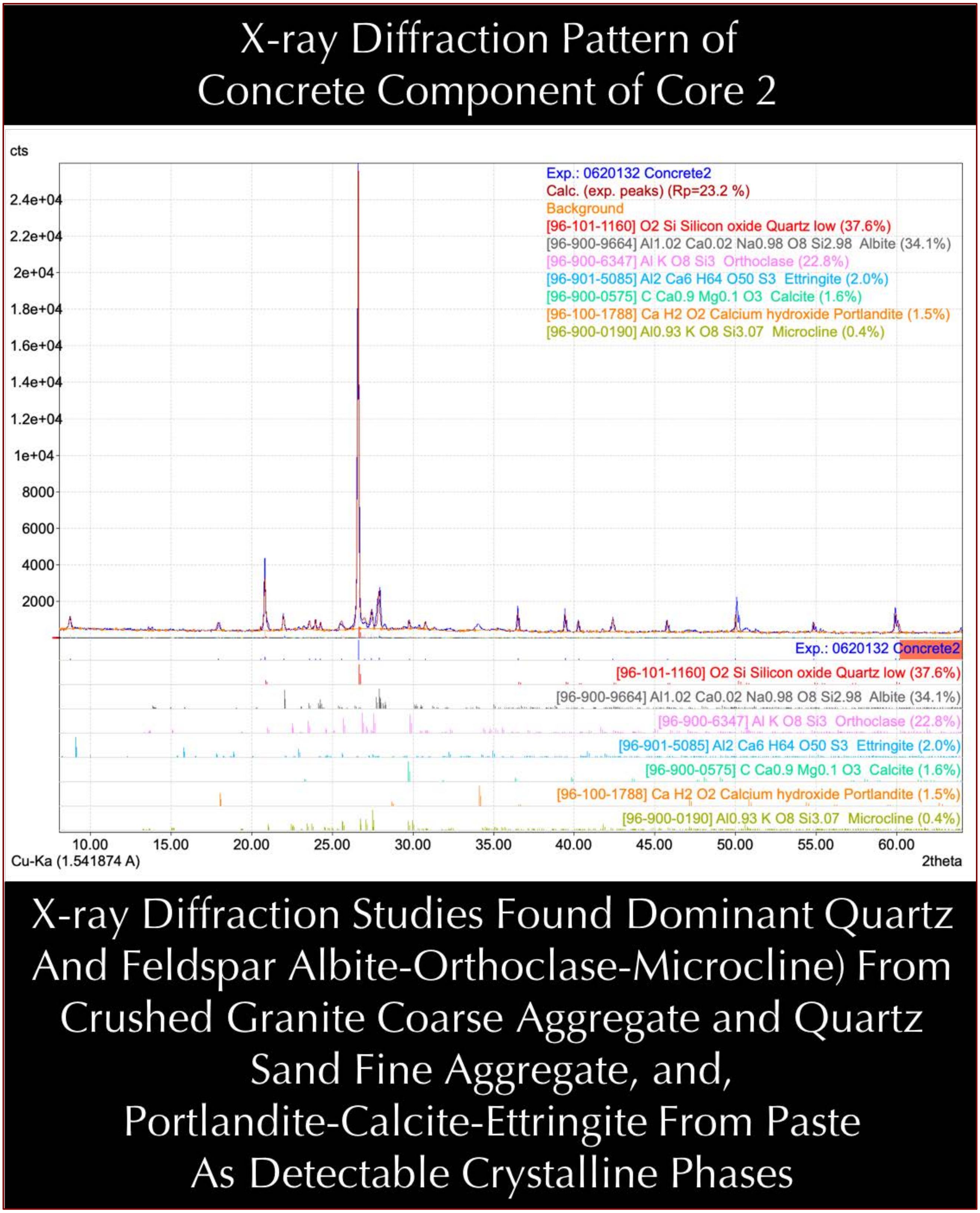

Figure 56: X-ray diffraction pattern of concrete component of Core 2.

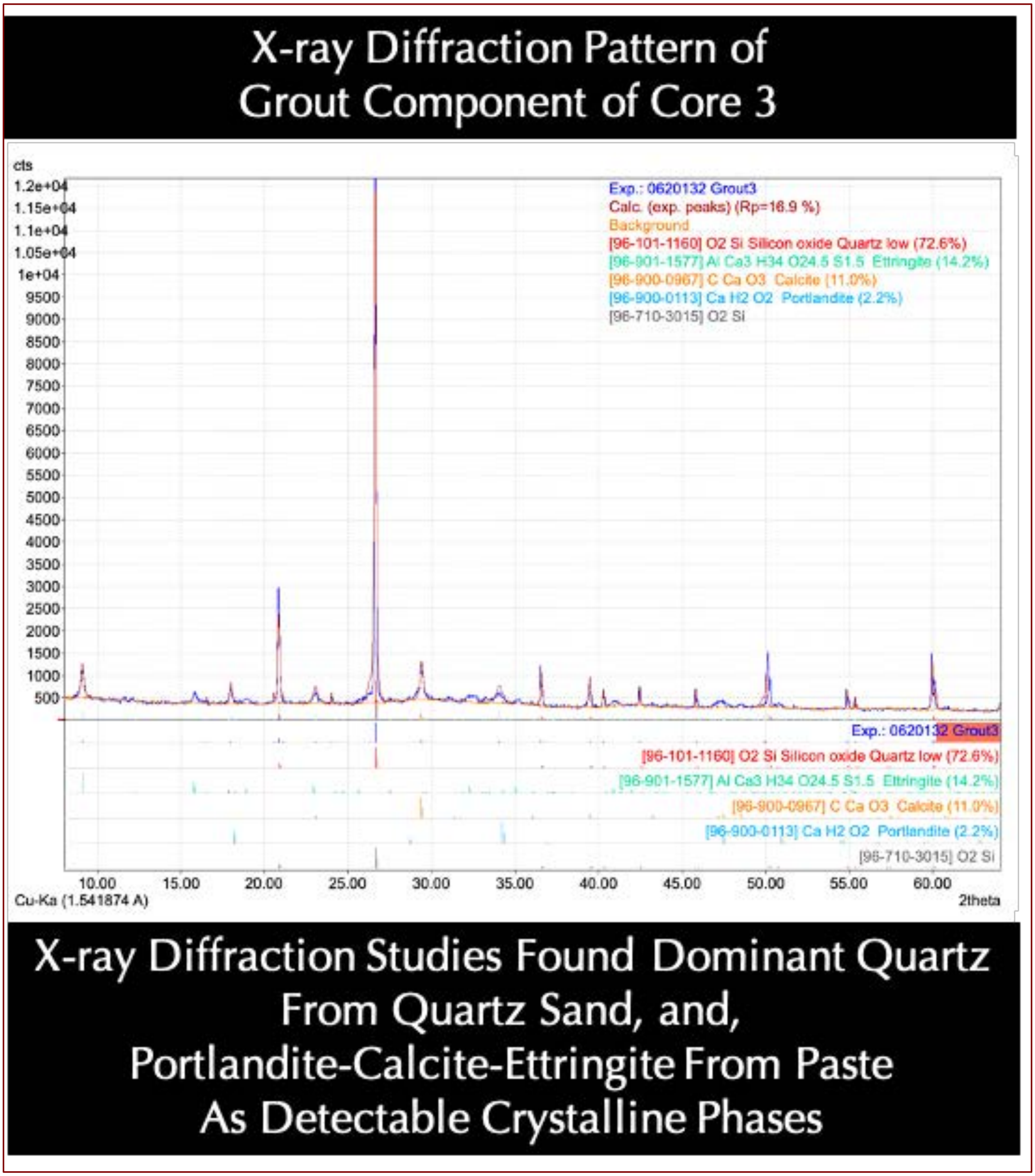

Figure 57: X-ray diffraction pattern of grout component of Core 3.

X-ray Diffraction Pattern of Concrete Component of Core 3

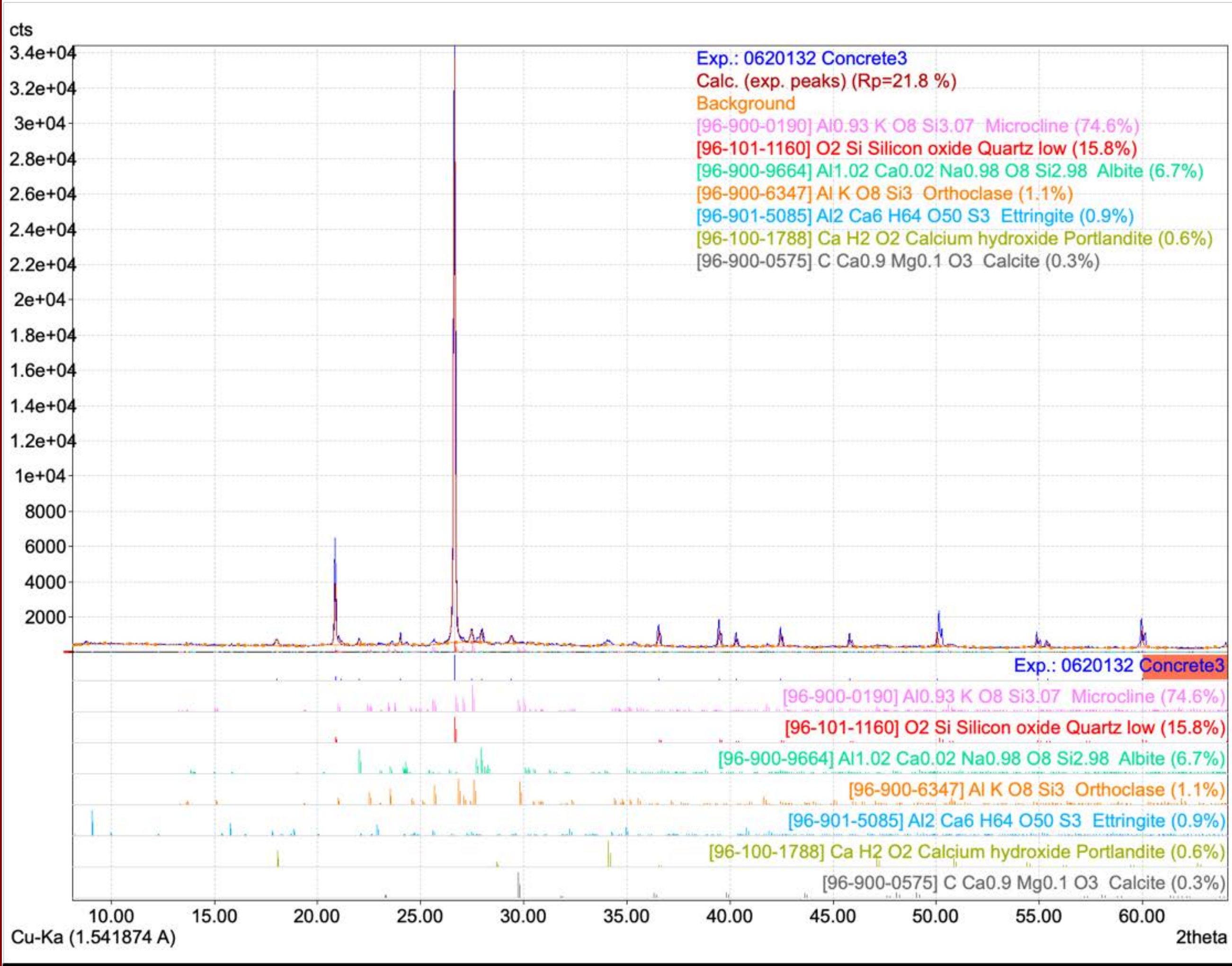

X-ray Diffraction Studies Found Dominant Quartz And Feldspar Albite-Orthoclase-Microcline) From Crushed Granite Coarse Aggregate and Quartz Sand Fine Aggregate, and, Portlandite-Calcite-Ettringite From Paste As Detectable Crystalline Phases

Figure 58: X-ray diffraction pattern of concrete component of Core 3.

X-RAY FLUORESCENCE (XRF) COMPOSITIONS OF GROUTS

X-ray Fluorescence Studies of Bulk Grout & Concrete in 3 Cores Showing Overall Compositional Similarities & Differences

Cores	Components	SiO2	Al2O3	CaO	MgO	Na2O	K2O	Fe2O3	TiO2	P2O5	SO3	Balance	Total
Core 1	Grout	31.3	2.71	22.3	1.54	0.163	0.258	1.78	0.299	0.0231	4.44	35.2	100
	Concrete	55.1	4.53	13.9	0.914	1.38	1.08	2.06	0.194	0.065	0.592	20.2	100
Core 2	Grout	33.9	2.81	21.1	1.49	ND	0.265	1.99	0.296	0.0271	4.21	33.8	100
	Concrete	54.5	6.19	10.7	0.857	1.96	1.9	2.08	0.234	0.0649	0.397	21.1	100
Core 3	Grout	27.6	2.61	23.8	1.65	ND	0.199	1.76	0.406	0.0154	5.08	36.8	100
	Concrete	54.0	4.43	12.3	0.99	1.16	1.47	1.71	0.222	0.0602	0.576	23.1	100

a. Grouts are uniform in compositions
b. Concretes are uniform in compositions
c. Grouts have consistently higher sulfate contents of ~4 to 5% as SO3 compared to ~ 0.5% sulfate in concrete
d. Grouts have consistently lower silica contents (~ 30%) compared to concrete (~ 55%)
e. Grouts have consistently lower alumina contents (~ 2.5-3%) compared to concrete (~ 4.5-6%)
f. Grouts have consistently higher lime contents (~ 20-23%) compared to concrete (~ 10-14%)
g. Grouts have lower alkali contents than concrete where alkali in concrete came from alkali-feldspar in crushed granite coarse aggregate in concrete

Figure 59: X-ray fluorescence spectroscopy of both grout and concrete components of all three cores showing overall similarities in bulk chemical compositions of grouts and concretes as separate components, as well as their main differences.

Sulfate contents in the concrete ranges from 0.4 to 0.6 percent, which is consistent with addition of approximately 15 percent by mass of Portland cement in the concrete having 3 percent sulfate in cement, which are the normal cement and sulfate contents in cement, respectively, for the concrete found in the present three cores. In other words, sulfate contents of concrete do not show any evidence of external introduction of sulfate from the adjacent grout or from any other source besides the Portland cement as the main contributor of sulfate in concrete. There is, therefore, no evidence of cracking in the concrete from external sulfate attack or introduction of sulfate from the grout.

Sulfate contents in the grout range from 4 to 5 percent, which is normal for a shrinkage-compensating anchoring grout where high sulfate contributed to an early expansion of the grout needed for anchorage. Sulfate contents, however, are not too high (e.g., >15 percent) as found in many gypsum-based anchoring grouts, where a lot of unused 'excess' sulfate stays after initial hydration reactions at the plastic state and those unreacted sulfate cause potential sulfate-aluminate reactions in the hardened state, which introduce late expansion at the hardened state and cracking in grout. The present grout is Portland cement based, not gypsum-based, which is confirmed from bulk sulfate content of the grout, which also removes the possibility of having an excess sulfate in the grout to cause late-stage expansion and cracking.

RESULTS

AGGREGATES IN GROUTS

The grout component in all three cores are compositionally similar and indicative of use of the same grout mix at all three core locations from three different floors. The grout sand is lightly crushed natural siliceous sand made using major amounts of quartz and subordinate amounts of quartzite, which are nominal 0.5 mm or less in size, clear, subrounded to angular, dense, hard, well-graded, well-distributed, equidimensional to elongated, unaltered, uncoated, and uncracked. There is no evidence of alkali-aggregate reaction of sand particles, which are present in sound condition during their service.

Properties and Compositions of Aggregates	Grout Sand
Fine Aggregate	
Types	Natural siliceous sand
Nominal maximum size (in., mm)	0.5 mm
Rock Types	Major amounts of quartz and subordinate amounts of quartzite
Cracking, Alteration, Coating	Variably colored, subrounded to angular, dense, hard, equidimensional to elongated
Grading & Distribution	Well-graded and Well-distributed
Soundness	Sound
Alkali-Aggregate Reactivity	None

Table 2: Properties of grout sand in all three cores.

HARDENED PASTE

Paste in the grout component in all three cores are very dense and hard. Most distressed grouts show soft, porous, dusty paste, which is not the case in these grout samples where paste shows no evidence of leaching or softening during service. Portland cement was used as the major cementitious component in the grout. There is no evidence of fly ash, or slag addition as a supplementary cementitious material, however, there are evidence of addition of some other pozzolanic and/or cementitious materials as minor component besides Portland cement, which were observed during optical microscopy of paste. Such evidence include some spherical fly ash-like empty particles that have vesicular glassy margins, but are not as ubiquitous as would have been if a fly ash component was added. There are also indications of possible addition of silica fume as evidenced by some brown clusters of ultrafine particles in the paste. A polymer component may also be added as polymers commonly impart a densified paste microstructure seen in the paste in present grouts. In summary, the paste microstructure shows more than that usually obtained from hydration of Portland cement. Densification of paste indicated use of a combination of a low-water-cementitious materials ratio, high cementitious materials content, and water-reducer/superplasticizer type mix, which did not leave any capillary pores in the paste to be detected by optical microscopy.

The basic mineralogical compositions of paste in a typical distressed anchoring grout shows: (a) gypsum, ettringite, and hydrates of calcium aluminate, sulfoaluminate, and silicate as the products of hydration of the original binder components of gypsum and Portland cement additives in the grout, as well as (b) secondary products of coarser gypsum crystals, and calcium carbonate, which were formed by dissolution of primary hydration products and precipitation of gypsum or atmospheric carbonation of gypsum to calcite (through dissolution of gypsum in the presence of moisture during service followed by atmospheric carbonation and precipitation as calcite). Extreme leaching of paste by moisture during service, and carbonation leaves secondary calcium carbonate in a skeletal microstructure of paste. Gypsum, trace residual cement, and calcium carbonates are some common products of alteration of paste in a distressed grout. However, none of the above-mentioned microstructures or secondary deposits of alterations of distressed paste are found in the dense sound paste of the present grout, which shows no such leaching or dissolution of grout or precipitation of secondary deposits by exposure to moisture during service.

Properties and Compositions of Pastes	Grout Paste
Color, Hardness, Porosity, Luster	Gray, Hard, Dense, Subvitreous
Residual Portland Cement Particles	Normal, 14 to 16 percent by paste volume
Calcium hydroxide from cement hydration	Normal, 10 to 14 percent by paste volume
Pozzolans, Slag, etc.	No evidence of fly ash or slag but other ultrafine pozzolanic and/or cementitious materials may have been added at minor amounts after adding Portland cement as the main cementitious component
Water-cementitious materials ratio (*w/cm*), estimated	Less than 0.40
Cementitious materials contents, estimated (equivalent to bags of Portland cement per cubic yard)	12 to $12^1/_2$
Secondary Deposits	None
Depth of Carbonation, mm	No carbonation of paste
Microcracking	None
Aggregate-paste Bond	Tight
Bleeding, Tempering	None
Chemical deterioration	None

Table 3: Properties and compositions of hardened cement paste in the grouts.

AIR

Grout samples in all three cores are excessively air-entrained having air contents estimated to be 18 to 20 percent by volume. Such high air entrainment has reduced the overall compressive strengths of grouts at the expense of added freeze-thaw durability during service. The observed cracks in the field are judged not due to any freezing-related distress on the grout *per se*.

MINERALOGICAL AND CHEMICAL COMPOSITIONS OF GROUTS

Both XRD and XRF studies of grouts showed the typical high sulfate contents of grout, and overall similarities in basic mineralogical and chemical compositions.

Bulk sulfate contents in the grout range from 4 to 5 percent, which is normal for a shrinkage-compensating anchoring grout where high sulfate contributed to an early expansion of the grout needed for anchorage. Sulfate contents, however, are not too high (e.g., >15 percent) as found in many gypsum-based anchoring grouts, where a lot of unused 'excess' sulfate stays after initial hydration reactions at the plastic state and those unreacted sulfate cause potential sulfate-aluminate reactions in the hardened state, which introduce late expansion at the hardened state and cracking in grout. The present grout is Portland cement-based, not gypsum-based, which is confirmed from bulk sulfate content of the grout, which also removes the possibility of having an excess sulfate in the grout to cause late-stage expansion and cracking.

XRD studies showed quartz as the dominant mineral from silica sand and minor portlandite and calcite from paste. None of the grout samples showed any potentially deleterious components or reactions to introduce cracking or affect the performance beyond what is anticipated for the chemistry and mineralogy of the grout.

COARSE AGGREGATES IN CONCRETE

Coarse aggregates are compositionally similar crushed granite in all three cores having nominal maximum sizes of 1 inch (25 mm). Particles are dense, hard, light to dark gray, brown, angular, equidimensional to elongated, unaltered, uncracked, and uncoated.

Coarse aggregate particles are well-graded and well-distributed. There is no evidence of any potentially deleterious alkali-aggregate reaction of crushed granite particles found in the cores. Coarse aggregate particles have been sound during their service and did not contribute to the observed cracking of balconies.

FINE AGGREGATES IN CONCRETE

Fine aggregates are compositionally similar crushed silica sand having nominal maximum sizes of $^3/_8$ in. (9.5 mm) and containing major amounts of quartz, and subordinate amounts of quartzite, feldspar, granite, and sandstone particles. Particles are variably colored, angular, dense, hard, equidimensional to elongated, unaltered, uncoated, and uncracked.

Fine aggregate particles are well-graded and well-distributed. There is no evidence of alkali-aggregate reaction of fine aggregate particles found in the cores. Fine aggregate particles have been sound during their service in the concrete and did not contribute to the cracking of balconies.

The following Table summarizes properties of coarse and fine aggregates in the samples.

Properties and Compositions of Aggregates	Concrete Aggregates
Coarse Aggregates	
Types	Crushed Granite
Nominal maximum size (in.)	1 inch (25 mm)
Rock Types	Alkali Granite
Angularity, Density, Hardness, Color, Texture, Sphericity	Dense, hard, light to dark gray, brown, angular
Cracking, Alteration, Coating	Equidimensional to elongated, unaltered, uncracked, and uncoated
Grading & Distribution	Well-graded and Well-distributed
Soundness	Sound
Alkali-Aggregate Reactivity	None
Fine Aggregates	
Types	Crushed silica sand
Nominal maximum size (in.)	$^{3}/_{8}$ in. (9.5 mm)
Rock Types	Major amounts of quartz, and subordinate amounts of quartzite, feldspar, granite, and sandstone particles
Cracking, Alteration, Coating	Variably colored, rounded to subangular, dense, hard, equidimensional to elongated
Grading & Distribution	Well-graded and Well-distributed
Soundness	Sound
Alkali-Aggregate Reactivity	None

Table 4: Properties of coarse and fine aggregates of concrete.

HARDENED PASTE IN CONCRETE

Properties and composition of hardened cement pastes in the concrete portions of cores are summarized in Table 5. Pastes are moderately dense, medium gray, and uniform in color throughout the depth of concrete. Freshly fractured surfaces have subvitreous lusters and subconchoidal textures.

Residual and relict Portland cement particles are present and estimated to constitute 8 to 10 percent of the paste volumes. Besides Portland cement, no other pozzolanic or cementitious materials are found. Hydration of Portland cement is normal in the interior bodies.

Properties and Compositions of Paste	Paste in Concrete
Color, Hardness, Porosity, Luster	Moderately dense, medium gray, uniform in color throughout the depth of concrete. Freshly fractured surfaces have subvitreous lusters and subconchoidal textures.
Residual Portland Cement Particles	Normal, 8 to 10 percent of the paste volumes
Calcium hydroxide from cement hydration	Normal, 10 to 14 percent by paste volume in the interior
Pozzolans, Slag, etc.	None

Properties and Compositions of Paste	Paste in Concrete
Water-cementitious materials ratio (*w/cm*), estimated	0.40 to 0.45
Cement Content (bags per cubic yard)	6 to 6$^1/_2$
Secondary Deposits	None
Depth of Carbonation, mm	3 to 4 mm from exposed surface
Microcracking	Microcracking from freezing of concrete at critically saturated conditions, and some shrinkage
Aggregate-paste Bond	Tight
Bleeding, Tempering	None
Chemical deterioration	None

Table 5: Proportions and composition of hardened cement pastes.

The textural and compositional features of the pastes are indicative of Portland cement contents estimated to be 6 to 6$^1/_2$ bags per cubic yard, and, water-cement ratios (*w/c*) estimated to be 0.40 to 0.45 in the interior bodies of concrete. Carbonation is 3 to 4 mm from exposed surface of balcony. Aggregate-paste bonds are tight.

AIR IN CONCRETE

Air occurs as a few near-spherical and irregularly-shaped voids that are characteristic of entrapped air in concrete. There is no evidence of intentional addition of an air entraining agent found in the concrete. Concrete in all three cores are non-air-entrained having air contents estimated to be 1 to 2 percent. Due to the non-air-entrained nature of the concrete, some of the observed cracks, if not all, could have been introduced from cyclic freezing and thawing of a non-air-entrained concrete at critically saturated conditions, especially in areas along the interfaces to grout pockets.

MINERALOGICAL AND CHEMICAL COMPOSITIONS OF CONCRETE

Sulfate contents in the concrete range from 0.4 to 0.6 percent, which is consistent with addition of approximately 15 percent by mass of Portland cement in the concrete having 3 percent sulfate in cement, which are the normal cement and sulfate contents in cement, respectively, for the concrete found in the present three cores. In other words, sulfate contents of concrete do not show any evidence of external introduction of sulfate from the adjacent grout or from any other source besides the Portland cement as the main contributor of sulfate in concrete. There is, therefore, no evidence of cracking in the concrete from external sulfate attack or introduction of sulfate from the grout.

XRD studies showed quartz and feldspar (microcline, orthoclase, and albite) as the dominant minerals from crushed granite coarse aggregate particles and minor portlandite, calcite, and occasional secondary ettringite from paste where secondary ettringite found in the XRD are innocuous, and similar to the ones found in optical microscopy lining the walls of air voids that are indicative of the presence of moisture during service.

DISCUSSIONS

ANCHORING GROUTS – PROPERTIES & TYPES, AND PROBLEMS

Properties that are vital for use of a proprietary prepackaged anchoring grout in railing posts are:

- Non-shrink behavior when set and hardened (hence also called nonshrink, or, shrinkage-compensating grout), which is achieved by an expansion at the plastic state (*pre-hardening expansion*) to fill available open or void spaces around railing post to provide successful anchorage and load-transfer from the railing to the surrounding concrete. Pre-hardening expansion reduces or eliminates subsequent shrinkage during hardening that a traditional Portland-cement-only grout system undergoes. Usually, the mechanism that provides the early expansion at the plastic state and thus the nonshrink behavior, if continues after hardening, contributes to the *post-setting/hardening expansions* with the failure of the grout system and/or the surrounding medium.
- Quick setting and high early strength, in order to reduce the time that posts are needed to be supported. Traditional Portland-cement-only grouts provide slow setting and strength gain, hence are commonly replaced by many newer-generations of proprietary grout products offering very fast setting and high early strengths (e.g., the current 'Anchor All' grout of Dayton Superior that achieves an advertised 4500 psi strength within 24 hours when mixed, used, and applied according to the manufacturer's recommendations).

The newer generations of nonshrink anchoring grouts are broadly classified into:

- Polymer Grouts (e.g., nonshrink epoxy grouts) that contain a filler and a polymer binder, or, a Polymer-Modified Grout, where a cementitious system is further densified with an impregnated polymer, or,
- Cementitious Grouts.

The present examined grout belongs to the category of cementitious grouts.

Cementitious grouts can have one of the following three primary types of binders that are traditionally used for repair materials, or, anchoring:

- Portland cement-based repair grouts, where Portland cement constitutes the dominant binder component. Due to the requirements of shrinkage-compensation, quick setting, and high early strength during anchoring applications, Portland-cement-only grout systems, as mentioned, are less common than the following two types. A Type III Portland cement, being more finely ground than Type I/II can provide high early strength, hence a better choice in a cement-grout.
- Gypsum-based, which provide fast, early set, which may contain gypsum as the sole binder component, or gypsum with a minor amount of Portland cement (usually less than 10 percent cement to provide some passivation of embedded metals, which, however, can also cause formation of deleteriously expansive

compounds like ettringite, a calcium sulfoaluminate hydrate, after initial hardening, if exposed to moisture during service, resulting in cracking of the grout itself and/or of the surrounding medium),

- Blended Portland cement and Calcium Aluminate Cement-based, or expansive calcium sulfoaluminate cement system, where sulfate-aluminate reactions during setting provide the necessary nonshrink behavior, which, however, can also contribute to distress if this reaction continues after setting i.e. during service in the continued presence of moisture.

The present examined grout belongs to the first category of Portland cement-based cementitious grout, which is determined to contain Portland cement as the major binder component, along with some other minor components of hydraulic cementitious materials. There is no evidence of calcium aluminate cement in the paste.

Both gypsum-based grouts and Portland cement/calcium aluminate cement-based grouts offer the necessary shrinkage compensation characteristic of a nonshrink grout. Many proprietary grout products contain other shrinkage compensation additives, such as:

- A shrinkage-compensating (expansive) cement, e.g., a Type K sulfoaluminate-type expansive cement, or a Type M expansive cement, which is a mixed Portland cement plus calcium aluminate cement plus calcium sulfate, or, a Type S expansive cement, which is a very high C_3A, as high as 20% C_3A Portland cement containing a stoichiometrically high amount of calcium sulfate - all of which undergo an expansive formation of ettringite during hydration thus provide the shrinkage-compensation (expansion) during the early hardening period after setting, and all are specified in ASTM C 845.
- A shrinkage-compensating/reducing chemical (e.g., organic, water-soluble) admixture (SRAs, however, are not covered in ASTM C 494 specifications for chemical admixtures), which operates by interfering with the surface chemistry of the air/water interface within the capillary pores, reducing surface tension of water in the capillary pores (which is the prime factor for drying shrinkage of Portland cement-based systems), and consequently reducing the shrinkage as water evaporates from within the grout or concrete.
- Oxidizing iron aggregate, or metallic powders (aluminum).

ANCHORING GROUTS – PROBLEMS

Three common types of problems of many anchoring grout systems related to *post-hardening expansions* are:

- Volume instability when exposed to moisture after hardening i.e. during service, resulting in expansion or degradation of the product itself,
- Migration into and reaction with the surrounding concrete, again, in the presence of moisture during service that causes dissolution of potentially deleterious water-soluble components from the grouts to the concrete, resulting in the formation of expansive chemical compounds and deterioration of concrete as cracking and spalling; and,

- Lack of passivation of embedded metal, particularly aluminum causing corrosion of metal.

Based on detailed petrographic examinations, the present grout is judged to have experienced no such potential distress from exposure to moisture during service or due to any usual composition (e.g., no excess sulfate for late reactions) of the grout materials used, which is found to be as anticipated for the intended anchoring purposes. The grout was reportedly covered with metal plates and prevented from moisture intrusion during service. The dense microstructure of paste showed no evidence of leaching of any moisture-related distress. There is no evidence of addition of excess water in the grout mix to soften the paste or increase the paste porosity.

ANCHORING GROUTS – EXCESS CALCIUM SULFATES & MECHANISMS OF POST-HARDENING EXPANSIONS AND DISTRESS

The primary cause for post-hardening expansion and associated distress of the grout and/or of the surrounding concrete is the presence of: (i) free calcium sulfate in the hardened grout, and (ii) moisture during service.

- After the rapid-setting/hardening grout has set, free calcium sulfate, if present dissolves if exposed to moisture during service, and then precipitates out as calcium sulfate again, when the material dries. After precipitation, the calcium sulfate is more loosely packed and occupies more space than the original free calcium sulfate, resulting in a friable deposit that expands within the material. This phenomenon is similar when a drywall, which is mostly calcium sulfate, gets wet and then dries out, forming an expanded, flaky residue.
- Also, when calcium sulfate is dissolved in water, it can migrate into the surrounding concrete, where it can react with the aluminates in the cement, resulting in deleterious expansions from sulfate-aluminate reactions and formation of secondary ettringite deposits.

As mentioned, none of the grout samples examined here showed evidence to support the above two mechanisms of grout distress to introduce the observed cracking in the field. There is no evidence of excess sulfate in the grout to cause sulfate-aluminate reactions at the hardened state in the presence of moisture during service.

For Portland-cement-only grouts, calcium sulfate originally present in the Portland cement (usually less than 3% by mass of cement when C_3A content of cement is 8% or less, or, less than 3.5% by mass of cement when C_3A content is greater than 8%) for set-controlling purposes (to control the flash set of C_3A in cement) is consumed during initial hydration of cement in the plastic state. If, however, 'excess' calcium sulfate is present after hydration that can, when exposed to moisture during service, cause several distress mechanisms in grout and/or surrounding concrete. That 'excess' calcium sulfate can: (a) readily dissolve in the moisture during service, and when the system dries out, it can recrystallize, thus occupying more volume than before it was wetted, thus causing disintegration of the grout. Additionally: (b) excess calcium sulfate in the hardened grout can migrate out to the surrounding concrete to form deleteriously expansive materials by sulfate-aluminate reactions, leading to cracking and spalling of concrete.

Despite having 4 to 6 percent bulk sulfate in the present grouts, dominance of Portland cement component in the binder prevented formation of any excess potentially deleterious sulfate in the grout for late expansions.

For gypsum-based grouts that, by definition, contain abundant free calcium sulfate at the hardened state, the system, though fast-setting, is extremely vulnerable to moisture during service, for the same reasons as mentioned for the fate of excess calcium sulfate in the Portland-cement-only grouts during service in a moist environment. Gypsum can: (a) expand during wetting (ready dissolution in water) and drying (recrystallization to larger masses); (b) gypsum can participate in deleterious expansive reaction with aluminates in Portland cement, if the grout formulation contains a minor cement additive, or with the hydrates of aluminate in the Portland cement in the surrounding concrete; (c) gypsum can cause expansive corrosion of aluminum posts, anchors, and clips that they may be in contact with when exposed to moisture during service; and (d) gypsum in a confined space can absorb a lot of moisture in the moist outdoor condition and expand during freezing at the moist state.

As mentioned, the present grout does not belong to this category.

For blended cement systems containing Portland cement and calcium aluminate cement, or an expansive (e.g., calcium sulfoaluminate) cement, pre-hardening expansion is achieved by sulfate-aluminate reactions and abundant primary ettringite formation from hydration of such systems, which provide the necessary expansion at the plastic state. Both Portland cement and calcium aluminate cement contain calcium sulfate for set-controlling purposes (3-3.5% maximum SO_3 for Portland cement and 2.5-15% SO_3 for calcium aluminate cement), where the former has a much tighter control on chemistry and a well-established ASTM standard (C 150) than the latter (which has no ASTM standard or a control of SO_3 content). Hence sulfate content in calcium aluminate cement can vary between products and formulations depending on the desired performance in a particular application. Hence two different products having the same SO_3 content may behave differently i.e. one could be expansive when exposed to moisture, while the other may not. Due to such uncontrolled, inconsistent calcium sulfate contents, it is difficult to know if a given batch will be durable prior to use. The binder in these newer-generation of grouts can also contain fly ash, limestone fines, silica fume, and other additives.

As mentioned, the present grout does not belong to this category.

ANCHORING GROUTS – MIX PROPORTIONING & CURING

In addition to the type of the binder present, a control on the amount of mix water added and adequate moist curing are critical. Sufficient mix water is needed for calcium sulfate to react at the plastic state, but ‘excess’ water can cause physical and/or chemical segregation, e.g., of aggregates at the bottom from binder at the top and/or different layers of compounds, respectively. It is crucial to follow manufacturer’s recommended amount of mix water. For blended cement systems, adequate moist curing is important since inadequate curing may cause reversal of chemical reactions changing the resulting chemical compounds to more expansive and lower-strength compounds (Papas 2014).

The present grout showed no evidence of addition of excess water during mixing to leave many capillary porosity in the paste. By contrast, paste showed very dense microstructure with no such capillary pores from excess mix water.

ANCHORING GROUTS – ASTM SPECIFICATIONS & TESTS

Presently, there is no ASTM standard that specifically addresses rapid-hardening grouts, particularly for use in an exterior environment where the hardened material will be exposed to moisture in service, *such as the case for the present grout*. The ASTM standards commonly associated with the repair and anchorage grout systems are:

- ASTM C 928, "Standard Specification for Packaged, Dry, Rapid-Hardening Cementitious Materials for Concrete Repairs," which covers packaged, dry, cementitious mortar or concrete materials for rapid repairs to hardened hydraulic-cement concrete pavements and structures i.e. elements that could be exposed to moist exterior environments during service.
- ASTM C 1107, "Standard Specification for Packaged, Dry, Hydraulic Cement Grout (Nonshrink)" is the specification that is often cited by manufacturers of prepackaged grouts, where the specification covers as stated in the scope "packaged dry, hydraulic cement material (nonshrink) intended for use under applied load (such as to support a structure, a machine, and the like) where a change in height below the initial placement heights is to be avoided." Many anchoring grout systems advertised to meet C 1107, however, are not consistent with intended use mentioned in the scope of C 1107.

Both standards require length change measurements at specific ages, but do not necessarily simulate the conditions that an anchoring grout may face during service. For example, ASTM C 928 uses mortar bars cured in both air and water but the length change is measured only at a single age of 28 days, which does not provide sufficient information to predict expansion potential of an anchoring grout. ASTM C 1107 uses a cylindrical specimen that is stored restrained for 56 days, which may simulate semi-restrained condition of anchoring grout but does not simulate the conditions that a repair grout in a deteriorated concrete would be exposed to after removal of the forms.

Two ASTM Tests followed by manufacturers of many nonshrink cementitious grouts are:

- ASTM C 827, "Standard Test Method for Change in Height at Early Ages of Cylindrical Specimens from Cementitious Mixtures;" and,
- ASTM C 1090, "Standard Test Method for Measuring Change in Height of Cylindrical Specimens for Hydraulic-Cement Grout."

ASTM C 827 evaluates vertical height change of nonshrink grout at the plastic state prior to hardening, where up to 90% of shrinkage can occur following the initial expansion; therefore, C 827 has been used widely as the starting point for specification of nonshrink grout. ASTM C 1107 sets the maximum height change requirements in the plastic state to be 4.0% when tested in accordance with C 827, but C 1107 does not set a minimum requirement for height change in the plastic state. Therefore, a grout can exhibit shrinkage in the plastic state and still meet the requirements of C 1107. Typical values of height change of nonshrink grouts tested *a la* C 827 and conforming to C 1107 are from 1% minimum to 4% maximum.

CONCLUSIONS

Laboratory examinations of anchoring grouts and adjacent concrete in three different cores collected from balconies in a condominium showing cracking in the concrete around grout pockets, however, showed no deleterious chemical and/or physical reactions either in the grout, or in the concrete *per se*, to introduce the cracks. The grout in all three cores is compositionally similar, dense, excessively air-entrained (18 to 20% air), silica sand and Portland cement-based, having 4 to 6 percent bulk sulfate (as SO_3), having a very dense low *w/cm* paste microstructure, and present in sound condition with no evidence of leaching, softening, carbonation, cracking, or any moisture-related alteration or distress of grout during service that are common in many other anchoring grouts showing expansion and cracking. Field photos of grout pockets showed no expansion, cracking, or softening of grout *per se*, except some visible cracks mostly confined to the concrete around the grout pockets. The high cementitious materials factor in the grout can introduce some shrinkage-related microcracks during drying. In fact, a few shallow-depth vertical surface microcracks found in the grout components in cores are judged to have formed from unaccommodated drying shrinkage which is not unusual for loss of some mix water during drying. Adequate curing of grout could delay formation of such surface microcracks but not necessarily prevent them from occurring at the hardened state after the curing period is over.

The concrete in three cores are compositionally similar and present in sound condition. However, the non-air-entrained nature of concrete can introduce some of the visible cracks in the field from cyclic freezing and thawing of concrete at critically saturated conditions. Excessive air in the grout pockets can absorb moisture and create a local moisture mass within the concrete to saturate the concrete during freezing and hence introduce cracking from freezing of concrete mostly at grout-concrete interfaces at saturated condition. The grout itself, however, should not crack by freezing due to its abundant entrained voids, which would accommodate all freezing-related expansions.

In summary, cracking of concrete around grout in the field photos are mostly formed due to one or a combination of the following factors: (a) continued expansion of grout after semi-plastic state to exert stresses to the neighboring concrete mass, which, however, seems unlikely due to reasonable 4 to 6 percent bulk sulfate content of grout to not leave any excess sulfate for continued sulfate-aluminate reactions at the semi-plastic or hardened states, or very dense and sound paste microstructure with no evidence of leaching, softening, or any moisture-induced alteration of paste during service; (b) restrain from expansion of grout at the plastic and semi-plastic state from concrete and metal plate installed above the grout; (c) freezing of concrete at critically saturated conditions at the grout-concrete interface; and (d) some other factors not possible to evaluate from the present study. The present study found no deleterious reactions within the grout or in concrete component to introduce the cracks.

REFERENCES

ASTM C 856 "Standard Practice for Petrographic Examination of Hardened Concrete," Vol. 4.02, ASTM International, West Conshohocken, PA, 2019.

Jana, D., "Sample Preparation Techniques in Petrographic Examinations of Construction Materials: A State-of-the-art Review," *Proceedings of the 28th Conference on Cement Microscopy*, International Cement Microcopy Association, Denver, Colorado, pp. 23-70, 2006.

Jana, D., Petrography – A Powerful Tool for Quality Assurance and Failure Investigation of Construction Materials, International Seminar on Non-Destructive Testing (NDT), India Chapter of American Concrete Institute and ACI (USA), 2006, pp. 117-131.

ASTM C 1090, "Standard Test Method for Measuring Change in Height of Cylindrical Specimens for Hydraulic-cement Grout," Vol. 4.02, ASTM International, West Conshohocken, PA, 2010.

ASTM C 1107, "Standard Specification for Packaged, Dry, Hydraulic Cement Grout (Nonshrink)," Vol. 4.02, ASTM International, West Conshohocken, PA, 2010.

ASTM C 157, "Standard Test Method for Length Change of Hardened Hydraulic-Cement Mortar and Concrete," Vol. 4.02, ASTM International, West Conshohocken, PA, 2010.

ASTM C 827, "Standard Test Method for Change in Height at Early Ages of Cylindrical Specimens from Cementitious Mixtures," Vol. 4.02, ASTM International, West Conshohocken, PA, 2010.

ASTM C 845, "Standard Specification for Expansive Hydraulic Cement," Vol. 4.01, ASTM International, West Conshohocken, PA, 2009.

ASTM C 928, "Standard Specification for Packaged, Dry, Rapid-Hardening Cementitious Materials for Concrete Repairs," Vol. 4.02, ASTM International, West Conshohocken, PA, 2010.

ASTM E 1019, "Standard Test Methods for Determination of Carbon, Sulfur, Nitrogen, and Oxygen in Steel, Iron, Nickel, and Cobalt Alloys by Various Combustion and Fusion Techniques," Vol. 3.05, ASTM International, West Conshohocken, PA, 2015.

Five Star Products, Inc. "A Professional's Guide to Grouting and Concrete Repair for Architects, Contractors, Engineers, Specifiers, and Owners," 2007.

Papas, S. M., "Cementitious Concrete Repair Materials and Grouts: When is Fast Too Fast?" Interface, pp. 18-24, April 2014.

Robl, T.L., Graham, U.M., Taulbee, D.N., and Giles, W., "The Effect of Carbonation Reactions on the Long Term Stability of Products made from Dry FGD Materials," Argonne National Laboratory, 2007.

Wang, H., Carbon Dioxide Sequestration with Flue Gas Desulfurization (FGD) Gypsum, Environmental Science and Information Application Technology, 2009.

✪ ✪ ✪ END OF TEXT ✪ ✪ ✪

END OF REPORT[1]

[1] The CMC logo is made using a lapped polished section of a 1930's concrete from an underground tunnel in the U.S. Capitol.